# WATER QUALITY MODELLING

# OF

# BUFFALO POUND LAKE

by
Julie Terry

A thesis submitted to the
College of Graduate and Postdoctoral Studies
University of Saskatchewan
in partial fulfilment of the requirements for the degree of

Doctor of Philosophy
in
The School of Environment and Sustainability

March 2020

PERMISSION TO USE

In presenting this thesis in partial fulfilment of the requirements for a Postgraduate degree from the University of Saskatchewan, I agree that the Libraries of this University may make it freely available for inspection. I further agree that permission for copying of this thesis in any manner, in whole or in part, for scholarly purposes may be granted by the professor or professors who supervised my thesis work or, in their absence, by the Head of the Department or the Dean of the College in which my thesis work was done. It is understood that any copying or publication or use of this thesis or parts thereof for financial gain shall not be allowed without my written permission. It is also understood that due recognition shall be given to me and to the University of Saskatchewan in any scholarly use which may be made of any material in my thesis.

Requests for permission to copy or to make other use of material in this thesis in whole or part should be addressed to:

Executive Director
School of Environment and Sustainability
University of Saskatchewan
Room 323, Kirk Hall
117 Science Place
Saskatoon, SK S7N 5C8, Canada

Or

Dean
College of Graduate and Postdoctoral Studies
University of Saskatchewan
116 Thorvaldson Building, 110 Science Place
Saskatoon, Saskatchewan S7N 5C9
Canada

# ABSTRACT

The highly variable climate of the Canadian Prairies causes high economic losses from floods and droughts. Prairie waterbodies can be ice covered over half of the year impacting water transfer capacities and influencing aquatic processes and water quality. Available winter studies show ice cover has a wide ranging influence on physical, chemical and biological processes. Water quality models are an emerging tool in the Prairies for understanding complex ecosystem responses. Water quality modelling has traditionally been focussed on open water periods with under-ice processes largely ignored during calibration and model simulations. Management plans based on model results applicable to just four or five months of the year will overlook water quality issues under ice that can be informed by modelling. This thesis presents the first application of a complex hydrological-ecological model CE-QUAL-W2 to Buffalo Pound Lake an impounded, cold polymictic, natural lake supplying the water needs of approximately 25% of the Saskatchewan population. Three research themes investigate if 1) water quality is driven more by the lake's catchment area or by internal lake processes, 2) how future flow management and climate change will affect the water quality of the lake, and 3) how under-ice processes can be successfully represented in the CE-QUAL-W2 model. Five water quality variables are simulated: Chlorophyll-a, ammonia (ammonium, $NH_4^+$-N), nitrate ($NO_3$-N), dissolved oxygen, and phosphate ($PO_4$-P).

This thesis is written in manuscript format. The first manuscript improves the predictive capabilities of the zero-order sediment compartment and adapts the model code to read a variable sediment oxygen demand rate in place of the existing fixed coefficient. A semi-automated calibration method finds an annual pattern between chlorophyll-a, summer oxygen demand and rate of winter decay. The second manuscript looks to improve the under-ice heat and light environment in the model by modifying the ice algorithm to incorporate a variable albedo rate. Simulated ice-off dates are found to be highly sensitive to the ending albedo value. Improvements to water quality predictions are limited by the connection of the ice and eutrophication modules in CE-QUAL-W2. A targeted monitoring program is suggested to reduce uncertainty with boundary data. The third manuscript tests the sensitivity of the model to catchment and in-lake boundary conditions. All five water quality variables are found to be most sensitive to modelled inflow

discharge. The final chapter summarises the findings of the three manuscripts and presents a scenario based flow management analysis for discussion. This research finds the Buffalo Pound Lake model is most sensitive to catchment boundary data. Water quality in the lake may be impacted by changing inflows resulting from lake management decisions and climate change.

# ACKNOWLEDGMENTS

This work is funded through the Natural Sciences and Engineering Research Council of Canada Strategic Project Grant, the Buffalo Pound Water Treatment Plant (WTP), the Water Security Agency (WSA), the Global Institute for Water Security (GIWS), and the School of Environment and Sustainability (SENS).

For the Buffalo Pound Lake project, I thank Heather Wilson (DEM preparation), and Dr. Helen Baulch (buoy data + funding support) from GIWS, and Paul Jones (boat sonar data) from SENS. I also thank John-Mark Davies (water-quality data), Dave MacDonald (GIS data), and Andrew Thornton (water demands) from the WSA. I am grateful to Curtis Hallborg from the WSA for hydrological data and his time in explaining the hydrology of the reservoir system. Water-quality data provided by Dan Conrad at the WTP is gratefully acknowledged.

For my PhD program, I sincerely thank my supervisor Dr. Karl-Erich Lindenschmidt and members of my supervisory committee: Professor Steven C. Chapra, Dr. John-Mark Davies, Dr. Andrew Ireson, Dr. Saman Ravazi, and Dr. Rebecca North and Dr. Helen Baulch for their mentorship, guidance and support. I also deeply thank Dr. Michael Kehoe and Dr. Amir Sadeghian for their endless encouragement and technical and statistical expertise. I am grateful to Irene Schwalm of SENS for program administration assistance and guidance throughout.

I thank all the University Faculty, employees and technicians that have contributed their expertise behind the scenes, and professionals in the field that have generously shared their knowledge.

TABLE OF CONTENTS

# LIST OF TABLES

Tables

LIST OF FIGURES

Figures

# LIST OF ABBREVIATIONS

This thesis contains the content of published manuscripts, and as such full descriptive names and abbreviations are used within individual sections and chapters as relevant to the text.

| | |
|---|---|
| BOD | Biochemical oxygen demand |
| BPL | Buffalo Pound Lake |
| Chl-a | Chlorophyll-a |
| DEM | Digital elevation model |
| DO | Dissolved oxygen |
| DOC | Dissolved organic carbon |
| DT | Distributed tributary |
| ECCC | Environment and Climate Change Canada |
| ELA | Experimental Lakes Area |
| GIWS | Global Institute for Water Security |
| HAB | Harmful algal bloom |
| LDief | Lake Diefenbaker |
| LDOM | Labile dissolved organic matter |
| LPOM | Labile particulate organic matter |
| $NH_4^+$-N | Total ammonia (Ammonium) |
| $NO_3$-N | Nitrate |
| OAT | One-factor-at-a-time |
| $PO_4$-P | Phosphate |
| RDOM | Refractory dissolved organic matter |
| RPOM | Refractory particulate organic matter |
| SOD | Sediment oxygen demand |
| TDS | Total dissolved solids |
| TN | Total nitrogen |
| WQ | Water quality |
| WSA | Saskatchewan Water Security Agency |
| WTP | Buffalo Pound Water Treatment Plant |
| W2 | CE-QUAL-W2 |

# CHAPTER 1

# INTRODUCTION

## 1.1 Background

Our freshwater resources are under stress. The unsustainable use of water has led to falling levels of groundwater, and loss of lakes, river flows, and wetlands (Wheater and Gober, 2015) in many world regions (Rodell et al., 2018). Water supplies and quality are progressively under threat from climate change and human activities (Vörösmarty et al., 2010, Watson and Lawrence, 2003) and are increasingly vulnerable to extreme climatic events (Wheater and Gober, 2015). Our total global lakes and reservoirs are approximately 43 times greater in volume than our total rivers (Likens, 2009). Their sustainability is of great importance for water security. Perhaps the greatest challenge facing these waterbodies is degradation of water quality (WQ). Lakes are considered "sentinels" of environmental change (Adrian et al., 2009, Schindler, 2009, Williamson et al., 2009) and human induced impacts (Minns, 2013). They are sensitive to climate related changes, and their responses can, with care, be used to infer global trends and regional variations in climate and the respective influence on ecosystems (Adrian et al., 2009, Williamson et al., 2009). A reason for using lakes as experimental units is their ecological complexity with internal and external drivers and feedbacks, and their rapid physical, biological and chemical response to change (Adrian et al., 2009). Lakes have measureable indicators and can react quickly to system perturbations as well as accumulating signals of longer changes over time. Their size facilitates whole-system studies that are impossible to conduct at a larger scale, and they are accessible units for researchers to monitor.

The Experimental Lakes Area (ELA) in Canada was created in the late 1960s as a test site for whole lake manipulation experiments at an unprecedented scale (Stokstad, 2008). These were selected, in part, due to their pristine condition from their remote location far from human and industrial influences (Stokstad, 2008). With an original research agenda of understanding eutrophication and then acid rain, additional research topics over time have included

biomanipulation, aquaculture, habitat disruption, toxicities, reservoir impacts and climate change. Although controversial for the methodology of polluting otherwise pristine lakes, the resultant data and images of ELA experiments have been sufficient to sway North American governmental policy on matters such as phosphates in detergents and the Clean Air Act (Stokstad, 2008).

Undoubtedly the ELA cannot answer all questions as there are few actual pressures on the ELA from human and industrial water demands (Blanchfield et al., 2009). With a growing human population, economic development, and increasing water security pressures more water will likely be abstracted from lakes over time. A relevant unit to study human impacts would be an impounded lake in a developed region (Fig. 1.1).

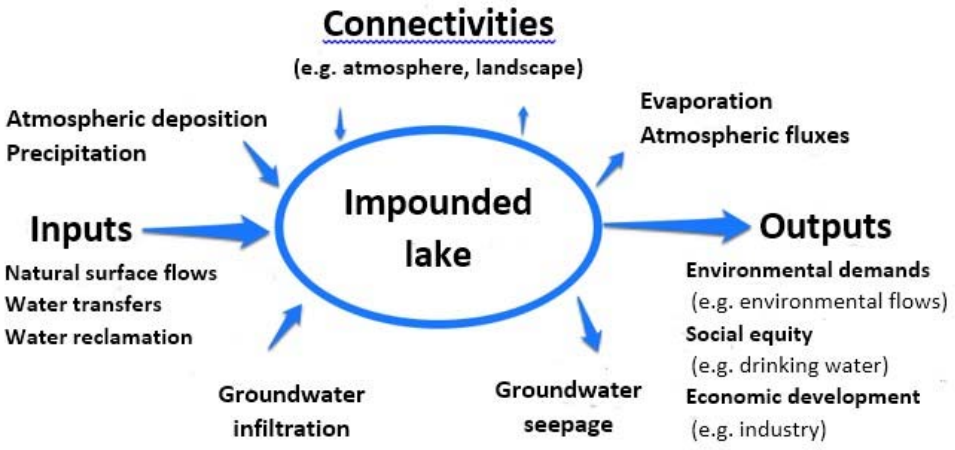


Figure 1.1. The inputs, outputs, and connectivities to atmosphere and landscape of an impounded lake.

One such example where lake research is critical is the study of algal bloom development. Algal blooms are inextricably linked to lake ecology and functioning (Michalak et al., 2013, Havens, 2008), and can lower the aesthetical value of a waterbody. A Harmful algal bloom (HAB) is a bloom with negative health implications for humans or ecosystems (Ho and Michalak, 2015). Some algal strains contribute to taste and odour (Kehoe et al., 2015) and toxicity (Taranu et al., 2015, Quiblier et al., 2013) problems in drinking water supplies, with high treatment costs for removal. Toxin forming strains of cyanobacteria ('blue-green algae') have also been linked to fatal dog poisonings from swimming in waters with bloom presence (e.g. Puschner et al., 2008).

In 2011 Lake Erie recorded its largest ever well documented HAB, with a peak bloom estimated by remote sensing at more than 5,000 $km^2$ – 3.3 times the size of the largest previously recorded bloom in 2008 (Michalak et al., 2013). In 2014 a HAB in Lake Erie forced a three-day tap water restriction in Ohio (Ho and Michalak, 2015). With a long history of algal blooms, the WQ problems of Lake Erie were the motivation for the phosphorus research conducted at the ELA (Venkiteswaran, 2012). While the responding policy implementations for phosphorus loading reduction were initially successful, HABs in Lake Erie have been steadily increasing since the mid-1990s (Michalak et al., 2013). Both climatic conditions, and rising trends in agricultural nutrient application have been proposed as the contributing factors for the 2011 bloom (Michalak et al., 2013). The spatio-temporal upscaling of research across 108 lakes, over a 200 year period, by Taranu et al. (2015) highlighted that human activities, in particular nutrient management, are the major driver of increasing cyanobacterial abundance.

Canada contains approximately 9% of global available surface freshwater, and yet water resources are a concern (Watson and Lawrence, 2003). In the South Saskatchewan River Basin, a 336,000 $km^2$ area that passes through the provinces of Alberta, Saskatchewan and Manitoba, agriculture is responsible for 82% of consumptive water use (Wheater and Gober, 2013). Water apportionment agreements exist between Alberta and downstream jurisdictions notably through the Master Agreement of Apportionment, which is administered by the Prairie Provinces Water Board. Water security challenges in the basin include drinking WQ concerns for indigenous communities, and provision of sufficient water resources for agriculture, industry and natural resource development (Wheater and Gober, 2013). This is a land subject to some of the most variable climate on Earth with high economic losses from persistent floods and droughts (Wheater and Gober, 2013). Waterbodies can be frozen over half of the year impacting water transfer capacities and influencing aquatic processes and WQ.

The implications of seasonal freezing is under-investigated in freshwater WQ research. Under-ice processes are often considered less important in a waterbody's overall trophic status (Hampton et al., 2017). Algal issues, in particular, are fewer in under-ice conditions due to low temperatures and limited light penetration. Fieldwork has traditionally been performed in the warmer, open water seasons. This is partly due to harsher field-work conditions in winter, and logistical difficulties collecting data at the season beginning and end when ice cover is less stable. The lack of winter data means WQ research has focussed largely on open water conditions. The

under-ice physical, chemical and biological environments remain severely understudied (Hampton et al., 2017, Oveisy et al., 2014).

This disparity is especially true with regards to WQ modelling applications. Previous attempts to link ice modules to WQ models have found the ice modules too simplified, or too disconnected to the under-ice WQ environment for lake management purposes (Oveisy et al., 2012). In warmer climates where ice cover may last only days, or one or two weeks at a time, the under-ice environment can be largely ignored in a WQ model with little danger of compromising the model results. On the Prairies, where surface waterbodies can be continuously ice covered for a longer duration than their open water season, data may not be reliable. Available studies show ice conditions can have wide-ranging influence on physical, chemical and biological processes (e.g. Hampton et al., 2017, Kirillin et al., 2012, Salonen et al., 2009, Adrian et al., 1999). In the populated areas of the Prairies setting best practice management methods based on model results applicable to just four or five months of the year may not account for a number of processes influencing annual lake succession.

## 1.2 Objectives and Thesis Structure

My project falls under the Global Institute for Water Security's (GIWS) research theme of Land-Water Management and Environmental Change. Buffalo Pound Lake (BPL), my study site, is located on the Upper Qu'Appelle River in Saskatchewan. The increasing pressure on BPL has led to numerous scientific studies over the years (e.g. Kehoe et al., 2015, McGowan et al., 2005, Hall et al., 1999, Hammer, 1971), and organisational reports from environmental consultancy firms (e.g. Clifton Associates Ltd, 2012) and agencies (e.g. Water Security Agency). In spite of this, WQ is a continuing concern in the lake. Almost all previous studies of the lake have been practical field-work and laboratory based experiments. BPL has only recently been included in a one-dimensional model grid of the Upper Qu'Appelle river-lake system using WASP7 (Hosseini et al., 2018). The overall objective of my research project is the first application of a two-dimensional, complex hydrological-ecological model CE-QUAL-W2 (W2) to the lake.

Three overall research themes interlink:

1) Is WQ in BPL driven by catchment processes, or the lake's internal processes?

2) How will future flow management strategy and climate change affect the WQ (Chl-a, DO, $PO_4$-P, $NH_4^+$-N, $NO_3$-N) of the lake?
3) Can under-ice processes be modelled successfully in a WQ model of BPL?

This thesis follows the guidelines set out by the College of Graduate Studies and Research, and is presented in manuscript format. The introductory chapter provides the theoretical basis and research purpose. Three manuscripts are then presented as single thesis chapters that each address a specific research question. Chapter prefaces introduce the objectives of each of the manuscripts. The final thesis chapter presents a synopsis of research findings and future implications along with a discussion on model uncertainties and limitations.

Adaptions to the original W2 model structure are: 1) the addition of two empirical coefficients in the ice module to reduce heat transfers at the ice-air interface, 2) a function for reading a variable sediment oxygen demand rate to replace a fixed model coefficient value, 3) a function for reading a variable albedo rate in the ice module to replace a fixed model coefficient value.

## 1.3 Copyright and Author Permissions

Chapters 2 through 4 of this thesis consist of manuscripts that are published or are currently in review. I provide the manuscript citations below in order to maintain consistency with copyright and author rights for each publisher. For all manuscripts, the student is the first author as per the College of Graduate Studies and research guidelines for manuscript style theses.

Chapter 2: Terry, J. A., Sadeghian, A., and Lindenschmidt, K-E. (2017) Modelling dissolved oxygen/sediment oxygen demand under ice in a shallow eutrophic Prairie reservoir. *Water, 9, 131.*

Chapter 3: Terry, J. A., Sadeghian, A., Baulch, H. M., Chapra, S. C., Lindenschmidt, K-E. (2018) Challenges of modelling water quality in a shallow prairie lake with seasonal ice cover. *Ecological Modelling, 384, 43-52.*

Chapter 4: Terry, J. A. and Lindenschmidt, K-E. Sensitivity of boundary data in a shallow prairie lake model. Submitted for publication to *Canadian Water Resources Journal* 29 May 2019 – in process as at March 2020

# PREFACE TO CHAPTER 2

This manuscript was designed to meet the current uncertainty on how best to describe sediment oxygen demand (SOD) in a water quality model with limited data. Oxygen is essential for a healthy aquatic system, and reliable prediction of oxygen deficits is paramount for aquatic managers. Buffalo Pound Lake (BPL) is a shallow system with a high sediment-water interface relative to water volume, and capturing SOD is crucial. Here, a novel modelling approach improves the predictive abilities of a simple sediment compartment with limited data. Presented are two methods of model calibration using observed data for dissolved oxygen and chlorophyll-a concentrations. By this method, the manuscript provides aquatic managers a methodology to model SOD in their waterbodies if they do not have the data for a full diageneses model. The findings are applicable to waterbodies across the world with similar attributes to BPL.

CHAPTER 2

# MODELLING DISSOLVED OXYGEN/SEDIMENT OXYGEN DEMAND UNDER ICE IN A SHALLOW EUTROPHIC PRAIRIE RESERVOIR

Julie A. Terry*, Amir Sadeghian, and Karl-Erich Lindenschmidt
* Corresponding author.

Water 2017, 9, 131; doi:10.3390/w9020131
Received 17 December 2016; Accepted 10 February 2017
Water (2017), 9, 131-16 pages


Author Contributions

Julie A. Terry, Amir Sadeghian and Karl-Erich Lindenschmidt conceived and designed the experiments. Julie A. Terry set up the Buffalo Pound Lake model. Amir Sadeghian wrote the MATLAB code and adapted CE-QUAL-W2 for snow cover and variable SOD. Julie A. Terry wrote the bulk of the paper with text inputs and conceptual edits from Karl-Erich Lindenschmidt. All authors proofread and approved the manuscript.

## 2.1 Abstract

Dissolved oxygen is an influential factor of aquatic ecosystem health. Future predictions of oxygen deficits are useful for risk assessment when maintaining water quality. Oxygen demands

depend greatly on a waterbody's attributes. A large sediment-water interface relative to volume means sediment oxygen demand has greater influence in shallow systems. In shallow, ice covered waterbodies the potential for winter anoxia is high. Water quality models offer two options for modelling sediment oxygen demand: a zero-order constant rate, or a sediment diagenesis model. The constant rate is unrepresentative of a real system, yet a diagenesis model is difficult to parameterise and calibrate without data. We use the water quality model CE-QUAL-W2 to increase the complexity of a zero-order sediment compartment with limited data. We model summer and winter conditions individually to capture decay rates under ice. Using a semi-automated calibration method, we find an annual pattern in sediment oxygen demand that follows the trend of chlorophyll-a concentrations in a shallow, eutrophic Prairie reservoir. We use chlorophyll-a as a proxy for estimation of summer oxygen demand and winter decay. We show that winter sediment oxygen demand is dependent on the previous summer's maximum chlorophyll-a concentrations.

## 2.2 Introduction

Oxygen is essential for a healthy aquatic system. The Canadian water quality (WQ) guidelines for the protection of aquatic life state that dissolved oxygen (DO) is the most important parameter in water (Canadian Council of Ministers of the Environment, 1999). Severe oxygen depletion can lead to fish kills (Robarts et al., 2005, Meding and Jackson, 2003), deformities in fish larvae (Canadian Council of Ministers of the Environment, 1999), and changes in community composition and lake trophic state (Ruuhijärvi et al., 2010, Meding and Jackson, 2003, Wetzel, 2001). The prediction of DO concentration is vital for fisheries, and for aquatic managers responsible for maintaining ecosystem health (Meding and Jackson, 2003).

The shallow lakes and reservoirs of the Canadian Prairies are naturally mesotrophic to eutrophic (Finlay et al., 2010), and display severe fluctuations in DO (Robarts et al., 2005). Large phytoplankton blooms can occur, and the waterbodies are subject to a highly variable climate with hot summers and ice covered winters. DO is additionally important in drinking water reservoirs as dissolved gas supersaturation can be an issue in water treatment (Scardina and Edwards, 2001). Low oxygen can also induce release of nutrients, and sulphide production.

Phytoplankton contribute greatly to DO in reservoirs by photosynthesis, as will macrophytes if present in large volumes (Hosseini et al., 2017, Meding and Jackson, 2003).

Periphyton may also contribute (Thornton et al., 1990). Additional DO will enter from inflows and reaeration from the atmosphere. As well as replenishing DO, inflowing waters also transport organic matter into a reservoir. This matter will settle in the sediments along with dead plants and algae. When this material decomposes both chemical oxidation and biological respiration exert a significant oxygen demand to the water column (Cross and Summerfelt, 1987), known as biochemical oxygen demand (BOD), and to the sediments, known as sediment oxygen demand (SOD). Both BOD and SOD have a positive relationship with reservoir productivity. Nitrification also contributes to oxygen demand.

In open water oxygen deficits are replenished through reaeration (Chapra, 1997) to the surface and mixed to the bottom by wind and turbulence. Reaeration is the exchange of gases at the air-water interface. In contrast, ice covered conditions bring significant changes to the DO dynamics. Under ice cover atmospheric gas exchange is removed from the oxygen balance (Golosov et al., 2007). If sufficient light penetrates through the ice, plants and algae continue to photosynthesise and produce oxygen (Vehmaa and Salonen, 2009). The cooler winter water temperatures slow the decomposition of organic matter and reduce the consumption of oxygen through bacterial activity (Wetzel, 2001, Canadian Council of Ministers of the Environment, 1999). Breaks in the ice can increase the oxygen balance by allowing gas exchange.

Conversely, heavy snow loads reduce light penetration to a point where photosynthesis is greatly reduced (Salonen et al., 2009, Wetzel, 2001, Fang and Stefan, 2000). The resultant decomposition of dying biota consumes further oxygen supplies (Golosov et al., 2007). Inflow volumes are often low in winter with less new oxygen inflow to offset consumptive processes (Martin et al., 2013). There may be no breaks in the ice and extended ice cover. The absence of wind on the water surface reduces the chance of oxygen mixing through the water column to deeper waters. Oxygen levels can reach the point of anoxic conditions at the bottom of reservoirs with high oxygen demands (Meding and Jackson, 2003).

Low winter DO concentrations have been linked to shallower lakes with sizeable littoral zones and prolonged ice cover (Leppi et al., 2016). Shallow waterbodies have a large sediment-water interface relative to water volume. This interface is where the organic matter and bacterial activity tends to be concentrated (Leppi et al., 2016). The relative influence of bottom decomposition on the water column is therefore greater in shallow systems (Chapra, 1997). While open waters are often well-mixed from wind action, under ice cover the shallow water depth means

that the anoxic zone could potentially thicken along the bottom sediments. SOD is highly sensitive to small temperature fluctuations at lower water temperatures, with small increases intensifying oxygen depletion (Kirillin et al., 2012). When modelling DO in a shallow, eutrophic system the ability to simulate SOD and the rate of SOD decay is important.

WQ modellers usually work in a series of steps: first is a water balance model followed by a water temperature and mixing model to set up the hydrodynamics for the system. Some modellers then choose to move to a full nutrient and phytoplankton model, and their DO predictions are part of the overall sources and sinks of the model. The danger with greatly increasing the complexity at once is that each additional state variable will require additional parameters and functions to control the escalating number of interacting processes. The result is a large number of parameters in relation to output variables and objective functions. An over-parameterised model is difficult to calibrate due to the greater number of parameter combinations that may provide non-unique optima as described by the equifinality thesis (Beven, 2006).

Another strategy is to approach the nutrient and phytoplankton modelling with a stepwise approach: building the model complexity in stages rather than adding all the WQ data at once. This method allows parameters to be constrained at a lower complexity (fewer output variables) before enabling further state variables, parameters and functions.

One of the simplest methods to begin a DO model is the Streeter-Phelps model, a long-standing model with the state variables BOD and DO (Chapra, 1997). In practice, the relative importance of BOD depends on the system being investigated. In Europe, for example, rivers have high loading of waste water BOD in areas of dense population and industry (Williams et al., 2012, Lindenschmidt et al., 2009, Lindenschmidt, 2006). The Prairie reservoirs in Canada are often in rural areas and BOD inflows can be small. For these shallow, eutrophic systems it is far more important to include SOD when modelling DO.

WQ models generally fall into two categories for modelling SOD: a full sediment diagenesis model, or a much simplified year-round SOD rate that varies in response to water temperature. A diagenesis model has the advantage that it can be calibrated for specific applications such as wastewater studies. The disadvantage is that, in reality, SOD is fairly difficult to measure in the field. The diagenesis model is useful when sediment core analyses are available, yet few aquatic managers and fisheries would have access to this kind of information.

A full WQ model is currently being built for Buffalo Pound Lake (BPL), a shallow eutrophic Prairie reservoir in the Canadian province of Saskatchewan. BPL has insufficient sediment data to properly parameterise a diagenesis model. A constant SOD rate, however, is unrepresentative of the processes in a shallow, eutrophic system that spends approximately half of the year under ice.

Our objective in this study is to test an alternative approach that allows us to increase the complexity in the constant rate SOD formulation with limited data. Our method extends the year-round constant rate by building an empirical model for SOD that considers both ice-on and ice-off periods. Modelling both winter and summer allows us to constrain certain parameters during certain seasons in order to better calibrate other parameters. For instance, setting reaeration to zero under ice covered conditions allows us to better describe the SOD parameterisation.

For the DO model, we use CE-QUAL-W2 (W2) (Portland, OR, USA) - a two-dimensional (vertical and longitudinal) coupled hydrodynamic and WQ model. W2 is a complex model suitable for reservoirs. W2 is chosen due to its suitability for BPL as a long, narrow waterbody, and the inclusion of an ice model. A full description of the hydrodynamics and transport processes of W2 is given in the user manual (Cole and Wells, 2015).

The results obtained by our simulations will allow us to constrain our baseline SOD within a sensible range for BPL. We will be able to maintain appropriate SOD rates as the model becomes more complex on incorporating algal-nutrient dynamics.

## 2.3 Materials and Methods

### 2.3.1 Site Description

Buffalo Pound Lake (BPL) is an impounded natural lake located on the Upper Qu'Appelle River in Saskatchewan, Canada (Fig. 2.1). The reservoir supplies the water demands of the cities of Moose Jaw, Regina, surrounding communities, and an expanding industrial corridor and potash mines. The reservoir forms part of the glacially formed upper Qu'Appelle River system described in detail in Hammer (1971). Annual mean precipitation is 365.3 mm and approximately 30% falls as snowfall (Environment and Climate Change Canada). Ice cover is typically November to late April. Air temperatures range between an average daily minimum of -17.7 °C in January to an

average daily maximum of 26.2 °C in July (Environment Canada). WQ issues such as eutrophication remain a challenge, and the reservoir has persistent problems with taste, odour, and algal blooms (Kehoe et al., 2015, Slater and Blok, 1983). Over 95% of the drainage basin is agricultural land (Hall et al., 1999), although the large majority of inflows into BPL are via controlled releases through the Qu'Appelle River Dam on Lake Diefenbaker (LDief) upstream. LDief waters therefore have more influence on BPL WQ than the agricultural catchment suggesting that non-point nutrient sources (diffuse pollution, overland run-off) may not factor in nutrient loading to BPL to the same extent as other prairie waterbodies.

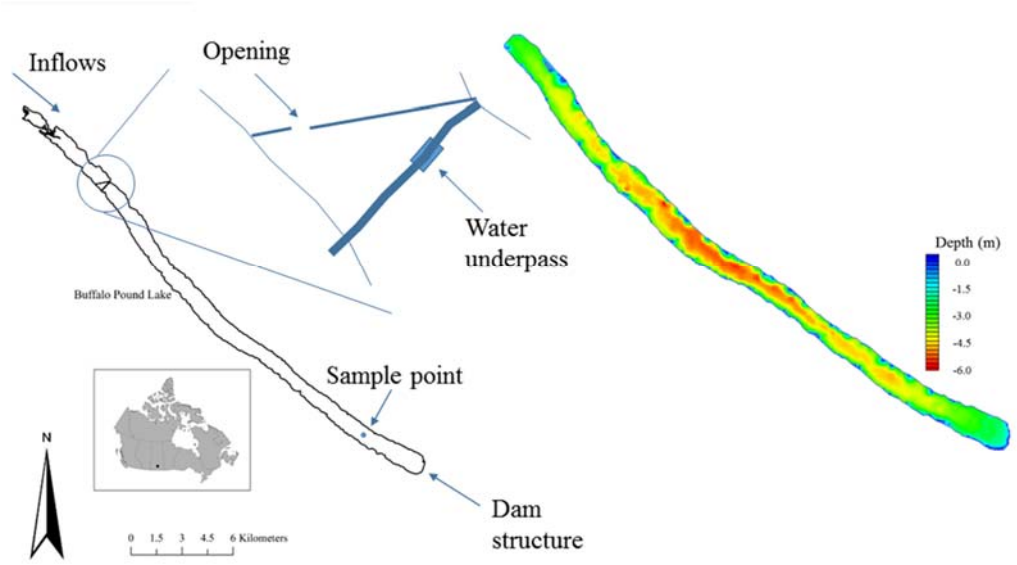


Figure 2.1. Buffalo Pound Lake, Saskatchewan, Canada. Mean depth is 3.8 m with a maximum depth of 5.98 m. Mean residence time is highly variable (6 to 30 months). Flow is in a southeast direction. The black reservoir outline is to the provided scale. The digital elevation model (DEM) shows bathymetry for the main body of the lake downstream of the underpass.

### 2.3.2 Model Setup

W2 needs full geometric data to operate. A digital elevation model (DEM) was prepared in ArcGIS 10.2.2 (ESRI Inc., Redlands, CA, USA). The DEM includes sonar data collected by boat in 2014, and a reservoir extent polygon and shoreline digital elevation data provided by the Saskatchewan Water Security Agency (WSA). The combined GIS data are interpolated using a

spline barrier method at 30 m resolution. The Upper Qu'Appelle flows into the northwest end of the reservoir with the dam located at the southeast end. In essence, the upstream area of BPL is split into separate waterbodies by Highway 2, which divides the reservoir down to the reservoir bed (Fig. 2.1). The first obstacle that the inflows meet is the old highway. Once the flows are through this they are then squeezed through a gap of 45 m (three connected 15 m sections) under the bridge of the new Highway 2, and into the main body of the reservoir. The north section of the reservoir is extremely shallow and macrophyte covered in summer, and could not be accessed by boat at the time of collecting sonar data. The top and main body of the reservoir will likely experience some differences in reservoir conditions making it less realistic to model the reservoir as just one waterbody. WQ data were available for under Highway 2 and so these are set as boundary data. The DEM and WQ model covers the whole main body of BPL downstream of Highway 2.

W2 discretises the waterbody into a finite grid of longitudinal segments, vertical layers and cross-sectional widths. The user specifies the space steps in the longitudinal and vertical directions. The cross-sectional widths are determined by the shoreline bathymetry as each cell spans the width of the waterbody. The prepared DEM has been segmented into a numerical grid in the Watershed Modelling System (WMS) (Aquaveo, Provo, UT, USA) for final output as a bathymetry text file for W2. Longitudinal segments average 100.9 m with a total length for all 256 segments of 25,834 m. Vertical layers are 0.25 m with the maximum number of layers being 26 at the deepest part of the reservoir. W2 requires boundary layers and segments that are all zero meters and these are included in these totals. Average width at the surface is 890 m.

### 2.3.3 Data Collection and Analysis

Hourly meteorological forcing data have been downloaded from Environment and Climate Change Canada (ECCC) for the Moose Jaw station located approximately 30 km south from BPL. In order to estimate the wind conditions at the reservoir surface, comparisons have been made of recent ECCC data against data from an in situ high-frequency data collecting buoy. This buoy has been deployed on BPL by the Global Institute for Water Security since 2014 for open water field seasons. Snowfall figures are also taken from the ECCC Moose Jaw station, and are monthly totals.

The “snow on the ground” measurement is the physical quantity of snow cover on the last day of each month.

Gauged averaged daily inflows have been downloaded directly from the ECCC website. Accurate inflow data are not available for the BPL boundary of Highway 2, and flows are from the nearest gauge (05JG004) 19 km upstream on the Upper Qu’Appelle River. This is land distance - the flows will travel further as the channel meanders. Monthly mean estimates of ungauged inflows are provided by the WSA and include minor tributaries located after the ECCC gauge, as well as overland run-off estimates.

The main outflows from BPL are dam releases and piped withdrawals. The dam releases have been derived using ECCC data for two downstream flow gauges. The withdrawal volumes are provided by the on-site Buffalo Pound Water Treatment Plant (WTP) and by SaskWater. Daily averaged water-level measurements are provided by the WSA for an in-reservoir gauge.

Monthly inflow DO and BOD measurements are provided by the WSA for a sample site at the Highway 2 boundary. The in-reservoir observed data are taken from a substantial weekly dataset provided by the WTP laboratory. The WTP weekly samples are normally taken around 07:20 a.m. at a sample site midway between the north and south shorelines near the downstream end of the reservoir, and approximately one meter off the reservoir bed. The reservoir is expected to be well-mixed at the sampling point. Water is withdrawn through an intake pipe at this location to the WTP’s pumping station, on the south shore, where sampling takes place before the water is pumped to the WTP itself. These samples are transported to the WTP laboratory for analyses. This procedure is performed weekly in both open water and under-ice conditions. Some spot sample WQ data are available for other locations across the lake, although not all constituents are measured regularly at these additional sites, and they have not been included in this study.

Weekly inflow temperatures are estimated through a linear regression ($R^2 = 0.861$; equation $y = 1.0598x - 2.7747$; 59 samples; no outliers removed) between WTP spot sample temperature measurements over 34 years at the site of the inflow gauge upstream, and the WTP weekly temperature data for the reservoir. Precipitation temperatures are set at dew-point temperature, or zero if the dew-point is negative.

Initial conditions for water temperature and DO are also taken from the WTP weekly dataset. Sediment temperature is set at the mean annual air temperature over the simulation period as per the W2 manual recommendation (Cole and Wells, 2015). Parameter coefficients are set

according to knowledge of the reservoir, or are left at W2 default values where data are not available to support a change. The kinetic coefficients for BOD and SOD are W2 defaults (Table 2.1).

For quality assurance, the WTP data span the complete simulation period and undergo strict quality control sample procedures. The flow data, water-level data and meteorological data downloaded from the WSA and ECCC websites are expected to have undergone quality control prior to commencement of the study. Metadata are available for the WSA WQ database that details the source and perceived accuracy of the measurements.

Table 2.1 W2 Default kinetic coefficients used in this study for the sediment oxygen demand (SOD) and biochemical oxygen demand (BOD) calculations.

| Coefficient | Description | Value | Units |
|---|---|---|---|
| TSED | Sediment temperature | 10.3 [1] | °C |
| CBHE | Coefficient of bottom heat exchange | 0.3 | W $m^{-2}$ $°C^{-1}$ |
| KBOD | 5-day BOD decay rate at 20 °C | 0.1 [2] | $day^{-1}$ |
| TBOD | Temperature coefficient (decay rate) | 1.02 [2] | |
| RBOD | Ratio of 5-day BOD to ultimate BOD | 1.85 [2] | |
| CBODS | BOD settling rate | 0.0 [2] | M $day^{-1}$ |
| SODT1 | Lower temperature for zero-order SOD or first-order sediment decay | 4.0 | °C |
| SODT2 | Upper temperature for zero-order SOD or first-order sediment decay | 25.0 | °C |
| SODK1 | Fraction of SOD or sediment decay at lower temperature | 0.1 | |
| SODK2 | Fraction of SOD or sediment decay at upper temperature | 0.99 | |
| REAERAT | Reaeration formulation | LAKE, 6 | |

[1] Where the value is different to the W2 default. [2] W2 uses CBOD as the model group; we are assuming that CBOD makes up the majority of our BOD.

### 2.3.4 Model Customisation

We have customised two components of the W2 model: SOD and the ice algorithm. This study uses W2 version 3.72, which includes a zero-order, or a limited first-order, sediment compartment for estimating SOD. The latest versions of W2 (v4.0 onwards) also includes a new sediment diagenesis model; however, with no sediment data to drive a full diagenesis compartment, there would be considerable uncertainty at the large scale of a reservoir. We opted for v3.72 as the complete source code for v4.0 was not available for download on commencement of our study, and we were unable to customise the later version for our specific objective.

W2 uses three different types of data for model calibration: the first group are set prior to the model run and remain constant throughout the simulation - examples being latitude for the calculation of solar radiation, bathymetry, and parameter coefficients. The second group are the time-varying state variables such as inflows, outflows, and meteorological data. The third group are the variables changing internally in the model at each time step; temperature, shear stress, and horizontal and vertical velocities are examples of this group.

DO is calculated in W2 as per Equation (1). The complete set of DO equations in W2 are more complex as the model recognises up to thirteen sources and sinks of DO (Cole and Wells, 2015). We present here the W2 equations we use in our own reservoir DO/SOD model.

$$S_{\mathrm{DO}} = \underbrace{A_{sur}K_L(\Phi'_{DO} - \Phi_{DO})}_{aeration} - \underbrace{\boldsymbol{SOD}\gamma_{OM}\frac{A_{sed}}{V}}_{zero-order\ SOD} - \underbrace{\sum K_{BOD}R_{BOD}\Theta^{T-20}\,\Phi_{BOD}}_{BOD\ decay} \qquad (1)$$

Where:

| | |
|---|---|
| $A_{sur}$ | water surface area, $m^2$ |
| $K_L$ | interfacial exchange rate for oxygen, $m \cdot s^{-1}$ |
| $\Phi'_{DO}$ | saturation DO concentration, $g \cdot m^{-3}$ |
| $\Phi_{DO}$ | dissolved oxygen concentration, $g \cdot m^{-3}$ |
| $\boldsymbol{SOD}$ | sediment oxygen demand, $g \cdot m^{-2} \cdot s^{-1}$ |
| $\gamma_{OM}$ | temperature rate multiplier for organic matter decay |
| $A_{sed}$ | sediment surface area, $m^2$ |
| $V$ | volume of computational cell, $m^{-3}$ |
| $K_{BOD}$ | BOD decay rate, $s^{-1}$ |
| $R_{BOD}$ | conversion from BOD in the model to BOD ultimate |
| $\Theta$ | BOD temperature rate multiplier |
| $\Phi_{BOD}$ | BOD concentration, $g \cdot m^{-3}$ |

The zero-order SOD is a user-defined constant rate that is temperature dependant. In the original source code the model reads the SOD at the start of the simulation, and uses the same rate in the equation for the whole simulation period. The zero-order SOD is displayed in bold text in Equation (1). In W2, BOD is imported as a time-varying variable in the inflow constituent file. We modified the W2 code to treat SOD in a similar manner and read SOD as a time-varying temperature dependent input file. The model checks for new values of SOD during each iteration and updates the zero-order SOD in Equation (1). The original constant SOD rate in W2 is now a variable rate in the DO equations, although the DO module itself is unchanged.

For the ice model W2 calculates the formation and melting of ice during simulations, and the relevant processes (e.g. light, wind, heat fluxes) are adjusted accordingly by the model. Snow

is not considered in the algorithm. Snow depth at BPL is often between 0.1 and 0.3 m as per the supplied WSA long-term data. To account for this lack of snow the ice model has been extended to include two empirical coefficients to the existing W2 algorithms, as have been previously applied (Sadeghian et al., 2015). The first coefficient α extends the ice growth and thickness equations and reduces the heat lost through back radiation from black surfaces. The second coefficient β extends the ice melt equations and reduces the heat conduction between air and ice. Both coefficients are assigned a value between zero and one to be multiplied by the appropriate equation parameter. For BPL, no ice thickness data are available for calibration of α. A 39-year data set of ice-on and ice-off dates has been provided by the WTP, and it is found that W2 predicts the ice-on dates to be closely matched with the observed dates. For this study, the coefficient α is set to have no contribution to the ice growth equation (given the value 1). Ice-off dates were difficult to match as the ice melts too quickly in the W2 simulations - up to a period of several weeks. The optimum value of coefficient β is found to be 0.24 to predict the best spring ice-off dates over the simulation period.

### 2.3.5 Model Setup and Application

The model simulates a continuous seven-year period (1 April 1986–31 March 1993). This period is chosen due to the availability of daily flow data recorded by two WSA gauges just above and below BPL that were subsequently discontinued.

The water balance, ice-on and ice-off dates, and the water temperature model were calibrated. The final temperature model shows good results (Fig. 2.2). Some discrepancy occurs in the winter of 1989/90 and 1991/92 with the model under-predicting the winter bottom temperature and possibly the stratification. The temperature profile can depend on the meteorological conditions at freeze-over. In addition, many of the temperature sensitive parameters and coefficients in W2 (e.g., sediment temperature, bottom heat exchange, surface albedo) are fixed in the model. It is likely that there is some temporal variance in these in-reservoir.

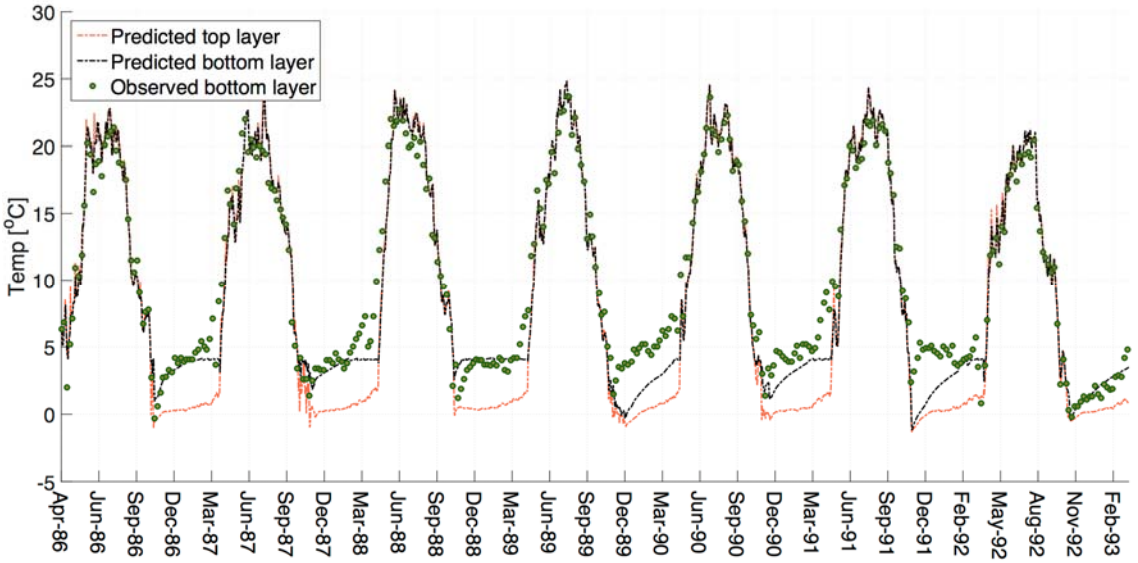


Figure 2.2. Results of the water temperature model. Compares predicted temperatures in the same grid cell as the Buffalo Pound Water Treatment Plant weekly observations. Note that CE-QUAL-W2 converts the negative water temperature modelled at the start of each winter to equivalent ice thickness. Root mean square error = 1.46 (to 2 dp); mean absolute error = 1.12 (to 2dp).

The monthly ungauged inflow estimates provided by the WSA are created to close their own water balance for BPL, and our respective water balances differ as a result of methodology and data. We chose not to use the provided estimates due to the uncertainty. Another limitation is that the downstream flow data, which we have included, have room for error due to the presence of wetlands, and the potential for backwater flows during the freshet from a tributary confluence downstream of the reservoir. To close our water balance we have incorporated a distributary tributary (DT) using the W2 in-built water balance tool. The total contribution of the DT flows is approximately 1.4% of total inflows and precipitation over the eight-year simulation period, although there are seasonal fluctuations. An exception is the winter of 1992/93 where the maximum contribution of DT flows to total inflows under ice reach 22%. This is likely due to uncertainty attributed to error in the withdrawals to the industrial corridor as they are reported on yearly totals. These final year DT flows equate to an approximate 6.5% of BPL volume based on our initial reservoir volume in the DEM (BPL water levels are controlled within a few cm). We aim to assign the DT flows to ungauged inflows and/or outflows once we calibrate the full WQ model - based on our chemical and nutrient data. For this study, we are assuming that constituent

concentrations are primarily introduced in the main river inflows, and that DO and BOD inputs are zero in the DT flows.

We first simulated a simple DO model of BPL with a constant SOD, for comparative purposes. We extended the calibrated temperature model by enabling the WQ variables DO and BOD (BOD as one group) in W2. We proceeded to calibrate the SOD rate as part of a Monte Carlo analyses for several coefficients. We used MATLAB to run W2 for these calibration iterations and attempted to fit the predicted DO to observed DO concentrations. Using a constant SOD we were only able to produce a moderately good fit (Fig. 2.3): with both underestimations and overestimations of DO throughout the simulation period.

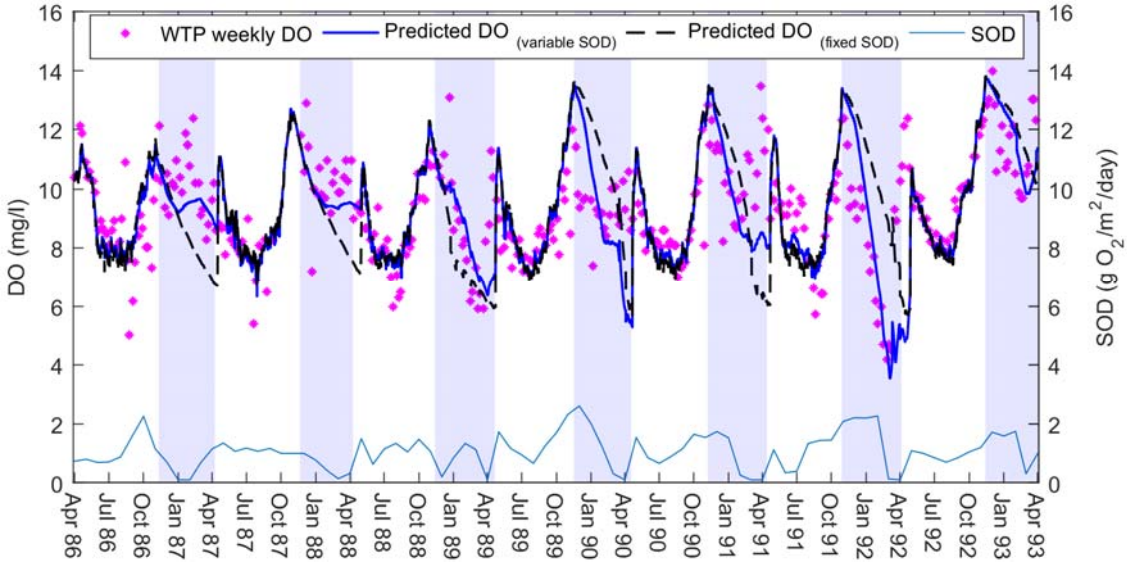


Figure 2.3. The dissolved oxygen (DO) model using variable sediment oxygen demand (SOD) rates found through a semi-automated calibration procedure to match weekly predicted and observed DO concentrations (WTP weekly DO). These SOD rates are maximum values, as used by CE-QUAL-W2. The black line represents the best fit we could achieve by Monte Carlo analyses using a constant SOD rate (root mean square error = 1.94 (to 2 dp); mean absolute error = 1.43 (to 2 dp). Ice cover days shown here in blue stripes are observed data from the Buffalo Pound Water Treatment Plant. Predicted DO concentrations using the variable SOD have root mean square error = 1.58 (to 2 dp); mean absolute error = 1.1 (to 2 dp).

To introduce a variable SOD we took the DO model of Figure 2.3 and implemented a semi-automated calibration through MATLAB. The code attempted to match W2's predicted DO to the observed data by changing the SOD at weekly intervals. We used simple rules: for each weekly period, if the predicted DO concentrations were overestimated then the MATLAB code

increased the SOD to increase consumption. If the predicted DO concentrations were underestimated then the SOD decreased that week. All weeks were changing simultaneously during the iterations and we ran the model until the SOD rates reached a stable condition.

We found that the DO model performed better with the variable SOD rates (Fig. 2.3). On examining the results of this new model, we noted that SOD followed a relatively consistent seasonal trend. SOD was high over summer, peaking towards the end of the season, and then gradually depleting over winter. The rates of SOD were different in magnitude each year, yet similar in behaviour.

We compared the new SOD results against observed in-reservoir water-quality data to look for trends. We noticed that the predicted SOD appeared to follow a similar pattern to the observed weekly summer chlorophyll-a (Chl-a) concentrations (Fig. 2.4) over the first few years: with SOD peaking not long after Chl-a. In light of this, we investigated if any relationships could be found between Chl-a abundance, and SOD. Our aim was to determine if Chl-a might be useful as an alternative measurement for estimating SOD. We approached the open water and under-ice periods differently due to the restriction of ice cover on reaeration. We wanted to maintain the assumption of having limited data with which to build a model, and we aimed for simple strategies.

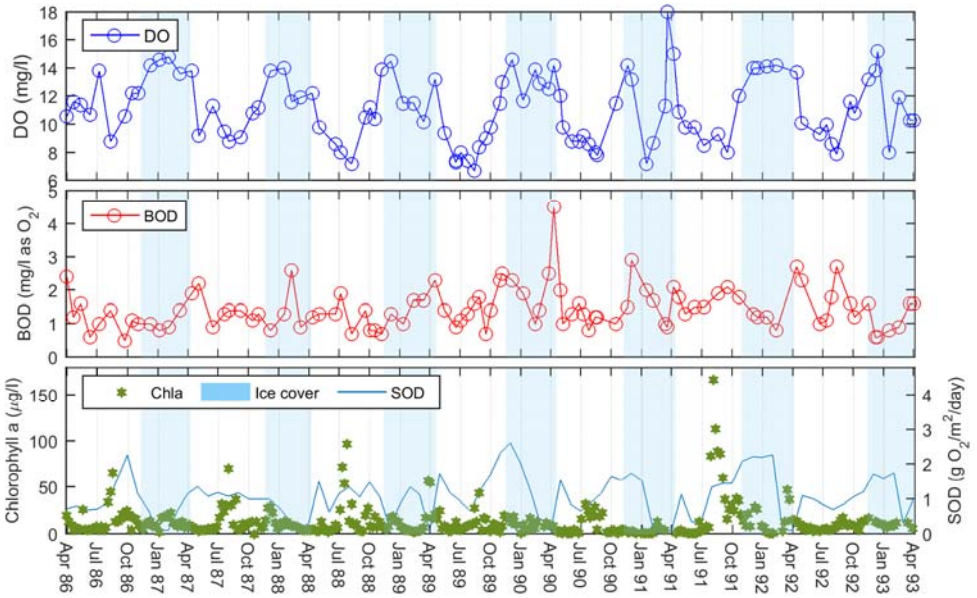


Figure 2.4. Observed dissolved oxygen (DO) and biochemical oxygen demand (BOD) inflow data, and in-reservoir Chlorophyll-a (Chl-a) concentrations in Buffao Pound Lake. The DO and BOD data are monthly measurements at the upstream boundary (BOD as the standard five-day BOD at 20 °C), and the Chl-a data are from the long-term weekly dataset, provided by the Buffalo Pound Water Treatment Plant, at the downstream sample point.

For open water seasons reaeration can replenish oxygen as it consumed, and we elected to keep our SOD constant over these periods. We allowed the model to have interannual variability by using individual SOD rates for each year. We began by averaging each summer variable SOD presented in Figure 2.3. Taking these averages, we found that the lowest and highest seasonal SOD occurred in the respective years of the lowest and highest maximum summer Chl-a concentrations in the reservoir. This made it simpler to assume the two SOD values as being our SOD range. We then used an equation based on these two variables (summer SOD = 0.0042 × max summer Chl-a + 0.9345) to set the remaining summer SOD rates based on the maximum summer Chl-a concentrations each year. By this method, we used the previous summer's maximum Chl-a concentrations as a proxy of the magnitude of biomass production that settled to the bottom sediments by the end of the open water season.

To simulate end of season algal bloom mortality and winter decay we again used MATAB to adjust the SOD rate, so that predicted DO fit to observed DO, from one-month before ice-on occurred until ice-off the following spring. We implemented the same weekly semi-automated calibration process as before, and the SOD rates generally peaked before the ice-on event. Under ice cover W2 automatically stops any gas exchange, and reaeration equals zero. This allows us to imitate a first-order decay rate during this time.

Once we had both the end of season peak SODs and winter SODs we were then able to back-calculate the winter SOD decay rates ($k$) for each year based on Equation (2):

$$\text{SOD} = \text{peak SOD} \times \text{weeks}^{-\text{decay}(k)} \quad (2)$$

Where the predicted winter SOD in W2 is assumed to be a function of the predicted peak SOD, and the number of weeks since the start of ice cover to the decay rate $k$; With $k$ being the unknown in this equation. These back-calculated decay rates were then plotted against summer Chl-a.

## 2.4 Results

### 2.4.1 Dissolved Oxygen Simulation

The final DO model shows good overall results (Fig. 2.5). The predicted DO observations follow the pattern of the observed DO measurements in most years. There is some underestimation

in the winters of 1986/87, 1987/88 and 1992/93. SOD follows a similar trend for each year with an end-of-season peak, and winter decay. The SOD remains high in the winter of 1991/92 due to a greater than average oxygen depletion that year. There is a clear connection in the model between the predicted DO, and the observed ice-on and ice-off dates provided by the WTP.

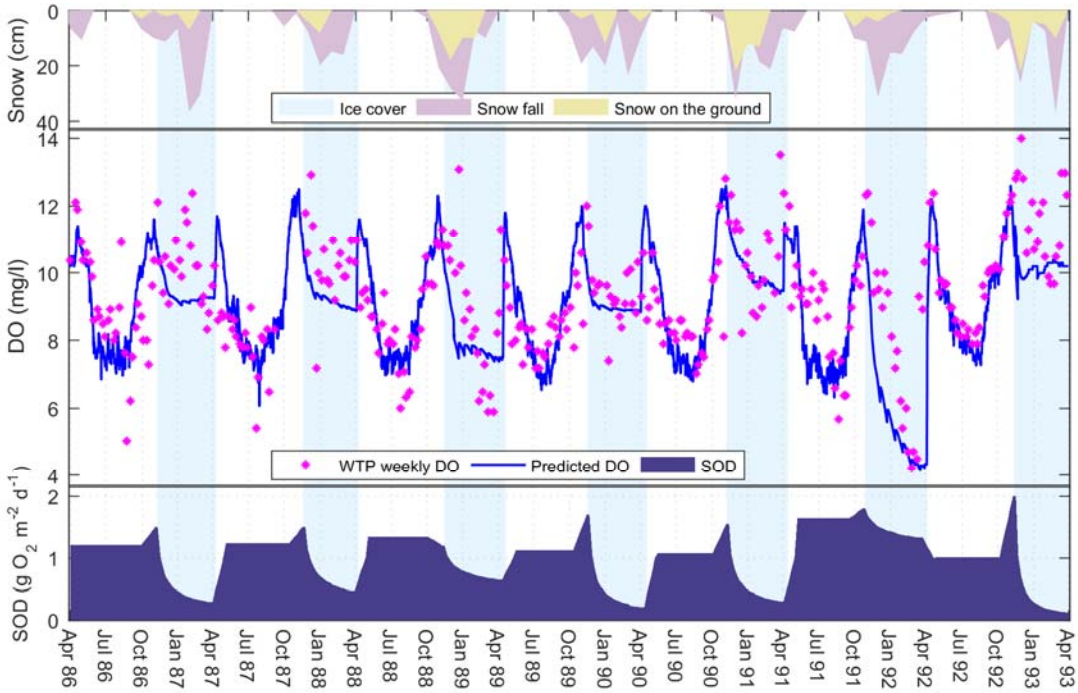


Figure 2.5. Dissolved oxygen (DO) model using summer sediment oxygen demand (SOD) rates based on the maximum summer Chlorophyll-a. The end of season peak and winter decay are found through a semi-automated calibration procedure to match weekly observed DO concentrations (WTP weekly DO). Ice cover days shown here are observed data from the Buffalo Pound Water Treatment Plant, and snow data are from Environment Canada. Snow on the ground is measured on the last day of each month. Predicted DO have root mean square error = 1.47 (to 2 dp); mean absolute error = 1.09 (to 2 dp).

### 2.4.2 Sediment Oxygen Demand Relationships

The late autumn peak SOD does not fit particularly well with the maximum or average summer Chl-a. Interestingly, in comparison with observed data for BPL, the peak SODs appear to have a high correlation ($R^2 = 0.85$) with the average BOD inflows included in our model for the open water period. (Fig. 2.6a). The winter SOD decay rates have a negative, exponential relationship with both the average and maximum summer Chl-a concentrations of the previous summer. The

relationship between SOD decay and the maximum Chl-a (Fig. 2.6b) is slightly stronger at $R^2$ = 0.88 (average Chl-a: $R^2$ = 0.84).

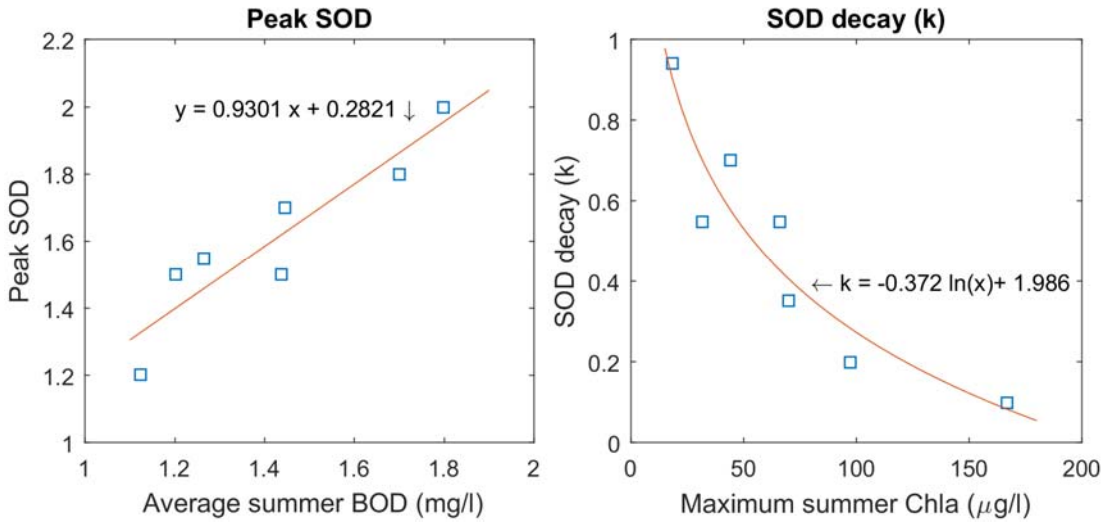


Figure 2.6. Relationships between sediment oxygen demand (SOD) (day-1), and observed Buffalo Pound Lake measurements, after the final dissolved oxygen model simulations: (a) Left: predicted peak SOD and average open-water biochemical oxygen demand inflows ($R^2$ = 0.85); (b) Right: back-calculated winter SOD decay, and observed maximum Chl-a concentrations of the previous summer ($R^2$ = 0.88).

## 2.5 Discussion

A zero-order approach for SOD that treats the demand as an input variable rather than a calculated one does not reflect the conversion of organic matter settling during the simulation (Cross and Summerfelt, 1987). Our original intention was to allow the model to find the changing SOD values through matching to observed DO concentrations. For this, the model was calibrated in MATLAB using a semi-automated iterative process that allowed the model to change the SOD weekly. The resulting SOD values were then to be read by W2 as an input file; this would imitate a first-order compartment, in essence, by varying through the simulation. The model indeed predicted DO concentrations more closely with this variable SOD file than with the W2's original fixed rate option.

Calibrating the SOD with the purpose that the model's DO predictions match with observed DO measurements can be an unsound technique as it assumes that other parameters such as reaeration and settling rates are already well known (Chapra, 1997). This method of calibration

also combines several reservoir processes that contribute to DO into one net value that is assumed to be SOD. While these points suggest that there are limitations to this approach, there remains the problem that few aquatic managers have sufficient data available to run the full diagenesis model. In view of this, we assessed the initial results to see if there were other trends that matched what we know about BPL, and that might suffice as a proxy measurement or explanatory variable.

The reservoir is a highly eutrophic system with high incidences of algal blooms. Deoxygenation can occur after the collapse of a summer algal bloom due to additional bacterial activity (Robarts et al., 2005). In general, the more enriched the system then the higher the rates of productivity and ultimately the greater the oxygen depletion from decomposition (Meding and Jackson, 2003). Chl-a has previously been used as a proxy for estimating in-lake BOD (Fang and Stefan, 2009). Based on this principal, and our knowledge of the reservoir, we are assuming that most of the autochthonous contributions to oxygen demand within BPL are related to algal activity (apart from nitrification and chemical oxygen demand). Any allochthonous inputs to oxygen demand are already included in our BOD time-series data in the inflow constituent file - with the caveat that we are using the W2 default BOD settling rate between upstream and our sample site on the reservoir.

We have found this approach to be successful, as shown in Figure 2.5. The summer SOD rates based on a correlation with the summer Chl-a concentrations act effectively as a substitute to our weekly variable SOD. This suggested link between oxygen depletion and productivity also agrees with our findings relating winter SOD decay to the Chl-a concentrations of the previous summer. This is noticeable in the results for the winters of 1988/89 and 1991/92 where the SOD remains high under ice cover following large summer algal blooms.

In contrast, a result of no correlation between Chl-a and DO consumption is found in other shallow prairie lake sites (Meding and Jackson, 2003). The study in question suggests that the most important predictor of DO consumption is macrophyte biomass due to the large contribution to particulate organic matter (POM). This is found to be also true in sites with abundant phytoplankton, although the authors point out that the algal derived carbon averages 150 times less than the macrophyte derived carbon in their study. In BPL, apart from the top section outside of the model boundary and the downstream end by the dam, the reservoir is not thought to have many macrophytes. This may explain why we are able to find a relationship between summer Chl-a and

winter SOD decay as the macrophyte contribution to POM is not important at the specific study site.

Our winter SOD decay pattern declines in an exponential manner with a rapid reduction at the onset of winter. This theory fits with the suggestion that the first three months of ice cover have the greatest oxygen consumption due to the rapid oxidation of certain organic materials over others, for example (Babin and Prepas, 1985).

The pattern between peak SOD and the average BOD inflows for the open water season is more surprising as we had suspected that the low values of BOD would have little impact in the reservoir. SOD and BOD are, in fact, often combined into one demand known as hypolimnetic oxygen demand (Kirillin et al., 2012). In an ideal model BOD and SOD would be kept separate. Our internal BOD is included with our SOD, as is reaeration. In addition, BOD inflows are based on monthly samples. The result is that we cannot ascertain for certain the relative importance of BOD flowing into the reservoir.

In the winters of 1986/87 and 1987/88, the model under-predicted the DO concentrations. However, in these years, it can be seen that although snowfall was still high in both years, there was little snow left on the ground at the end of each month. It is possible that the reservoir winter albedo is relatively low in these years and light can penetrate the ice to allow photosynthesis to take place. This is evident in the observed winter Chl-a concentrations (Fig. 2.4). This is a winter phenomenon that we are unable to capture in the model as we do not simulate primary productivity, and our SOD equations are founded on summer Chl-a. While snow on the ground is also minimal in the winter of 1991/92, this year is different as the intense summer algal bloom preceding this year results in the DO concentrations falling and the SOD remaining high.

What is interesting in the winter of 1992/93 is that the snow cover is high throughout the winter, suggesting low light availability, and yet DO concentrations are high. On examination of the temperature model (Fig. 2.2), it can be seen that the observed bottom water temperatures are much lower in this year than in previous years. Cold water holds more oxygen than warm water (Wetzel, 2001), and estimating DO inputs based on monthly samples may be missing occasional elevated DO concentrations in cold river inflows during periodic snowmelts. The winter of 1992/93 also has the greatest contribution of the distributary tributary inflows, which indicates that there may be a larger amount of ungauged inflows contributing to the water balance in W2 with no corresponding DO input file.

Another point to consider is that oxygen consumption rates are shown to be temperature dependent with lower consumption rates at lower temperatures (Golosov et al., 2007). Both the summer temperatures of 1992 and winter temperatures of 1992/93 were colder than previous years. This suggests that less heat may be stored in the sediments. The sediment temperature in W2 is a fixed user parameter, and in our model has been set at the average annual air temperature over the simulation period (where temperature >0 °C). The observed sediment temperature may be colder than this average value in the final winter, and, in reality, the sediment oxygen requirements are lower than we are modelling.

An equation for the effect of water temperature on SOD shows how temperature and SOD have a positive relationship with each other: SOD starts to decline more rapidly after temperatures go lower than 10 °C, and reduces towards zero as water temperatures drop below 5 °C (Chapra, 1997). Part of the pattern of SOD changes in BPL will also be a function of bottom water temperature. Our SOD decays rapidly to near zero levels quite early in the colder water temperatures of winter 1992/93. The temperatures in BPL are fairly consistent year-on-year until the summer of 1992, and the winter decreases and summer increases of SOD in response to temperature are expected to be comparable up to this point. This leaves Chl-a explaining the SOD variance between the individual years.

W2 uses four SOD temperature-rate multipliers to adjust the rate of SOD decay as a function of temperature in the model. They are model calibration parameters, and can be helpful in reproducing the changing rate of consumption of DO. We used the default settings in W2 (Table 2.1). The variable SOD values that we include in W2 as an input file are maximum SOD rates - the same as the model format for a constant SOD rate. Figure 2.7 shows the temperature adjusted rates that W2 is actually using during the simulations based on these default calibration parameters. A contributing reason for the end of summer SOD peaks, for example, might be that the rapid decreases in the temperature adjusted SOD are too extreme. The model may potentially increase the maximum SOD to compensate for this temperature effect when calibrating SOD to match the predicted DO with observed DO. We had no data with which to justify changing the default values. Likewise, we did not wish to increase our model uncertainty by expanding the number of parameters with no additional data. We instead chose to adjust just one parameter (SOD) for our purposes.

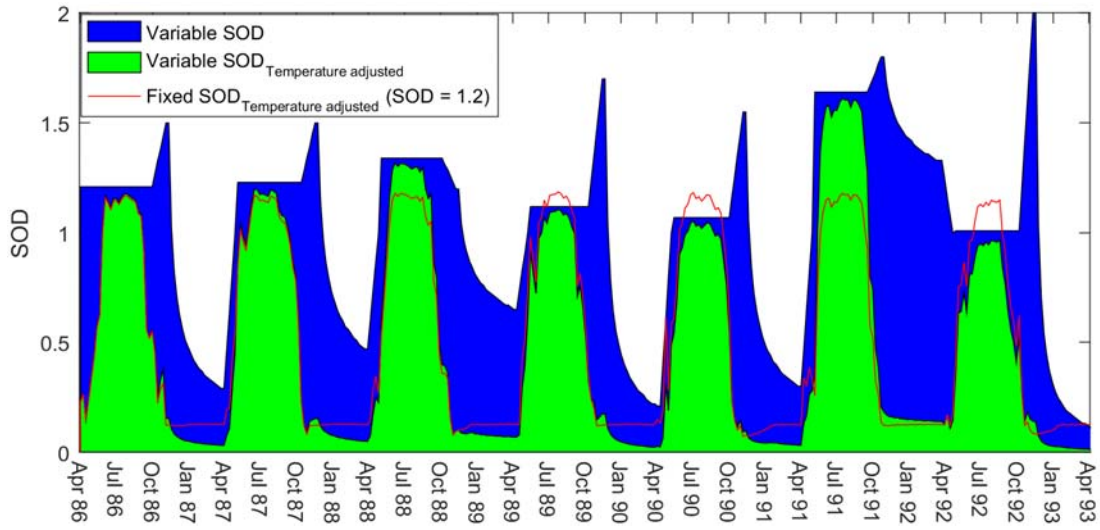


Figure 2.7. A comparison of the maximum sediment oxygen demand (SOD) rates that we input into the model (blue) against the temperature adjusted rates that the model is actually using based on W2 default values for the four temperature-rate multipliers (green). Also shown is the temperature adjusted rates for the fixed SOD simulations.

There are a few differences between SOD found by using MATLAB to vary SOD each week to fit the predicted and observed DO to each other (weekly model - Fig. 2.3), and SOD found through basing the demand on summer Chl-a (final model - Fig. 2.5). The winter decay in the final model agrees well with the drops in SOD in the weekly model except for the winter of 1991/92. In this year, the weekly model drops the SOD to zero when the DO levels are extremely low and then increases SOD as the oxygen levels rise. The behaviour of the final model in this time period is more realistic. The relatively large peak in SOD at the end of this summer may possibly be due to the BOD inputs being higher this year (Fig. 2.4).

In reality, the rapid peaks in SOD shown in Figure 2.5 are also likely a result of our holding the SOD at a constant rate over the summer period. The final model uses average summer rates, and will miss some of the variability that would naturally occur. In the semi-automated calibration of Figure 2.3, we show that when the model uses variable weekly SOD rates there is a general (with some fluctuations) increase over the course of the summer. This agrees with our assumption that SOD in BPL cumulates to a peak due to biota dying towards the end of the season. By holding the model at an average seasonal SOD, instead, we are likely overestimating the SOD in spring, and underestimating the SOD in autumn - if we are to assume that SOD increases as suggested by Figure 2.3. We found that our winter decay relationship with Chl-a was stronger if we allowed

MATLAB to adjust SOD so that the predicted DO fits to the observed DO at the onset of ice-on. In order to achieve this, we had to release the model from the fixed SOD rate at the end of the season - thereby simulating the end of season peak. We chose a one-month period prior to ice-on as a sensitivity analysis showed that this gradient of SOD adjustment gave us the best overall results for summer and winter.

This summer averaging method is responsible for the sudden increase in SOD at ice-off in April. There will be natural processes leading to an increase in SOD (e.g. warmer water, spring blooms, and spring turnover) that will be exaggerated by the need for the SOD to instantly increase to the average summer rate at the start of spring. Other methods may be to allow the model to increase gradually over the whole summer duration, either linearly or exponentially, although we would need to consider some way of verifying the manner in which it increased. Our strategy was to approach the problem as if having little to no data to verify the predicted SOD rates (except using DO data). We decided to constrain the model to using an average summer rate based on a relationship found with Chl-a, and then allow the SOD to decay over winter dependent on a fixed equation. Thus, the aquatic manager would only need to find (and ideally verify) limited points, such as the end of season peak rate, rather than weekly SOD rates.

Figure 2.7 is useful to evaluate the extent to which using a variable SOD function has modified model performance. By constraining the variable SOD over the open water period, the temperature adjusted rates used by W2 were similar in both scenarios when the constrained variable rates were in the region of the estimated average fixed SOD rate. The effort involved in modifying the code and estimating the variable rates are perhaps worthwhile only during periods when actual SOD in a waterbody differs greatly from average (e.g. as modelled in the summer of 1991). In the under-ice periods, however, the benefit of using the variable rate is clearer in Figure 2.7 as the variable rate allows the SOD to decay in the model. This should allow more accurate DO calibration in a full eutrophication model that includes primary productivity.

One limitation to our study is the disconnection between the top and main section of the reservoir. While our inflow constituent file is based on observed data from under Highway 2, and the boundary of our model, the inflows themselves relate to a gauge further upstream on The Upper Qu'Appelle River. It is uncertain at present what effect the top section of the reservoir, the old road, and the 45 m gap under the highway have on our inflow boundary data.

Finally, while our extended W2 ice model is a suitable model for seasonally ice and snow-covered waterbodies, the W2 model has a fixed albedo coefficient through the simulation. The extension to the ice model stops the ice melting too quickly by keeping the snow on the ground, yet does not help with modelling the correct amount of light penetrating the ice. This will make it difficult to calibrate DO, when primary production is added to the model, with just one value for high and low snow years, and different ice structures. This is due to the influence of light on photosynthesis and oxygen production, as indicated in the observed data in the winters of 1986/87 and 1987/88. Our future plans include modifying the ice model further to include a function for a variable albedo. We think that this will be an interesting step to take forward and is a missing link in modelling DO/SOD relationships in ice covered reservoirs.

## 2.5 Conclusions

From the modelling, we show that winter SOD decay is inversely dependent on the previous summer's maximum Chl-a concentrations. The decay rate is faster when less algae are produced. A constant SOD value suffices during the summer half-year; however, a better DO simulation is obtained in winter when the SOD rate decays during the course of the winter. This implies that the biomass supply during winter is limited and much of the draw on DO is diminished by the end of the winter. This result is backed by several field studies. We have shown that for a Prairie shallow reservoir with few macrophytes and BOD inputs variable SOD can be used in a WQ model to represent additional oxygen demand after an algal bloom. The summer SOD and winter SOD decay can be estimated by treating the open water and under-ice period individually in the model. This variable SOD over-time can be estimated for both summer and winter conditions based on summer concentrations of Chl-a. This concept can be widely applied to similar systems that do not have data to support a full diagenesis model, yet would benefit from a more representative estimation of SOD than is provided by a zero-order constant SOD rate.

# PREFACE TO CHAPTER 3

This manuscript was designed to address how water quality (WQ) models may better link under-ice processes with open water dynamics in seasonally ice covered lakes and reservoirs. The influence of ice cover on nutrient concentrations and algal succession is well known in field experiments and theoretical work. WQ models, as yet, are studying summer eutrophication issues, while ice phenology is left to the temperature and mixing models. This means WQ models are not factoring for this ice cover effect in multi-year simulations. Here, a novel modelling approach improves the predictive abilities of CE-QUAL-W2 - one of the few WQ models that includes an ice module. Presented is a method of model calibration that uses a variable albedo rate in the ice equations in place of the model's own fixed value. By this method, the manuscript provides aquatic managers a methodology to model a changing winter heat and light environment in their waterbodies. The model has a number of challenges to overcome that relate to both the study site, and to the modelling of shallow waterbodies – in particular data availability. A monitoring program is proposed that would allow parameterisation of the model. The findings are applicable to waterbodies across the world with similar attributes to Buffalo Pound Lake.

CHAPTER 3

# CHALLENGES OF MODELLING WATER QUALITY IN A SHALLOW PRAIRIE LAKE WITH SEASONAL ICE COVER

Julie A. Terry*, Amir Sadeghian, Helen M. Baulch, Steven C. Chapra, and Karl-Erich Lindenschmidt

* Corresponding author.

https://doi.org/10.1016/j.ecolmodel.2018.06.002

Received 24 February 2018; Received in revised form 4 June 2018; Accepted 5 June 2018

Ecological Modelling 384 (2018) 43–52

0304-3800/ 

Author Contributions

Julie A. Terry, Amir Sadeghian and Karl-Erich Lindenschmidt formulated the experiments. Julie A. Terry set up the Buffalo Pound Lake model, conceived and designed the paper's research question, and directed the methodology to completion. Amir Sadeghian wrote the MATLAB code and adapted CE-QUAL-W2 for variable albedo. Julie A. Terry wrote the bulk of the paper with text inputs and conceptual edits from Karl-Erich Lindenschmidt. All authors proofread and approved the manuscript.

## 3.1 Abstract

The link between under-ice processes and open water eutrophication dynamics has been proven in the field. Water quality models still lack the capability to capture the connection between both environments. The hydrodynamic-ecological model CE-QUAL-W2 is being applied to a

eutrophic drinking water reservoir on the Canadian Prairies as part of larger collaborative research project. CE-QUAL-W2 is one of the few water quality models that includes an ice algorithm, yet is restricted by a fixed albedo coefficient. Field studies have shown albedo to change through the ice cover season – varying the solar radiation that reaches the ice-water interface as a result. In order to better represent the light and heat environment during the under-ice periods we modify the ice algorithm to incorporate a time-variable albedo rate. We find ice-off dates in the model to be sensitive to end-of-season albedo values. While assessing the modified version of CE-QUAL-W2 on the reservoir we encounter a number of challenges during the calibration process. These challenges pertain to difficulties with modelling the under-ice environment, and with modelling shallow lakes and reservoirs. We recommend a targeted monitoring program to supplement available data that will reduce the uncertainty associated with the results of the reservoir model.

## 3.2 Introduction

Buffalo Pound Lake (BPL) is a shallow, eutrophic, impounded natural lake. BPL has a history of water quality (WQ) challenges and algal blooms (e.g. Kehoe et al., 2015, Slater and Blok, 1983). Treatment and processing costs are high for the on-site Buffalo Pound Water Treatment Plant (WTP) due to the need to run degasification systems for supersaturated waters, and frequent problems with unpleasant taste and odour. Of key importance are the winter processes under ice cover (range of 4.5 months to more than 6 months per year over a 39 year period). Salonen et al. (2009) argue that winter should be considered a fundamental part of summer lake functioning, and lake annual succession, stating that a frequent misconception is that biological activities are not important in this period due to low light and cold water. Heterotrophic growth instead provides competitive advantage for heterotrophic and mixotrophic species during ice cover conditions (e.g. Wetzel, 2001). As winter comes to an end, earlier ice off corresponds to earlier increases in water temperature (as incoming heat starts warming waters below after melting the ice), and the earlier light becomes available for phototrophic productivity triggering spring blooms. Algae may grow in an under ice layer (Vehmaa and Salonen, 2009, Kelley, 1997) and within certain forms of lake ice (Leppäranta, 2010) when snow cover is minimal and light can still penetrate. With ice-melt any impurities or algae confined in the different layers of ice will be

released into BPL. Algal succession is therefore influenced by ice cover duration, and winter snowfall quantity (Leppäranta, 2014).

Algal blooms require high water treatment costs for removal, particularly in waterbodies used for drinking water. Nonetheless, the relationship between ice cover and algal dynamics in BPL remains unexplored. Canada has seen a trend in earlier lake ice break-up dates attributed to warming spring air temperatures (Duguay et al., 2006). For the WTP to mitigate against bloom induced water restrictions, and processing costs, incorporating the influence of the under-ice environment into management planning would be beneficial. The growing evidence that lake dynamics during the open water season are connected to winter processes (Hampton et al., 2017, Sommer et al., 2012) suggests it may even be possible to anticipate bloom occurrence on ice-off by monitoring the preceding winter conditions. To do this, winter water temperature, nutrients, ice characteristics, and light penetration estimates would be vital information to collect due to their respective stimuli on phototrophic processes (Bertilsson et al., 2013).

BPL is the focus of a team of researchers investigating how temporal changes within the reservoir affect water chemistry and lead to algal blooms. Part of the objectives include the first application of a coupled hydrodynamic-ecological model to the system for long-term scenario development. This type of model has not been previously applied in Saskatchewan, in part due to a history of very limited monitoring. Traditionally, these more complex coupled WQ models have treated open water and under-ice periods in seasonally frozen waterbodies separately. WQ models have generally been applied to spring/summer eutrophication problems, and any complex winter modelling has tended to focus on hydrodynamics, ice characteristics and temperature. Research that explores the link between the under-ice environment, and spring algae and nutrient dynamics has so far been based around field sampling studies and theoretical discussions. WQ models have yet to capture under-ice chemical and biological feedback mechanisms, and are essentially simulating spring and summer processes without factoring for antecedent winter conditions. This limits the predictive capability of the model somewhat for a multi-year simulation.

In earlier work a dissolved oxygen and sediment oxygen demand model was applied to BPL (see Terry et al., 2017) for a seven-year continuous simulation using CE-QUAL-W2 (W2) (Portland, OR, USA). W2 is a public domain two-dimensional, laterally averaged, hydrodynamic and WQ model suitable for long, narrow waterbodies, and incorporating an ice model component. W2 is a complex model that has been applied to numerous lake systems worldwide (Deliman and

Gerald, 2002, Boegman et al., 2001, Gelda et al., 1998, Martin, 1988), and is capable of investigating the WQ issues and algal bloom dynamics of BPL. Studies on the application of W2 to simulate ice cover, and under-ice processes are much less available.

Although the W2 model includes an ice algorithm of its own to represent ice cover, the inflexibility of the coefficients and the under-laying assumptions of the algorithm mean the under-ice conditions in the model are not representative of the actual waterbody environment. This means model calibration is somewhat of an exercise and limits the accuracy of multi-year simulations. W2, like many WQ models, is set up for more temperate climates than the Canadian Prairies. In Terry et al. (2017) the authors discuss how W2 does not account for snow on top of the ice. Snow depth at BPL is generally between 0.1 to 0.3 m based on 99 snow depth measurements recorded by the Water Security Agency (WSA), for sites across the reservoir, between 1975 and 1996. Ice thickness growth is slowed down by early snow cover as conduction of heat fluxes is reduced due to the low conductivity of snow (Leppäranta, 2015). W2 may over-estimate the ice thickness in years with early snow events. This in turn may delay breakup of ice in the model. On the other hand, ice melting is strongly influenced by surface albedo and snow thickness (Kirillin et al., 2012) and W2 has the potential to simulate earlier breakup dates by absorbing extra solar radiation due to the perceived lack of snow cover.

To test the influence of a variable albedo on ice duration and WQ we develop a full WQ model for BPL. We modify the ice algorithm to include our variable albedo function. A number of challenges present themselves during model setup and calibration; these include difficulties in parameterising the reservoir in W2, and challenges pertaining to BPL reservoir itself. Many of the issues represent difficulties that can be faced when modelling any shallow Prairie lake in Canada. Other issues characterise complications in modelling the WQ of cold polymictic lakes. Here we present our findings. To our current knowledge we are the first to attempt to properly parameterise the ice algorithm of a popular off-the-shelf complex dynamic WQ model to better represent winter under-ice conditions (previous work by Sadeghian, 2015, and Terry, 2017, added two empirical coefficients to fix the ice cover prediction errors). The end objectives of this research are to better understand the factors limiting the ability to reproduce the under-ice environment of BPL in a WQ model, and to make recommendations for future WQ monitoring of the reservoir.

## 3.3 Methods and Model Description

### 3.3.1 Site Description

BPL is situated on the prairies of Saskatchewan, Canada along the Upper Qu'Appelle River System. BPL forms part of a landscape of lakes along a glacially formed (Hammer, 1971) river basin. Residence time is highly variable at approximately 6-36 months (Buffalo Pound Water Administration Board, 2015). The Upper Qu'Appelle drainage basin is primarily agricultural, and the Prairies have a high incidence of soil erosion and nutrient cycling (Meding and Jackson, 2003). The main inflows into BPL, however, are through controlled releases from the upstream Lake Diefenbaker and much of the drainage basin run-off does not find its way to the lake. The Upper Qu'Appelle River channel, between the two reservoirs, is a combination of improved channelized river (35 km) and meandering natural river channel (62 km). Soil type along the channel is mostly fine-grained alluvium (Acharya and Kells, 2005), and the channel suffers erosion, sedimentation and macrophyte growth (Clifton Associates Ltd, 2012).

The climate of the Canadian Prairies is highly variable (Wheater and Gober, 2015). Daily air temperatures range from an average daily low −17.7 °C to an average daily high of +26.2 °C, and approximately 30% of an annual mean precipitation of 365.3mm falls as snowfall (Environment and Climate Change Canada). Of key importance are the winter processes under ice cover (range of 4.5 months to more than 6 months per year over a 39 year period). BPL is a cold polymictic lake that mixes frequently through the open water season.

The morphology of BPL is unique - being a long, narrow reservoir with a relatively high throughflow (Fig. 3.1). The reservoir is essentially split into two waterbodies at the upstream end by Highway 2, which reaches down to the reservoir bed. Inflowing waters are first directed through an opening in a section of the old highway. The flows are then pushed through a 45m wide gap consisting of three connected 15m sections under Highway 2 and into the main body of the reservoir. The upper section of the reservoir is macrophyte bedded and extremely shallow.

With BPL there is the extra complication that the reservoir receives backflows from downstream Moose Jaw River (see Fig. 3.1) when flood waters at the confluence back up the Qu'Appelle River and flow back over the dam into BPL, although this does not occur with a high degree of frequency among years.

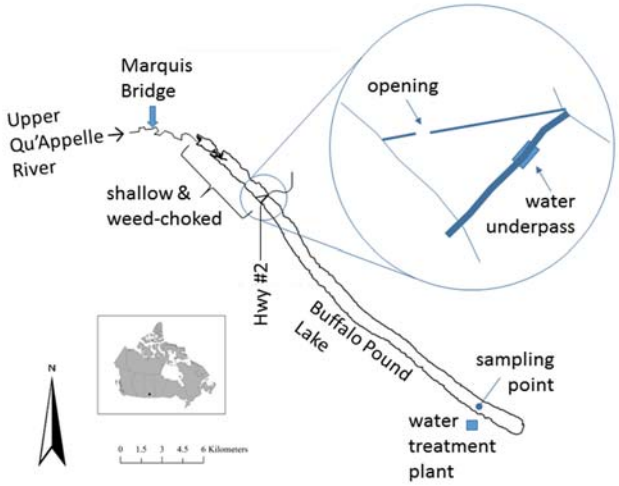


Figure 3.1. Buffalo Pound Lake, Saskatchewan, Canada. The black reservoir outline is to the scale provided. The magnified section illustrates the Highway 2 water underpass and the opening in the old highway. The reservoir has a mean depth of 3.8 m and a maximum depth of 5.98m. Average surface width of the main reservoir body is 890 m.

### 3.3.2 Available data

Gauged daily averaged inflows are provided by Environment and Climate Change Canada (ECCC) for gauge 05JG004 approximately 19 km directly upstream (river sinuosity increases this distance) of the Highway 2 underpass. Inflow temperatures are estimated by regression from long-term historical spot sample data at Marquis Bridge (Fig. 3.1), and weekly in-reservoir temperature measurements (see Terry et al., 2017). Inflow constituent data are from a monthly dataset belonging to the WSA for a site near the Highway 2 underpass. The WSA also provide monthly mean estimates for ungauged inflows. For outflows, dam releases are derived using two downstream ECCC flow gauges. Piped withdrawal volumes are provided by the WTP, and by SaskWater. Daily averaged water level measurements are provided by the WSA for an onsite gauge.

Hourly meteorological data are from an ECCC station located approximately 30 km south of BPL. The hourly data includes a description of the weather condition, which is used to estimate cloud cover based on ECCC guidelines (Environment and Climate Change Canada, 2015). Solar radiation is calculated by the model based on the estimated cloud cover, air temperature (longwave), and W2's computed angle of the sun's inclination (shortwave). Precipitation rates are from a station at BPL and precipitation temperatures are set using dew point temperature.

Historical records of the ice-on and ice-off dates for the reservoir, over a 39-year period, are provided by the WTP.

For the in-reservoir observed data, the WTP have a substantial long-term data set of physicochemical variables and major constituents processed by the onsite laboratory. The data spans between 10-30 years, depending on the parameter, and are sampled weekly throughout the year around 07:20 a.m. Data pass a rigorous quality control sample procedure. The sample site is located approximately four kilometres from the downstream end of the reservoir midway between the north and south shorelines, and approximately one metre off the reservoir bed (Fig. 3.1). Water is withdrawn through an intake pipe to the south shore pumping house, and samples are taken there before the water is drawn into the plant itself. Initial conditions for water temperature and constituents are from this long-term database. Sediment temperature is set as the mean annual air temperature as per W2 recommendations (Cole and Wells, 2016).

### 3.3.3 Model Set-up

Our WQ model is built on the temperature model, presented in Figure 3.2 of Terry et al. (2017), for a continuous seven-year simulation period (1 April 1986–31 March 1993). The simulation period was initially chosen due to the availability of ECCC flow data for gauges just above and below the reservoir. In the earlier work, the temperature model included an extended ice melt equation to account for the lack of snow in W2's own ice model algorithm. We use the default model equations for this current work. We use the same bathymetric map that covers the reservoir downstream of Highway 2. For our WQ model we split the numerical grid into longitudinal segments of approximately 300 m with a total length of 25,834 m for 87 segments. Vertical layer depth is 0.75 m (bounding layers are 0.25 m) with a maximum depth of 10 layers in the reservoir's deepest section. Note that W2's built-in bounding layers and segments are included in these totals.

### 3.3.4 Model Customisation – Ice Model

In W2's ice model, albedo is a user-defined constant rate that forms part of the equation for calculating the amount of solar radiation penetrating the ice (see Cole and Wells, 2016). The absorbance of solar radiation by the ice sheet and the water below it acts as the primary catalyst

for the ice melt process, and melt events are thus strongly dependent on the albedo value (Kirillin et al., 2012). Figure 3.2 illustrates the basic premise of the built-in W2 ice model. In the original W2 ice model the model reads a single albedo value at the onset of the simulation and uses this same value until the end of the run. We have customised the ice algorithm in W2 to read the ice albedo as a time-varying input file. The modified ice algorithm now checks for a new albedo value during each iteration of the simulation. We use W2 version 4.0.

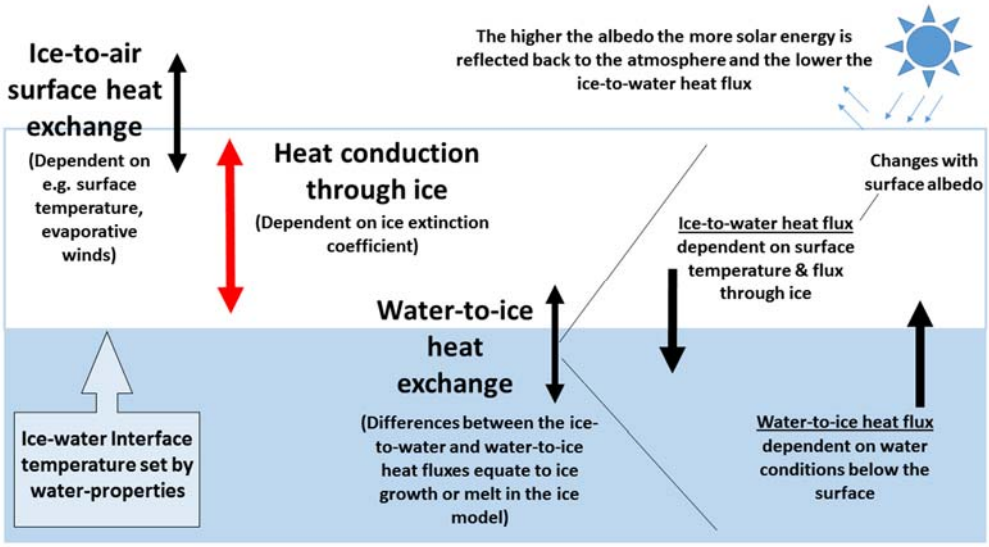


Figure 3.2. Water-to-ice-to-air system in CE-QUAL-W2 ice model calculations.

Solar radiation is used in two ways in the WQ model: solar energy as heat, and solar energy as light. Solar energy as heat is used to heat the water column, and controls the kinetic rates of the WQ constituents. W2 includes a temperature rate multiplier in the equations of each constituent. Solar energy as light is used in the growth equations of algae. W2 uses solar radiation to calculate available light for simulation of photosynthesis, photoinhibition, and light limitation.

## 3.4 Model Calibration

### 3.4.1 Ice Model Calibration

The first step is testing the ice model's sensitivity to changes in albedo rates during the simulation. Albedo rates for lake snow and ice are highly variable and site specific (Svacina et al.,

2014, Semmler et al., 2012, Vavrus et al., 1996). Svacina et al. (2014) find lake ice and snow albedo values progressively increase through winter at three sample sites with different types of snow and ice cover. Each site has a total of 70 albedo measurements over the winter field season, with snowfall events precipitating the greatest increases in value. Based on the authors' findings, for our sensitivity test we randomly generate 100 seven-year time-variable albedo files using MATLAB constraining the starting (i.e. at ice-on) albedo values between 0.25 and 0.55, and ending (at ice-off) albedo values between 0.65 and 0.95. We run 100 simulations, using a different albedo file each time, and plot the difference in days between the predicted and observed ice-on and ice-off dates.

For testing the connection between the ice model and the WQ model, we create an additional, non-randomised, variable albedo file where we control the albedo rates. For the initial simulations we assume an average starting albedo of 0.4, and an ending albedo value of 0.9 for all seven years. We use MATLAB to linearly interpret between the values each winter based on the number of ice cover days for that year. A more detailed year-by-year analysis of albedo rates will be made when the WQ model is fully parameterised.

### 3.4.2 Water Quality Model Calibration

Our model uses five WQ constituents to represent eutrophication in BPL: chlorophyll-a (Chl-a), phosphate ($PO_4$-P), ammonium ($NH_4^+$-N), nitrate ($NO_3$-N) - *modelled as nitrate/nitrite (NOx) in W2* - and dissolved oxygen (DO). Parameter coefficients are set according to known lake processes, literature reviews, or default values recommended in the W2 manual (Table 3.1). The W2 equations for each constituent can be found in the W2 user manual (Cole and Wells, 2016).

Chl-a is calibrated based on three algal groups: A fast growing low temperature group able to take advantage of spring conditions on ice-off (group 1 e.g. diatoms); a fast growing but highly edible group (group 2 e.g. green algae); and a warm temperature adapted summer bloom group (group 3 e.g. cyanobacteria). Algal rates are set as before based on data, literature, or W2 default values (Table 3.2).

For this initial WQ comparison we run three simulations using the same WQ model parameters for everything other than the ice model albedo rates. We first run two simulations using the original W2 ice model with fixed albedo rates of 0.5 and 0.8 respectively. We then run the model again using our modified ice model and the variable albedo file.

Table 3.1 W2 Kinetic coefficients used in the water quality model.

| Coefficient | Description | Default | Value | Units |
|---|---|---|---|---|
| HWI | Coefficient of water-ice heat exchange | 10.0 | 10.0 | W $m^{-2}$ °$C^{-1}$ |
| BETAI | Fraction of solar radiation absorbed in the ice surface | 0.6 | 0.6 | - |
| GAMMAI | Solar radiation extinction coefficient | 0.07 | 0.07 | $m^{-1}$ |
| ICEMIN | Minimum ice thickness before ice formation is allowed | 0.05 | 0.02 | m |
| ICET2 | Temperature above which ice formation is not allowed | 3.0 | 0 | °C |
| TSED | Sediment temperature | - | 10.3 | °C |
| CBHE | Coefficient of bottom heat exchange | 0.3 | 0.3 | W $m^{-2}$ |
| WSC | Wind shelter coefficient | - | 0.9 | °C |
| CHEZY | Bottom friction solution | - | 70.0 | $m^2$ $sec^{-1}$ |
| EXH20 | Light extinction coefficient for pure water | 0.25 | 0.25 | $m^{-1}$ |
| AX | Longitudinal eddy viscosity | 1.0 | 1.0 | $m^2$ $sec^{-1}$ |
| DX | Longitudinal eddy diffusivity | 1.0 | 1.0 | $m^2$ $sec^{-1}$ |
| AZMAX | Maximum value for vertical eddy viscosity | 1.0 | 1.0 | $m^2$ $sec^{-1}$ |
| EXSS | Extinction due to inorganic suspended solids | 0.1 | 0.01 | $m^{-1}/(g\ m^{-3})$ |
| EXOM | Extinction due to organic suspended solids | 0.1 | 0.01 | $m^{-1}/(g\ m^{-3})$ |
| BETA | Fraction of incident solar radiation absorbed at the water surface | 0.45 | 0.55 | - |
| SSS | Suspended solids settling rate | 1.0 | 1.0 | m $day^{-1}$ |
| NH4REL | Sediment release rate of ammonium (fraction of SOD) | 0.001 | 0.001 | - |
| NH4DK | Ammonium decay rate | 0.12 | 0.12 | $day^{-1}$ |
| NO3DK | Nitrate decay rate | 0.03 | 0.1 | $day^{-1}$ |
| NO3S | Denitrification rate from sediments | 0.001 | 0.001 | m $day^{-1}$ |
| SOD | Zero-order sediment oxygen demand | - | 1.2 | g $O_2$ $m^{-2}$ $day^{-1}$ |

Table 3.2 Algal rates used in the water quality model.

| Rate | Description | Default | Group 1 | Group 2 | Group 3 | Units |
|---|---|---|---|---|---|---|
| AG | Maximum algal growth rate (gross production) | 2.0 | 2.5 | 1.0 | 0.9 | $day^{-1}$ |
| AR | Maximum algal respiration rate | 0.04 | 0.04 | 0.04 | 0.04 | $day^{-1}$ |
| AE | Maximum algal excretion rate | 0.04 | 0.04 | 0.04 | 0.04 | $day^{-1}$ |
| AM | Maximum algal mortality rate | 0.1 | 0.1 | 0.15 | 0.1 | $day^{-1}$ |
| AS | Algal settling rate | 0.1 | 0.02 | 0.15 | 0.1 | $day^{-1}$ |
| AHSP | Algal half-saturation for phosphorus limited growth | 0.003 | 0.003 | 0.003 | 0.003 | g $m^{-3}$ |
| AHSN | Algal half-saturation for nitrogen limited growth | 0.014 | 0.014 | 0.014 | 0.010 | g $m^{-3}$ |
| AHSSI | Algal half-saturation for silica limited growth | 0 | 0.003 | 0 | 0 | g $m^{-3}$ |
| ASAT | Light saturation intensity at maximum photosynthetic rate | 100 | 75 | 75 | 75 | W $m^{-2}$ |
| AT1 | Lower temperature for algal growth | 5.0 | 2.0 | 10.0 | 10.0 | °C |
| AT2 | Lower temperature for maximum algal growth | 25.0 | 8.0 | 30.0 | 35.0 | °C |
| AT3 | Upper temperature for maximum algal growth | 35.0 | 15.0 | 35.0 | 40.0 | °C |
| AT4 | Upper temperature for algal growth | 40.0 | 24.0 | 40.0 | 50.0 | °C |
| AK1 | Fraction of algal growth rate at AT1 | 0.1 | 0.01 | 0.01 | 0.01 | - |
| AK2 | Fraction of maximum algal growth rate at AT2 | 0.99 | 0.99 | 0.99 | 0.99 | - |
| AK3 | Fraction of maximum algal growth rate at AT3 | 0.99 | 0.99 | 0.99 | 0.99 | - |
| AK4 | Fraction of algal growth rate at AT4 | 0.1 | 0.1 | 0.1 | 0.1 | - |
| ALGP | Ratio between algal biomass and phosphorus | 0.005 | 0.005 | 0.005 | 0.005 | - |
| ALGN | Ratio between algal biomass and nitrogen | 0.08 | 0.08 | 0.08 | 0.08 | - |
| ALGC | Ratio equivalent between algal biomass and carbon | 0.45 | 0.45 | 0.45 | 0.45 | - |
| ALGSI | Ratio equivalent between algal biomass and silica | 0.18 | 0.18 | 0 | 0 | - |
| ACHLA | Ratio between algal biomass and chlorophyll a | 0.05 | 0.05 | 0.04 | 0.1 | mg algae/µg chla |
| ALPOM | Fraction of algal biomass converted to particulate organic matter on death | 0.8 | 0.8 | 0.8 | 0.8 | - |
| EXA | Algal light extinction | 0.2 | 0.1 | 0.1 | 0.1 | $m^{-1}/(g\ m^{-3})$ |

## 3.5 Results

### 3.5.1 Ice Model Sensitivity Test

We find the simulated ice-on dates to be insensitive to changes in both the starting and ending albedo values. There appears to be no connection between the albedo rates used and the date the model begins simulating ice cover. The lack of dependence of ice-on dates to albedo is found in other lake models (Martynov et al., 2010). The simulated ice-off dates are also found to be insensitive to the starting albedo values with no apparent relationship between the two variables. The ice cover periods at BPL are lengthy, and the influence of the starting albedo on the ice characteristics will be dominated by the time to ice breakup. The simulated ice-off dates, however, are shown to be highly sensitive to the ending albedo value (Fig. 3.3). In both 1986 and 1987 the simulated ice-off date improves at the higher values of our chosen ending albedo range. In 1988 and 1989 an ending albedo in the region of 0.8 simulates an ice-off date closest to the observed ice-off date. What is interesting to see in 1989 is that ice melt in W2 can occur more than 15 days in advance of the actual ice breakup date depending on the albedo value chosen. A degree of instability in the ice model had been noted during calibration runs with ice-on and ice-off dates quite variable during similarly parameterised runs. This instability is the most likely cause of this large change in ice off dates in 1989 rather than the small change in albedo rate.

On examination of the ice equations in W2 we see albedo has no connection to a light extinction coefficient. The coefficient BETAI sets the fraction of light absorbed in the ice surface, and GAMMAI is the light decay through the ice. Using a variable albedo it is only possible to change the heat budget under ice, but not the light environment. To change both heat and light then the three coefficients (albedo, GAMMAI, BETAI) must be calibrated individually within the ice model.

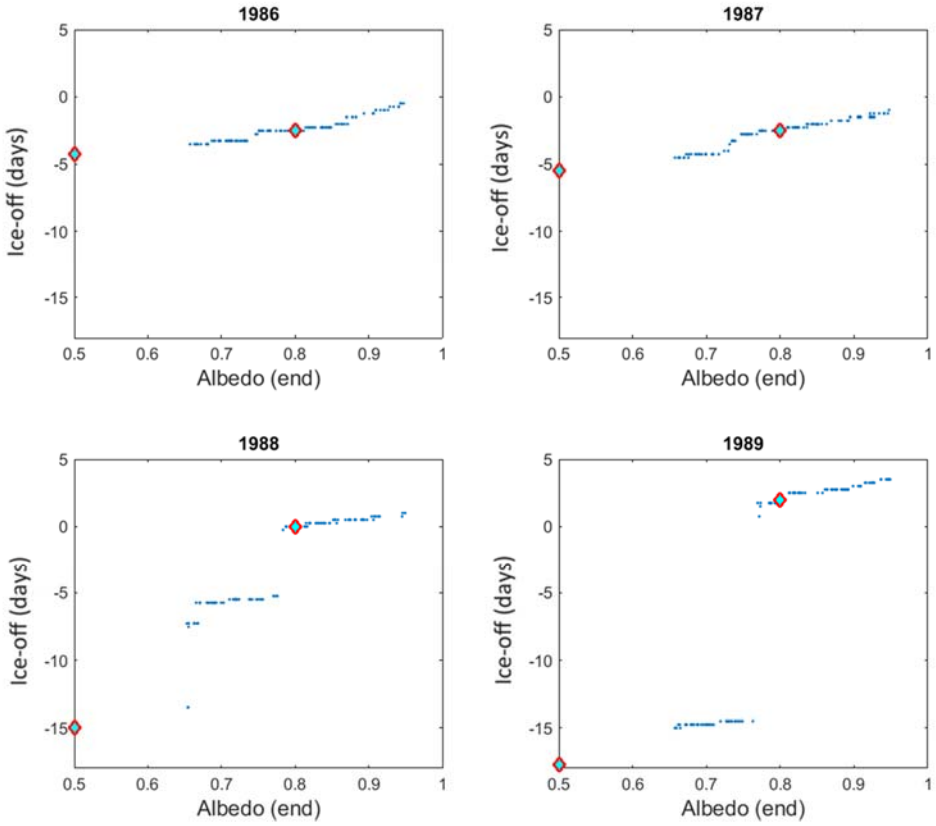


Figure 3.3. Results of the variable sensitivity test. Blue dots represent the difference, in days, between the predicted ice-off dates for each of the 100 runs and the observed ice-off dates (0 on the y axis). The red diamonds indicate the results for two comparative runs with the model's normal fixed albedo algorithm at albedo values of 0.5 and 0.8.

### 3.5.2 Water Quality Simulation

From a visual inspection of the fixed albedo results, the model appears to capture spring and summer increases in Chl-a that would relate to algal blooms in the reservoir (Fig. 3.4). The model predictions for the timing of the blooms, however, are poor with most simulated spring blooms occurring too late in the season. Conversely the model is simulating the summer blooms mostly in advance of the observed dates. Further, the model does not capture variance of bloom size among years.

Switching to the variable albedo ice algorithm delays the timing of the simulated spring blooms. This result is to be expected as the ice thickness is greater with the variable albedo just

before ice-off. Ice-off is also delayed. Unfortunately, as the fixed albedo model is already simulating the spring blooms too late in the season, the variable albedo does not help with the Chl-a calibration. The effect of the variable albedo on the summer bloom predictions is mixed with four of the years showing no apparent difference in results and the remaining three years all responding differently.

$PO_4$-P concentrations are overestimated throughout the year, and neither model captures the 1987 summer peak. Likewise both models miss certain autumn and winter concentrations in $NH_4^+$-N. There appears to be a high degree of sensitivity, or noise, in the $NH_4^+$-N values over summer indicating an issue with the model. $NO_3$-N predictions are within range autumn through spring, but are overestimated before the onset of the summer blooms. Both models are able to capture summer DO dynamics, but not the depletion of oxygen in late winter.

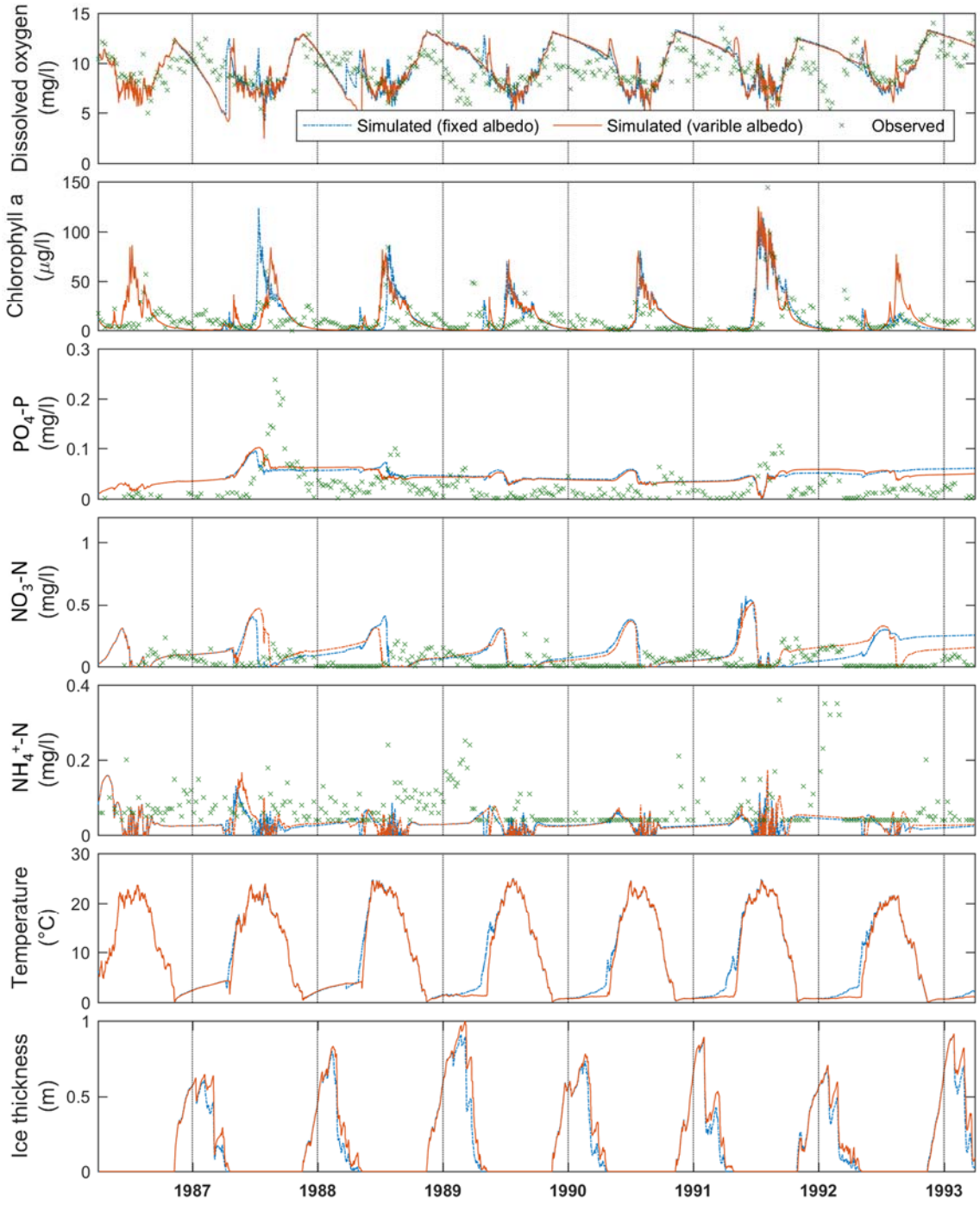


Figure 3.4. Water quality simulation results for Buffalo Pound Lake with a fixed-rate albedo of 0.8, and with a variable albedo that increases through the winter. Date lines indicate 1 January, with the model simulation beginning 1 April 1986.

## 3.6 Discussion

Although the inclusion of a variable albedo rate improves the ice cover duration at our sample location, it seems to have little influence on the main WQ model. In summer, solar radiation is a primary source of thermal energy reaching the water column (Sadeghian et al., 2015). This energy gradually attenuates at depth dependent on the light extinction coefficient, and the temperature rate multipliers in the kinetic equations of the WQ constituents are affected over multiple layers. When ice cover is present the solar radiation is attenuated by the ice extinction coefficient and a much reduced amount of thermal energy reaches the top surface layer of the water column. Much of this thermal energy is then used within the W2 ice-melt equations. The result is that very little changes in the temperature component of the WQ constituent calculations. It would appear no matter how much we change the albedo it will have little impact on the modelled WQ.

As a shallow reservoir on the Canadian Prairies, BPL presents some unique modelling challenges. A great source of uncertainty for the WQ model has been capturing the timing and magnitude of water movement in BPL. We have estimated wind speed on the lake surface by comparing ECCC climate station data with recent buoy data collected in-situ, yet wind direction remains for the station 30 km south as no in-lake data are available. W2 may incorrectly measure fetch in wind-induced motions, such as shear stresses, if the model is given time-series data incorrectly showing wind to be blowing across the width of the lake rather than along the length, for example.

For flows, the inflow gauge is upstream of ungauged tributaries draining into the river channel. In addition we have no data to determine the impact of the shallow upper reservoir section, old highway, and Highway 2 underpass on the flow velocities. As the inflow constituents are measured at Highway 2, which acts as the upstream boundary of our DEM, there is a timing disparity between the inflows and corresponding inflow constituents. Small or shallow lakes have a low buffer for inaccuracies in input data, which makes a WQ model sensitive to small amounts of error.

The Moose Jaw River waters are a poorer quality than BPL and the contributions to constituent concentrations during flood events are challenging to calculate. Based on the two downstream flow gauges, backflows into BPL were calculated on 12 days over the modelled period – reaching a daily average high of 3.14 $m^3/s$ during July 1991. Simple assumptions for WQ variables may be complicated in these wet periods. Shallow lakes also react quickly to changes in

meteorological conditions, and variable weather patterns from year-to-year can increase the complexity of nutrient patterns and productivity (Taranu et al., 2010).

Another sizable source of uncertainty is the WQ boundary data. Inflow constituents are interpolated in W2 from monthly records provided by the WSA. Monthly samples are an extremely coarse frequency for WQ constituents that can fluctuate greatly in just a matter of hours. The performance of a WQ model is restricted by the quality of its input and boundary data (Sadeghian et al., 2018, Hosseini et al., 2017), and W2 has shown poor WQ results due to boundary data limitations previously (Debele et al., 2008, Deliman and Gerald, 2002). Inflow constituents can be interpolated, or stepped, between sample dates in W2, yet neither method will accurately describe the dynamics over our simulation period.

We are also unable to validate our simulated spatial and temporal distribution of constituents due to limited profile data for earlier years. The weekly dataset of the WTP originates from sampling the plant's water withdrawals at the pumping house. The very action of withdrawing a large quantity of water through a pipe close to the reservoir bed may distort the nearby hydrodynamics, and, potentially, the observed constituent data. The intake pipe is approximately 300 m to the sample point in the pumping house (3000 m in total to the WTP) and data may begin to change as water is withdrawn from the reservoir. The segment we are trying to calibrate is therefore a difficult one.

One of the most challenging aspects of modelling shallow lakes is correctly identifying sediment oxygen demand (SOD), and the contribution of internal loading from the sediments to constituent concentrations. Due to their volume to sediment ratios shallow lakes have a relatively strong relationship with bottom decomposition (Chapra, 1997). This is especially true under ice where shallow, productive lakes can become oxygen depleted due to high SOD levels and the lower oxygen carrying capacity of a smaller volume of water. The correct representation of SOD is paramount, and yet data are rarely available to parameterise a comprehensive sediment diagenesis module included in WQ models such as W2 (Mooij et al., 2010). Likewise, internal loading of nutrients can be substantially greater than external sources (Taranu et al., 2010). Our lack of understanding of the lagged response of internal loading in polymictic lakes to changes in external nutrient loads (Taranu et al., 2010) makes shallow lake models susceptible to substantial error when internal loading data are missing.

For BPL, phosphorus internal loading (P-flux) data are available, for the years 2014 and 2015, for three sites in the main reservoir body (D'Silva, 2017). There are no data for other fluxes, such as ammonia. As we have insufficient data to run the sediment diagenesis model, we use the zero-order sediment compartment in our WQ model. In this compartment, W2 calculates internal loading with a user-defined flux coefficient that represents the fraction of the SOD rate that is released under anoxic conditions (coefficient * SOD = flux). As we have no spatial profile data for almost all of our variables the SOD rate we use is the same throughout the model grid. This means W2 would calculate the P-flux as being the same over the reservoir, and when under anoxic conditions. The actual internal loading data show that the P-flux rates vary spatially with the greatest flux occurring approximately two-thirds of the way into the reservoir from the upstream direction. The data also show that the P-flux is high, and occurs in substantial amounts in both summer and winter and in both anoxic and oxic conditions.

Uncertainty stems from assumptions and calculations in the W2 model. W2 uses labile and refractory dissolved organic matter (LDOM and RDOM), and labile and refractory particulate organic matter (LPOM and RPOM) to account for organic phosphorus (P); nitrogen (N); carbon (C); and silica (SI) cycling through the system. The only inflow and in-reservoir data we have available to us is dissolved organic carbon (DOC). If error exists in our conversion of DOC to the DOMs and POMs then that error will be propagated through the model results. Uncertainty and error resulting from using organic matter pools in W2 have been discussed by other authors (Debele et al., 2008). In general, we find our model to be highly sensitive to slight adjustments in algae and nutrient coefficients; the model output tends to rotate between high and low $PO_4$-P, $NO_3$-N, $NH_4^+$-N and Chl-a concentrations as we change parameter values making calibration difficult.

The WTP have collected algal count data since 1996. On review we see that the behaviour of the taxonomic groups can vary considerably from year-to-year. We note that W2's algal productivity equations have no connection with water movement other than the algae settling rates. Algal dynamics are quite unique in shallow well-mixed lakes. Non-motile species can remain suspended in the water column through wind stress turbulence, upwelling and Langmuir circulation, for example (Kelley, 1997). Competitive advantage may then shift between species in respect to nutrients, temperature, light, and water column stability (Yang et al., 2016, Taranu et al., 2012). Non-motile species can still be at the mercy of turbulent vertical mixing that cycles them through the eutrophic zone and dictates their available light for photosynthesis (Jewson et

al., 2009, Folkard et al., 2007); this is also true of some motile species that can only retain their position up to a particular turbulence threshold (Huber et al., 2012). With strong Prairie winds blowing over the surface, and high throughflow, BPL owes part of the observed variability of algae to water movement.

A sizeable challenge is attempting to resolve these uncertainties while modelling up to six-months per year under ice cover. Knowledge of under-ice processes in lakes is still relatively new, and WQ models are often based on open water limnology. The denitrification rate in W2, for example, is corrected with a temperature rate multiplier with default fractions being 1% denitrification at the lower temperature and 99% denitrification at the higher temperature. Recent work on BPL and other Prairie lakes has found that despite large water temperature differences denitrification rates were similar in both summer and under ice as nitrate concentrations represent a primary control of denitrification under ice, and temperature only the secondary control (Cavaliere and Baulch, 2018).

Both ice and snow cover on lakes have a dynamic complex nature with little uniformity on which to estimate the constant coefficient values, such as albedo, that must be specified in W2. Seasonal ice cover shows large variability and may be comprised of a transparent congelation ice (black ice), or white snow-ice (Leppäranta, 2015). Snow may accumulate on top of the ice and be pushed into patchy drifts depending on wind strength and direction. Ice can melt partially in spring forming slush and then refreeze with new melt water into new ice formations. Flooding can occur when ice is pushed under the surface by the weight of snow (when snow thickness>1/3 of ice thickness (Kirillin et al., 2012)). As a further complication, ice breaks up first along the shoreline due to its shallower depth with the released ice then free to move around the lake and break up further as a function of wind and water movements (Leppäranta, 2015). Most WQ models do not have the capacity to parameterise ice dynamics over a multi-year run.

The ice formation and breakup dates provided by the WTP are for the portion of lake directly in front (and thus visible) of the shoreside pumping station. Ice-on is defined to be the date when the visible portion of the reservoir is continuously ice covered, and ice-off the date when half of the visible portion is clear of ice. Total melting in front of the pumping station is rapid with only 1 or 2 days before the visible section of reservoir is clear of ice (Dan Conrad, personal communication). Recent Landsat imagery indicates that this visible area becomes ice free well in advance of the rest of the reservoir. Ice cover could still be seen on most of the reservoir weeks

after the ice-off date provided by the WTP. The observed area is also the location of the WTP intake pipe, and we suggest that the altered hydrodynamics in the immediate surroundings of the pipe are causing the ice cover to melt more rapidly.

## 3.7 Recommendations

Model simulations are greatly influenced by the upstream boundary conditions (Hosseini et al., 2017). To improve water quality modelling predictions, high-frequency WQ sampling is suggested at gauge 05JG004, immediately upstream of the top section of the reservoir, and near Highway 2. Manual flow measurements should be taken at the inflow to the top shallow section of reservoir, and near Highway 2. The combination of WQ and flow data at gauge 05JG004 and top section inflow will provide Upper Qu'Appelle River contributions, and the ungauged inflows and nutrient run-off in the remaining river channel. The WQ and flow data from Highway 2 will act as boundary data and reveal the buffering capacity of the top section of reservoir. Ongoing spot sample flow and constituent measurements are advised at the dam wall when Moose Jaw River waters are back-flowing into BPL. Finally, it is useful to monitor inflowing ephemeral streams around the reservoir perimeter during spring melt to consider nutrient run-off from surrounding agricultural fields.

In addition to boundary data, profile data of the reservoir is needed. It is recommended that a sampling strategy is in place to map the spatial location of constituents in a range of environmental conditions. Ideally one sample location should be close to the current WTP sample site, although outside the influence of the intake pipe, for comparison. Spatial profiling of sediment nitrogen-fluxes, and sediment oxygen demand is particularly encouraged. Other research groups are studying the sediments in greater detail and there is an opportunity for data collaboration between institutions.

Groundwater is not considered to be a significant contribution to the water balance; however, there are several small communities surrounding the reservoir that use septic tanks for domestic waste. The potential for seepage and point-source pollution should be re-evaluated periodically.

In winter, we advise that the WTP make note of ice type (e.g. clear ice, frazzle ice) when they record the ice-on date to assist the ice model parameterisation. Albedo measurements should be taken as often as logistically possible from various locations around the lake, along with snow

depth and ice thickness. The entire reservoir ice formation should ideally be monitored in some form, and not just the visible area in front of the pumping house.

Since 2014 there has been an in-reservoir data collecting buoy in the open-water seasons. The buoy includes a weather station and the relationship between wind direction at the reservoir surface and the ECCC weather station data should become clearer over time. To protect the equipment the buoy is removed from the reservoir during ice cover periods. It would be useful to have a weather station placed on top of the pumping house over winter.

## 3.8 Conclusions

In seasonally ice covered lakes and reservoirs the connection between under-ice processes and spring/summer WQ dynamics is becoming ever more important in response to changing ice phenology. Drinking water reservoirs are particularly at risk as unforeseen WQ troubles can lead to expensive treatment costs and water restrictions. WQ models have yet to successfully model uninterrupted open water and under-ice periods during multi-year simulations. The current 'stopstart' method of summer eutrophication and winter ice modelling leads to inaccurate assumptions during calibration efforts, and models lose predictive capabilities as a result. Yet the solution is not simple. Here, our attempt to improve the ice model of W2 with a variable albedo rate highlights challenges faced when modelling interannual dynamics in a cold-polymictic shallow reservoir. Our work is made the more difficult by the extreme variability in response mechanisms of shallow lakes and reservoirs to eutrophication problems (Scheffer, 2004). Most of the challenges stem from insufficient data to fully parameterise the model during calibration. In conclusion, a targeted monitoring program will go a long way to tackling uncertainty in model results and indicate if the WQ model can be calibrated to Buffalo Pound Lake without further modifications to the ice module code.

# PREFACE TO CHAPTER 4

This manuscript was designed to provide guidance to the Water Security Agency (WSA), the reservoir management agency of Buffalo Pound Lake (BPL), in how best to allocate their monitoring resources to collect the necessary data for developing models and monitoring tools. The existing water quality model of BPL has been difficult to calibrate due to uncertainty in boundary data. This manuscript tests the sensitivity of the model to its boundary conditions to assess which boundary conditions are having the biggest impact in model results. This is the first time such an investigation has been performed on the reservoir. Through sensitivity analyses it is ascertained that the BPL model is influenced primarily by catchment processes and is highly sensitive to changes in inflow discharge in particular. By this method, the manuscript provides the WSA with a plan to collect the most pertinent data for improving water quality modelling of BPL. The methodology is applicable to inland water management agencies across the world.

# CHAPTER 4

# SENSITIVITY OF BOUNDARY DATA IN A SHALLOW PRAIRIE LAKE MODEL

Julie A. Terry and Karl-Erich Lindenschmidt*
* Corresponding author.

Submitted to Canadian Water Resources Journal

Author Contributions

Julie A. Terry and Karl-Erich Lindenschmidt conceived and designed the experiments. Julie A. Terry performed the sensitivity analyses and analysed the results. Julie A. Terry wrote the bulk of the paper with text inputs and conceptual edits from Karl-Erich Lindenschmidt. Both authors proofread and approved the manuscript.

## 4.1 Abstract

A good predictive water quality model needs sufficient data to characterise the waterbody, yet monitoring resources are often limited. Inadequate boundary data often contribute to model uncertainty and error. In these situations, the same water quality model can also be used to determine where sampling efforts are best concentrated for improving model reliability. A sensitivity analysis using a one-factor-at-a-time approach on a shallow, eutrophic, impounded Prairie lake model investigates which boundary conditions are contributing most to variability in the model. The results show the lake model has greater sensitivity to its modelled catchment processes than to its modelled in-lake processes. Flows are shown to have the greatest influence on model predictions for all water quality variables tested, followed by air temperature. The lake is facing pressure from climate change, and future water management strategy. Results indicate an

accurate water balance will be a crucial factor in future monitoring programs and modelling efforts of the lake's management agencies.

## 4.2 Introduction

Water quality (WQ) models are increasingly directing management decisions for maintaining lakes and reservoirs (referred to as simply lakes from here on). Over 100 surface WQ models are now available (Wang et al., 2013). The result is that there is a wide range of models that can be applied to almost any surface waterbody, and numerous ways to meet modelling objectives.

WQ models are largely used as prediction tools. One of the WQ issues being investigated through modelling is eutrophication (over enrichment). Eutrophication is an increasing problem worldwide - a detrimental consequence of increasing human pressure on lakes (Wetzel, 2001). Simple static steady-state, and regression models have been widely used by lake managers since the 1970s to study eutrophication (Mooij et al., 2010). These simple models are easy to use and relatively quick to provide answers. Their disadvantage is they often fall short of capturing lake dynamics that differ from a general pattern (Mooij et al., 2010). Eutrophication is a complex problem that is closely connected with environmental conditions, lake morphology, and ongoing lake processes. A static model that is time-invariant and calculates a system in equilibrium would unlikely capture all key processes simultaneously.

Model choice must consider the question being asked. Static models use general relationships and can be used for initial assessment of a lake's trophic status, for example. They can point you in the direction of which processes may dominate in a waterbody. Dynamic models are designed to describe changes through time. Dynamic models use mathematical formula to simulate the physical behaviour of a system over time and space (Shoemaker et al., 2005). Dynamic models have greater spatial and temporal resolution than static models and greater flexibility in their application. Unfortunately, there is a trade-off between the maximum complexity of a model, the data available to parameterise the model, and the uncertainty a model can manage before it becomes unreliable (Chapra, 1997). When evaluating model output, uncertainty in the parameter settings and values used during model calibration, uncertainty in

boundary input data and initial values, and uncertainty due to model structure are essential considerations (Lindenschmidt et al., 2007).

This paper focusses on the second source of uncertainty: that arising from unknowns in boundary input data and initial values. A good WQ modelling effort requires sufficient data to adequately characterise the limnology of a waterbody (Cole and Wells, 2016). This includes in-pool data under a range of environmental conditions, and high-frequency time-varying boundary data covering the modelled period (Cole and Wells, 2016). In reality, monitoring resources are often limited (Reckhow, 1999), and financial, temporal, and logistical constraints are placed on sampling frequency and number of variables monitored. WQ models can be built using data recorded only monthly or less frequently. Yet observations show that boundary physical, chemical, and biological processes can fluctuate within hours (Sadeghian et al., 2018). Data used as time-varying boundary conditions for driving the model needs to be as accurate as possible (Cole and Wells, 2016). In one lake study model simulation RMSE error was consistently greater in WQ variables with only coarse field measurements (Sadeghian et al., 2018).

As well as being a scenario tool, a WQ model can also be used to explore where sampling efforts are best concentrated when monitoring resources are limited. A sensitivity analysis can investigate the most influential WQ variables through assessing the sensitivity of model output to a change in model input values. Several sensitivity analyses noted from the literature for lakes use a 'one-factor-at-a-time' (OAT) approach (Hosseini et al., 2017, Singleton et al., 2013, Knightes et al., 2009). OAT is a method where uncertain factors are changed one-by-one in the model while the others are kept constant (Saltelli and Annoni, 2010). In example, Knightes et al. (2009) established through OAT analyses that a shallow lake's response to a reduction in atmospheric mercury deposition was highly sensitive to changes in sediment burial rates and active sediment layer depth. Their second site, a catchment-dominated shallow farm pond, had little sensitivity to these same sediment parameters – being driven entirely by catchment processes.

Shallow lakes are particularly challenging for WQ modelling - being highly sensitive to small amounts of error from input data inaccuracies (Terry et al., 2018). One such lake is Buffalo Pound Lake (BPL) in Saskatchewan, Canada. An impounded natural prairie lake, BPL supplies the water needs of approximately 25% of the provincial population (Kehoe et al., 2015). Plagued by algal blooms the lake necessitates ongoing expensive treatment costs for the onsite Buffalo Pound Water Treatment Plant (WTP). Water shortages have occurred as a result of treatment

processes slowed by WQ issues. The lake is the focus of a research group developing models and monitoring tools to investigate conditions leading to harmful algal blooms. One objective of the research is to inform the strategic planning of the WTP, and provide critical information to the Water Security Agency (WSA) who manage flows to and from the lake.

An application of the CE-QUAL-W2 (W2) WQ model to the lake has been difficult to calibrate due to notable challenges and uncertainty in the model's boundary data (see Terry et al., 2018). Recommendations for improving the model are to strengthen the available data (see Terry et al., 2018). This study extends the work of Terry et al. (2018) and uses OAT sensitivity analyses to ascertain which boundary conditions are contributing most to variability in model output. This will provide recommended insight into where the WTP and WSA should concentrate their WQ monitoring resources for improved WQ modelling.

## 4.3 Materials and Methods

### 4.3.1 Site Description

BPL is a shallow (mean depth 3.8 m, maximum depth 5.98 m) impounded natural lake on the Upper Qu'Appelle River system. Annual mean precipitation is 365.3 mm with most rainfall occurring between May-July (~61%), and ~30% of precipitation falling as snowfall (Environment and Climate Change Canada). Ice cover is from November to late April (Hall et al., 1999, Hammer, 1971). The lake is wind-driven and mixes frequently through the open water season. Brief thermal stratification events and microstratification can occur (Baulch et. al., 2018, personal communication). Air temperatures range between an average daily minimum of -17.7°C (daily average -12.3°C) in January to an average daily maximum of 26.2°C (daily average 19.3°C) in July (Environment and Climate Change Canada).

Flows from the upstream Lake Diefenbaker (LDief) are released by the WSA to maintain water levels in BPL with an annual fluctuation in the lake of less than 0.25 m. The upper 35 km of the river reach between LDief and BPL is constructed channel, with the 62 km lower reach being natural channel. Two main tributaries and many smaller creeks join along the 97 km stretch (Fig. 4.1a). Highway 2 cuts through the lake at the upstream end (Fig. 4.1b). The highway is constructed on the lake bed, and essentially splits BPL into two waterbodies. Inflows first pass through an

opening in the old highway before passing under the bridge at Highway 2 with a 45 m inflow gap made up of three 15 m widths divided by pillars.

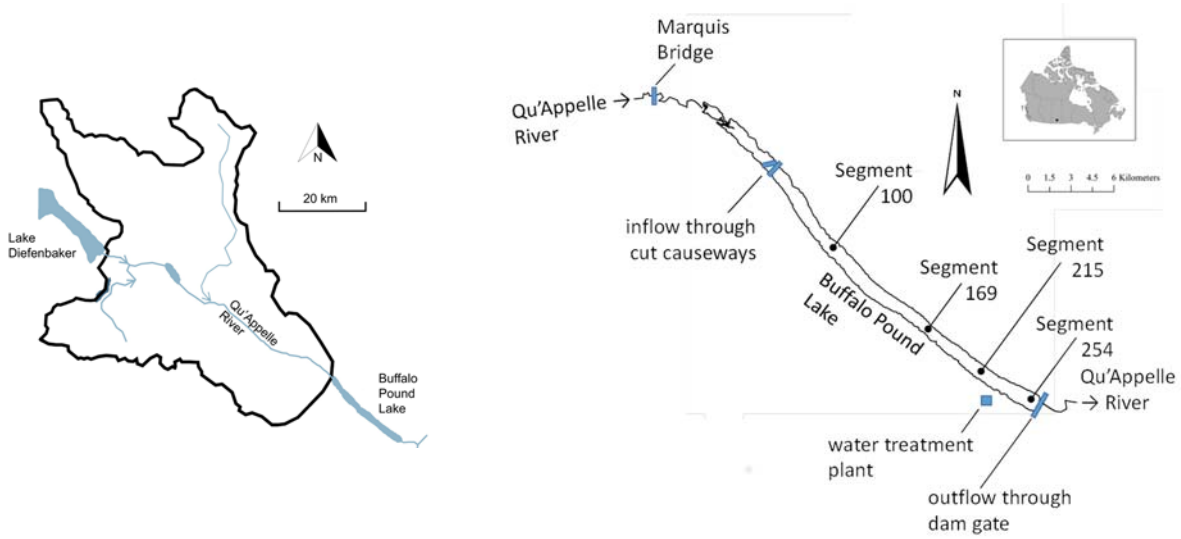


Figure 4.1. 4.1a (left): Upper Qu'Appelle catchment area for Buffalo Pound Lake. 4.1b (right): Buffalo Pound Lake, Saskatchewan, Canada. The black lake outline is to the scale provided. The lake has a mean depth of 3.8 m and a maximum depth of 5.98 m. Average surface width of the main lake body is 890 m. The black dots indicate the locations of the segments selected for model output.

## 4.4 Model Set-up

### 4.4.1 Model Description and Data

W2 is a two-dimensional coupled hydrodynamic and WQ model. W2 is a complex dynamic model suitable for rivers, estuaries, lakes, and reservoirs (Cole and Wells, 2016). Several branches and tributaries can be added to a waterbody, and waterbodies can be linked together in one simulation. W2 can be linked with catchment models such as SWAT (e.g. White et al., 2010, Debele et al., 2008). The longitudinal segments and vertical layers are user defined, and can be variable throughout the grid. The most recent versions of the model (V4 -V4.2) now incorporate an internal sediment diagenesis module.

W2 is considered a capable hydrodynamic and transport model. Various options exist for inflow placement, both longitudinally and vertically. Several types of inflow (including

precipitation) can be specified each with their own temperature and constituent file. Numerous hydraulic structures and withdrawals can be placed throughout the grid, and there are a variety of turbulence schemes from which to choose. The model's numerical scheme allows for direct coupling between the hydrodynamic and WQ processes and W2 uses the same time step and spatial grid (Zhang et al., 2015).

The simulation period covered seven consecutive years (1 April 1986 – 31 March 1993) that led up to the discontinuation of Environment and Climate Change Canada flow gauges just above and below the lake. The seven years covered a relatively dry period that was both preceded and followed by flood event years. Mean monthly summer (June-August) air temperatures ranged from 20.8°C (1988) to 16.5°C (1992). Mean monthly winter air temperatures (November-February) ranged from -3.6°C (1987) to -10.7°C (1989). Available input data frequency ranged from hourly meteorological data to monthly (or less) inflow constituent data sampled at Highway 2 (Fig. 4.1b). Observed in-lake constituent data were provided weekly from a laboratory analyses at the WTP. Inflows were daily averages measured at gauge 05JG004 upstream of BPL. For a full description of data sources and calculations see Terry et al. (2018).

Parameter coefficients were set as per Terry et al. (2018) according to known lake processes, literature reviews, or default values recommended in the W2 manual (Table 4.1). Equations for each constituent can be found in the W2 user manual (Cole and Wells, 2016) and are too numerous to provide here. As per Terry et al. (2018) the zero-order sediment model was used, and the variable-albedo function was added to the W2 ice model to improve ice coverage. The BPL model grid had a total of 256 segments of approximately 100 m longitude each and equalling 25,834 m in total. Vertical layers were 0.75 m in height with the deepest segment of the lake having 10 layers plus two 0.25 m boundary layers used by the W2 model.

Table 4.1 Main kinetic coefficients used in the water quality model. Additional kinetic and algal coefficients are listed in Terry et al (2018).

| Coefficient | Description | Default | Value | Units |
|---|---|---|---|---|
| TSED | Sediment temperature | - | 10.3 | °C |
| CBHE | Coefficient of bottom heat exchange | 0.3 | 0.3 | W $m^{-2}$ |
| SOD | Zero-order sediment oxygen demand | - | 1.2 | g $O_2$ $m^{-2}$ $day^{-1}$ |
| PO4R | Sediment release rate of phosphorus (fraction of SOD) | 0.001 | 0.001 | |
| NH4REL | Sediment release rate of ammonium (fraction of SOD) | 0.001 | 0.001 | - |
| NH4DK | Ammonium decay rate | 0.12 | 0.12 | $day^{-1}$ |
| NO3DK | Nitrate decay rate | 0.03 | 0.1 | $day^{-1}$ |
| NO3S | Denitrification rate from sediments | 0.001 | 0.001 | m $day^{-1}$ |
| SSS | Suspended solids settling rate | 1.0 | 1.0 | m $day^{-1}$ |
| EXSS | Extinction due to inorganic suspended solids | 0.1 | 0.01 | $m^{-1}/(g\ m^{-3})$ |
| EXOM | Extinction due to organic suspended solids | 0.1 | 0.01 | $m^{-1}/(g\ m^{-3})$ |
| EXH20 | Light extinction coefficient for pure water | 0.25 | 0.25 | $m^{-1}$ |
| BETA | Fraction of incident solar radiation absorbed at the water surface | 0.45 | 0.55 | - |
| WSC | Wind shelter coefficient | - | 0.9 | °C |
| HWI | Coefficient of water-ice heat exchange | 10.0 | 10.0 | W $m^{-2}$ $°C^{-1}$ |
| BETAI | Fraction of solar radiation absorbed in the ice surface | 0.6 | 0.6 | - |
| GAMMAI | Solar radiation extinction coefficient | 0.07 | 0.07 | $m^{-1}$ |
| ICEMIN | Minimum ice thickness before ice formation is allowed | 0.05 | 0.02 | m |
| ICET2 | Temperature above which ice formation is not allowed | 3.0 | 0 | °C |
| | **Algal Coefficients** | **Group 1** | **Group 2** | **Group 3** |
| AG | Maximum algal growth rate, day-1 | 2.5 | 1.0 | 0.9 |
| AM | Maximum algal mortality rate, day-1 | 0.1 | 0.15 | 0.1 |
| AS | Algal settling rate, m day-1 | 0.02 | 0.15 | 0.1 |
| AHSP | Algal half-saturation for phosphorus limited growth, g m-3 | 0.003 | 0.003 | 0.003 |
| AHSN | Algal half-saturation for nitrogen limited growth, g m-3 | 0.014 | 0.014 | 0.010 |
| AT1 | Lower temperature for algal growth, °C | 2.0 | 10.0 | 10.0 |
| AT2 | Lower temperature for maximum algal growth, °C | 8.0 | 30.0 | 35.0 |
| AT3 | Upper temperature for maximum algal growth, °C | 15.0 | 35.0 | 40.0 |
| AT4 | Upper temperature for algal growth, °C | 24.0 | 40.0 | 50.0 |
| ACHLA | Ratio between algal biomass and chlorophyll a in terms of mg algae/µg chl a | 0.05 | 0.04 | 0.1 |

### 4.4.2 Sensitivity Analysis

To determine the boundary conditions that most influence model output, a local sensitivity analysis was performed using the OAT approach. With this method each boundary condition was perturbed once, by a certain amount, while holding the rest of the model constant. The new model output was then compared with the original simulation results (the base model), and the total variance for each variable was quantified using root mean square error (*rmse*). The variables tested were chlorophyll-a (Chl-a), dissolved oxygen (DO), ammonium ($NH_4^+$-N), nitrate ($NO_3$-N) – simulated in W2 as nitrate/nitrite (NOx) - and phosphate ($PO_4$-P). The boundary conditions

investigated are listed in Table 4.2 and thought to be the most influential factors for BPL based on knowledge of the lake and calibration of the existing WQ model of Terry et al. (2018). Equal perturbation was applied to each boundary condition for comparability in the sensitivity output. A 10% increase was chosen as the experimental value as being within the realm of realistic variability while being sufficient perturbation to elicit a response. W2 considers each model grid cell individually when solving the water balance equations. Once the water balance is calibrated it is then difficult to decrease inflow discharge without recalibration of the outflows. If this is not done then the upstream cells can be left with insufficient volume. This returns an error code and terminates the simulation. The sensitivity analysis was restricted to testing a 10% one-directional sensitivity assessment (positive perturbation) only so that this recalibration step was not required for the one inflow scenario, and all scenarios were then tested using the same criteria.

Table 4.2 Boundary conditions perturbed during the sensitivity analysis. Each boundary condition was tested by increasing the model input values (time-series or model parameter) by 10% while holding the remaining boundary conditions and parameters constant.

| **Boundary Condition** | **Perturbation** |
|---|---|
| Air temperature | Increase by 10% |
| Inflows | Increase by 10% |
| Inflow constituent concentrations | Increase by 10% |
| Inflow water temperature | Increase by 10% |
| Opening balances (all constituents) | Increase by 10% |
| $PO_4$-P & $NH_4^+$-N sediment release (as a fraction of SOD) | Increase by 10% |
| SOD | Increase by 10% |
| Wind speed | Increase by 10% |

Air temperature, inflow discharge, inflow constituent concentrations, inflow water temperature, and wind speed were subject to a 10% increase in the time series data in W2 boundary input files. These represent the external forces on the lake driven by the catchment (wind speed being part of the catchment's climate). All air temperatures were perturbed in the positive direction meaning negative winter air temperatures became 10% warmer. In general, the absolute Kelvin scale should be used when calculating a percentage increase for temperature due to the Fahrenheit and Celsius scales having an arbitrary zero point. However, the W2 model requires air temperature to be entered as degrees Celsius in the meteorology time-series file. As the objective was to test the model response to each boundary condition in a comparable manner, we chose to apply the percentage increase to the Celsius scale rather than use a fixed interval increase. This is not entirely

appropriate to treat temperature in degrees Celsius as a continuous variable. It is recognised that this may introduce some uncertainty into results of the relative influence of air temperature. As 10% of 0°C is not possible, instances of 0°C were assigned the new air temperature of 0.1°C. The influence of this on the analysis is considered minor as these values represented <0.4% of the hourly air temperature measurements. Inflow temperatures were treated in the same manner as air temperature with 0°C representing <0.9% of the weekly inflow temperature measurements. Inflow constituents included in the W2 model of BPL were $PO_4$-P, $NH_4^+$-N, $NO_3$-N, DO, dissolved silica, four organic matter groups (labile and refractory dissolved, and labile and refractory particulate), and three algal groups (diatoms, green algae, cyanobacteria). Note that W2 uses organic matter as a means to account for organic phosphorus, nitrogen, carbon, and silica cycling through the system. This analysis considers the first four inflow constituents listed above plus Chl-a.

The in-lake boundary conditions are represented by the opening balances (the initial constituent concentrations specified in the model at the start of the simulation), the fluxes of $PO_4$-P and $NH_4^+$-N from the sediment bed, and the specified SOD rate. The fluxes for $PO_4$-P and $NH_4^+$-N are entered in W2 by the user as the sediment release rate under anoxic conditions as a fraction of SOD, and modified by the SOD temperature multiplier (Cole and Wells, 2016). When W2 is predicting anoxia then the flux becomes the (SOD rate) * (sediment release rate) in units of $g/m^2$/day. For a detailed description of how the model uses SOD, and the SOD temperature multiplier see Terry et al. (2017). In the sensitivity analysis the sediment release rate was increased by 10%, and the SOD rate increased by 10% as two separate tests. Four segments (100, 169, 214, and 254) are chosen for output comparison based on availability of field data for comparison. Segment numbering runs from upstream to downstream with segment 100 being approximately 10 kms from the upstream boundary (see previous section).

## 4.5 Results

### 4.5.1 Base Model

Figure 4.2 presents the base model results for the five variables considered for four segments spaced along the lake. The mid-depth layers are compared for each segment for Chl-a, $NH_4^+$-N and $NO_3$-N and the bottom layers are compared for each segment for DO and $PO_4$-P.

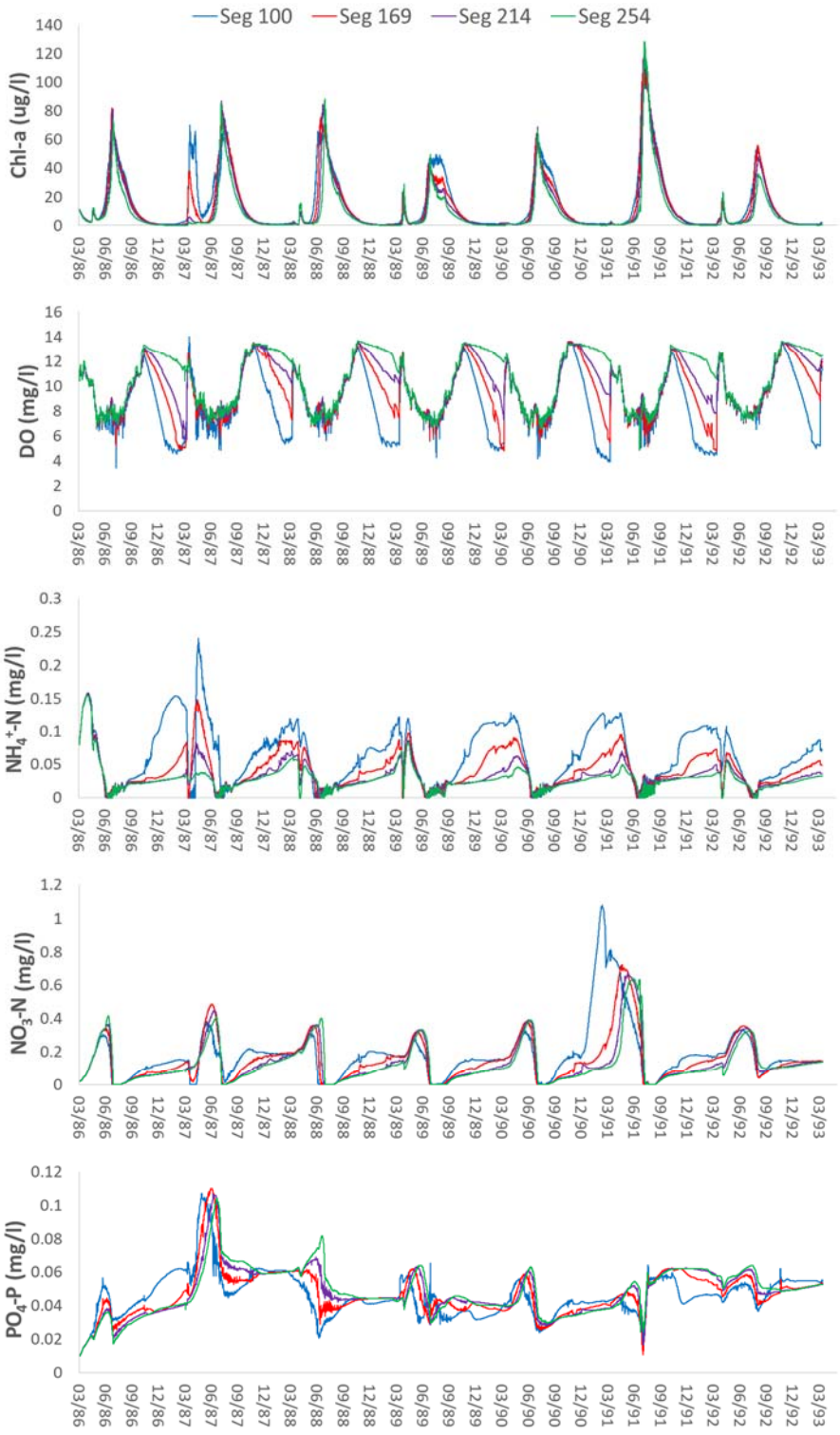


Figure 4.2. Base model simulation results. Output is for four segments (100, 169, 214, and 254) at mid-depth for chlorophyll-a (Chl-a), ammonium ($NH_4^+$-N), and nitrate ($NO_3$-N), and near the bottom for dissolved oxygen (DO), and phosphate ($PO_4$-P).

Modelled Chl-a concentrations generally decrease in the flow direction with greatest variation occurring in the year when Chl-a concentrations are at their lowest in the lake overall. DO concentrations are generally modelled to be the same throughout the lake during the open-water season, although there is a marked gradient from low to higher concentrations in the flow direction during winter. At all segments, DO decreases during the winter due to the oxygen demand imposed by the sediments and the lack of reaeration due to the ice cover capping the lake. Allochthonous inputs of organic material at the upstream boundary settle faster in winter due to the lack of wind induced resuspension of sediments. The oxygen demand gradient for decomposition of allochthonous material decreases in the direction of flow. This helps explain the opposite behaviour of the DO gradient. In addition, W2 simulates a dynamic ice cover, and predicts occasional breaks in the ice at various segments along the lake allowing reaeration and possible photosynthesis to be simulated.

Dissolved nutrients are generally at their lowest concentration during the summer peaks when algal activity is at its maximum (highest Cha-l concentrations). However, there is a strong decreasing gradient in the flow direction for the nitrogenous nutrient components under ice covered conditions which persists into spring. Particularly during the 1990/1991 winter, $NO_3$-N concentrations become particularly high in the upstream portion of the lake. This result is attributed to a large outlier in the inflow $NO_3$-N constituent data leading to substantially high loading over a two-month period. Spring phytoplankton prefer $NH_4^+$-N uptake over $NO_3$-N, and $NH_4^+$-N is depleted before $NO_3$-N in summer. Low nitrogen can result in the nitrogen fixing cyanobacteria outcompeting other species, and the resulting cyanobacterial blooms draw on substantial amounts of phosphorus as seen in the decreasing $PO_4$-P concentration in late summer. $PO_4$-P concentrations in the lake replenish again during winter when algal growth is minimum and a $PO_4$-P flux is still present. An exception occurs during the spring of 1987 where high $PO_4$-P values are simulated after the ice cover breakup. Observed data from the WTP indicates the real $PO_4$-P peak to be greater than our model predictions due to unusually high loading this year.

### 4.5.2 Sensitivity Analysis Scenarios

The *rmse* values of the differences between the perturbed *Op* and base run *Ob* output can be used as a sensitivity measure when comparing the impact of the boundary condition changes on each constituent individually. These impacts were summarised by first summing all of the

squared daily differences over the course of the simulation time domain, dividing by the total number of simulation days, *n*, and then taking the square root of that value (equation 4.1).

$$rmse = \sqrt{\frac{\sum_{i=1}^{n}(O_p - O_b)^2}{n}} \quad (4.1)$$

The sensitivities of the simulated variables to each of the eight boundary condition scenarios are visualised in Figure 4.3. The different levels of shading refer to the size of the *rmse* value relative to the other *rmse* values for the same variable, and are scaled in rows. Darker shades indicating a greater sensitivity to the change in boundary conditions.

All five variables are most sensitive to inflow discharge in all four segments. Chl-a *rmse* values range from 8.1 for inflow discharge to 1.87 for SOD, and DO *rmse* values range from 0.74 for inflow discharge to 0.08 for inflow temperature. DO, $NH_4^+$-N and $NO_3$-N concentrations gradually decrease in sensitivity to inflows from upstream to downstream (*rmse* DO: 0.74 (seg100) – 0.44 (seg254); *rmse* $NH_4^+$-N: 0.025 (seg100) – 0.009 (seg254); and *rmse* $NO_3$-N: 0.124 (seg100) – 0.064 (seg254)). Nitrogen is rapidly taken up by phytoplankton or nitrified, hence the influence of inflows on $NH_4^+$-N and $NO_3$-N concentrations will be reduced with distance from the inflow. DO in inflows can be consumed rapidly on entering a water body leading to a similar sensitivity gradient. $PO_4$-P results indicate the same sensitivity trend from upstream to downstream although to a far lesser degree.

Air temperature has the second greatest influence on model variables. The strong influence on DO results from the decreased DO saturation capacity of water at higher temperatures, along with accelerating organic decay processes as a function of temperature. The impact of air temperature on DO is greater at the upstream end (*rmse* 0.57 (seg100) – 0.28 (seg 254)). Air temperature is also relatively impactful on $PO_4$-P concentrations in the lake due to concurrent changes in simulated algal nutrient uptake. For Chl-a concentrations, sensitivity is greatest at the downstream end of the lake (*rmse* 5.36 (seg100) - 7.1 (seg254)).

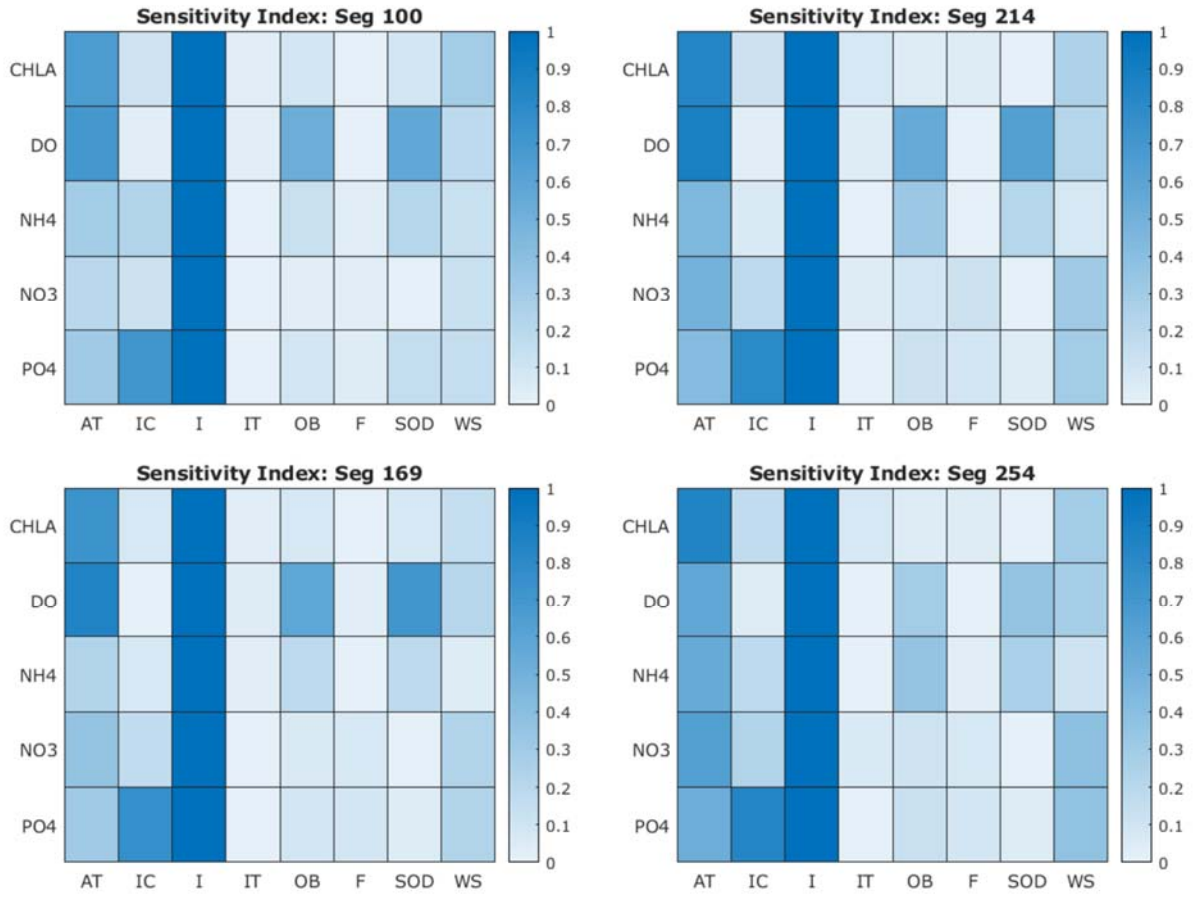


Figure 4.3. Sensitivity analysis based on the relative root mean square errors for each variable for each of the eight boundary conditions. Colours are scaled per row, and the four segments are treated individually for the scaling. Sensitivity is ranked from 0 (lowest) to 1 (highest). Where AT = air temperature, IC = inflow constituent concentrations, I = inflows, IT = inflow water temperatures, OB = opening balances, F = sediment flux, SOD = sediment oxygen demand, WS = wind speed, CHLA = chlorophyll-a, DO = dissolved oxygen, $NH_4^+$-N = ammonium, $NO_3$-N = nitrate, and $PO_4$-P = phosphate.

The plots in Figure 4.4 present the actual differences between the base run and scenario results as a year-by-year comparison for segment 214. This segment encompasses the sampling point location for the observed in-lake constituent data provided by the BPWTP.

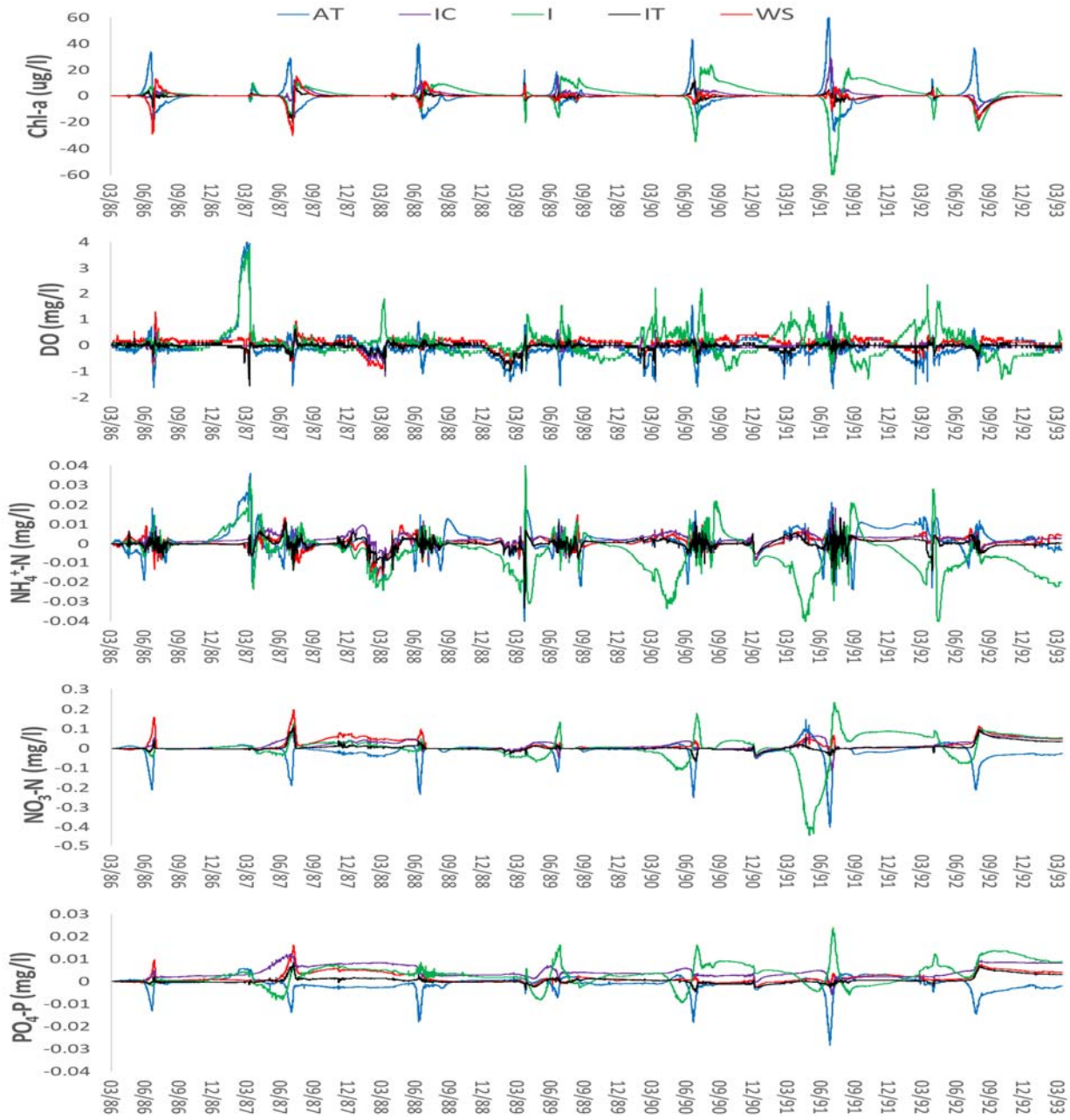


Figure 4.4a. Year-by-year comparison of actual difference between scenario and base run output concentrations for segment 214. Where AT = air temperature, IC = inflow constituent concentrations, I = inflows, IT = inflow water temperatures, OB = opening balances, F = sediment flux, SOD = sediment oxygen demand, WS = wind speed, CHLA = chlorophyll-a, DO = dissolved oxygen, $NH_4^+$-N = ammonium, $NO_3$-N = nitrate, and $PO_4$-P = phosphate. The plots are shown for catchment driven boundary conditions.

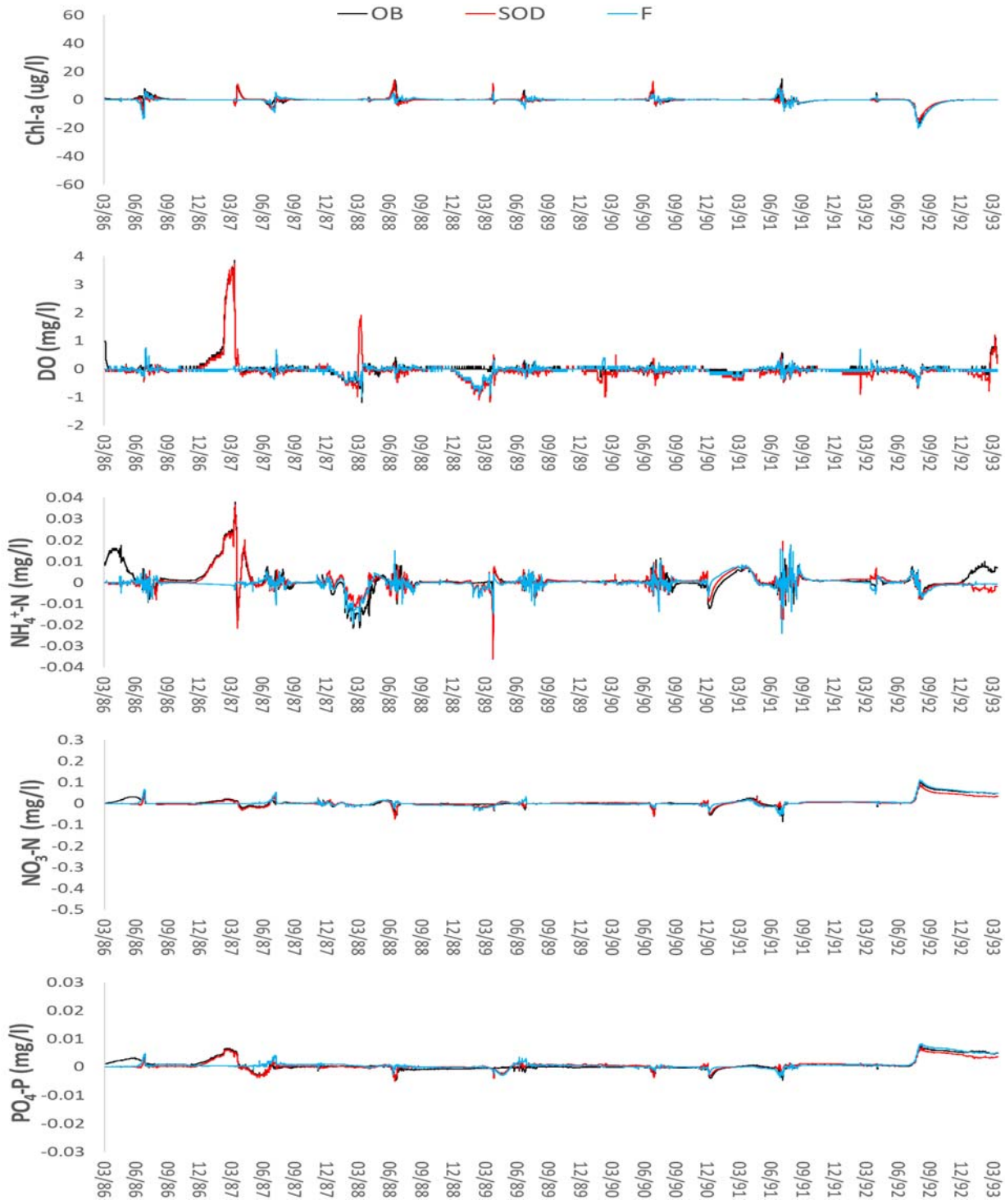


Figure 4.4b. Year-by-year comparison of actual difference between scenario and base run output concentrations for segment 214. Where AT = air temperature, IC = inflow constituent concentrations, I = inflows, IT = inflow water temperatures, OB = opening balances, F = sediment flux, SOD = sediment oxygen demand, WS = wind speed, CHLA = chlorophyll-a, DO = dissolved oxygen, $NH_4^+$-N = ammonium, $NO_3$-N = nitrate, and $PO_4$-P = phosphate.

The plots are shown for in-lake processes boundary conditions.

The air temperature scenario consistently shifts the timing of the algal blooms to earlier in the open water season than the baseline scenario blooms, as well as increasing bloom amplitude. The plot shows the large plotted positive difference in Chl-a at the start of each season. The blooms then subside earlier than the baseline scenario leading to the plotted negative difference between the two scenarios at the end of the seasons. The model shows early nutrient decreases associated with these early blooms. The algae's modelled preferred form of N, $NH_4^+$-N, displays a similar temporal response to air temperature's influence on algal growth and mortality. Wind speed and inflow discharge cause the opposite behaviour in Chl-a concentrations to air temperature. Increasing air temperatures lead to an early spring/summer algal bloom and then subsequent population decline. In reverse, increasing wind speed or inflow discharge results in an apparent early decline in population before the subsequent bloom occurrence.

The model appears less sensitive to inflow concentrations (other than $PO_4$-P), inflow temperatures, initial state opening balances, fluxes, SOD and windspeed.

## 4.6 Discussion

The results indicate that the BPL model is most sensitive to catchment processes. All five modelled WQ variables are most sensitive to a 10% increase in inflow discharge throughout the lake. This supports concerns discussed in Terry et al. (2018) that a large majority of the uncertainty in the model results relates to issues encountered when calibrating the water balance and the subsequent impact on WQ predictions. Flow is reported as being a dominant factor in model calibration (Sadeghian et al., 2018). The hydrology in the BPL catchment is complex with a contributing area that varies depending on amount of precipitation, and that functions on the percentage change between wet years and dry years (pers. Comm. Chris Spence, Environment and Climate Change Canada).

Both Chl-a and DO are found to be sensitive to air temperature. This result is unsurprising as both algal growth, and DO saturation are influenced greatly by water temperature in real life. Other modelling studies have found air temperature to have the most significant contribution to lake temperature uncertainty (Hondzo and Stefan, 1993). Above average spring temperatures, and calm, thermally stratified conditions have indeed led to early algal blooms in BPL. Note that while

ice off dates are similar between the two scenarios (except 1986 where ice off is 30 days earlier in the air temperature scenario), the ice on date is delayed by up to two weeks on average, and ice thickness is less in the air temperature scenario. Both the ice formation and ice growth equations in W2 are a function of air temperature. Thinner ice has more potential for light penetration for photosynthesis, and warming of the water, which in turn can lead to early bloom occurrence.

The onset of the blooms are within one to two days of each other between the wind and baseline scenarios; however, the blooms grow less rapidly and reach their peak later in the wind scenario. This leads to a plotted negative difference in Chl-a earlier in the season followed by a positive difference as the baseline peaks subside before the wind scenario peaks. BPL is a very wind-driven, well-mixed lake and it is possible the increased wind speed surpasses a critical point of turbulence for some algal species, and species competition and bloom temporal dynamics are altered as a result. In the simulated wind scenario the cyanobacteria group are consistently smaller each year in response to the increased wind speeds. In a controlled lake and modelling experiment Huisman et al. (2004) record how diatoms and green algae outcompete cyanobacteria for light when artificial mixing is switched on and within a certain turbulent diffusivity range. The dominant species of cyanobacteria in BPL are *Dolichospermum spp.* (*Anabaena*) (Buffalo Pound Water Treatment Plant, weekly lab data 1995-2011), which has been shown to be negatively affected by turbulence previously (Lindenschmidt and Chorus, 1998).

For some of the in-lake processes the model results are not surprising. Initial conditions, for example, quickly lose their importance during long simulations of waterbodies with short residence times (Debele et al., 2008). In contrast, an increase in fluxes would be expected to have more of an impact in a shallow lake with a high sediment to volume ratio, and long periods of ice cover. Terry et al. (2018) notes that fluxes are particularly difficult to quantify and model due to a lack of data to parameterise the sediment diagenesis model in W2. In the alternate zero-order sediment compartment fluxes are calculated internally by the model as a fraction of SOD released under anoxic conditions. Fluxes cannot be added directly to the model. The default release rates as a fraction of SOD for $PO_4$-P and $NH_4^+$-N in W2 are both 0.001. Defaults are used as there are no data to evidence applying a different rate. The same SOD rate is used throughout the model grid for the BPL model. With an SOD of 1.2 the release rate for each of the nutrients becomes 1.2 $mg/m^2/day$ and the 10% increase brings this to 1.32 $mg/m^2/day$. These rates are fairly low for BPL, and the small increase that is calculated as a result likely explains the low sensitivity of the model

variables to the 10% increase in fluxes. Recent field data shows the phosphorus flux varies spatially in BPL and occurs under both oxic and anoxic conditions in both summer and winter (soluble reactive phosphorus: summer oxic (6–21 mg/$m^2$/day); summer anoxic (23-40 mg/$m^2$/day); winter oxic (0-1 mg/$m^2$/day); winter anoxic (1-8 mg/$m^2$/day)) (D'Silva, 2017). Fluxes are therefore under accounted for in the model and the WQ calibration has been performed under the assumption of the majority of $PO_4$-P and $NH_4^+$-N entering the lake via inflows in the simulation period.

As shown in Terry et al. (2018) the BPL study site presents a number of unique modelling challenges for a WQ model. Much of this uncertainty is attributed to the lake's boundary conditions. In particular, the difficulty in capturing the timing and magnitude of water movement in the lake is described. Figure 4.5 plots observed constituent data provided by the Buffalo Pound Water Treatment Plant for two field sample sites. One field site (Highway 2) is located at the lake model boundary and provides the inflow constituent boundary data. The second field site (Marquis) is located upstream on the Upper Qu'Appelle River close to the location of the nearest Water Security Agency flow measurement gauge (05JG004) that provides the inflow discharge boundary data. As described in Terry et al. (2018) between the two sample locations exists a large, shallow, macrophyte-bedded section of the lake (Figure 1b) that is disconnected from the main body, and for which no data exists for the simulation period. Figure 4.5 depicts a comparison conducted prior to this current study where constituent data for Marquis is compared against the model boundary constituent data at Highway 2. The flow on the plots is as measured at gauge 05JG004. The correlations of the constituent concentrations are poor with R2 values of 0.21 ($NO_3$-N), 0.04 (total phosphorus), 0.13 (total iron). There are clear indications that the unknown reduction in flow moving from riverine to lacustrine conditions reduces constituent concentrations - most likely due to retention of sediments and nutrients (Hosseini et al., 2018), and possible uptake by algae as the flow transport momentum slows down. A timing disparity is suspected between fluctuations in inflow discharge, and the expected corresponding fluctuations in inflow constituents. Thus flow is suggested as a principal driver for uncertainties in boundary constituent data.

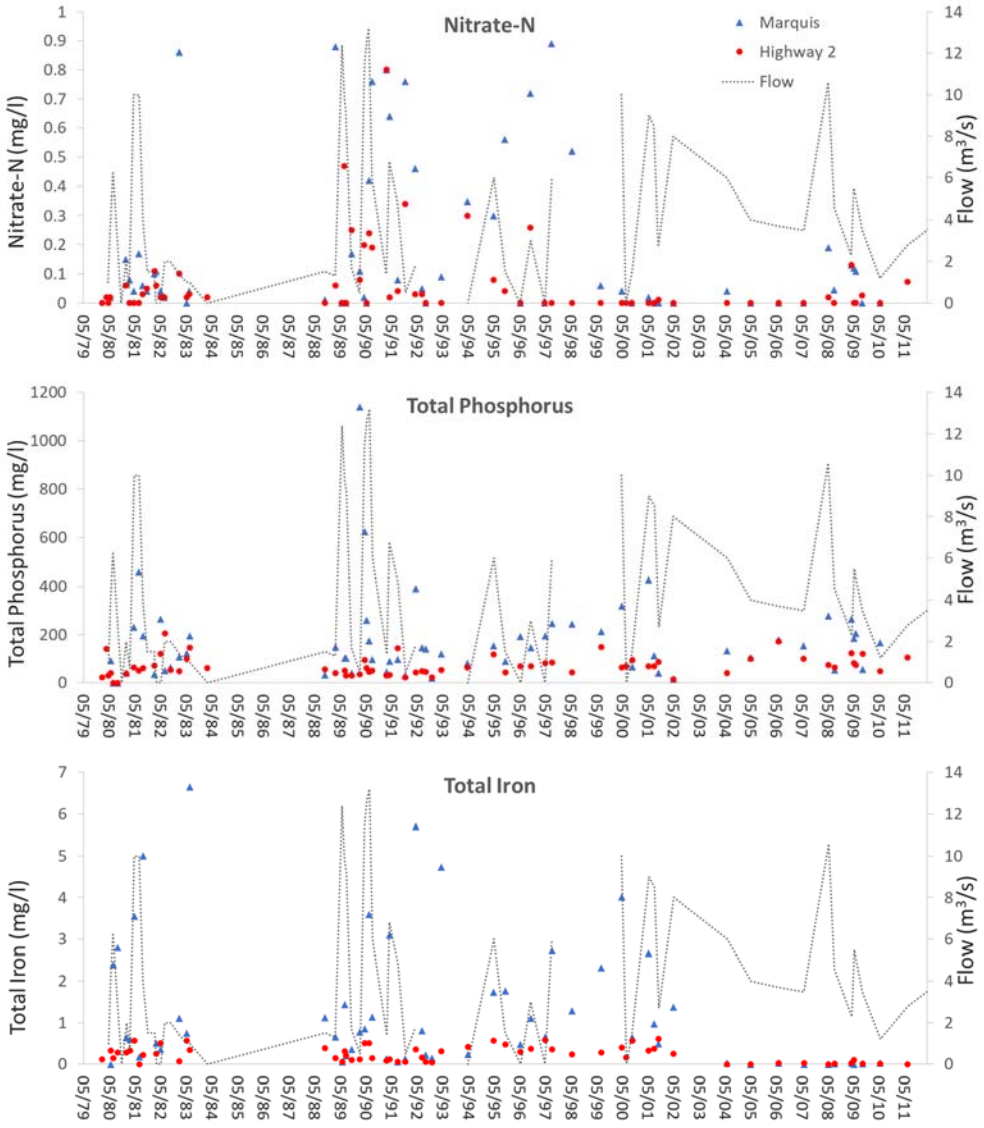


Figure 4.5. Comparison of constituent concentrations sampled from our model boundary site at Highway 2, and the upstream Marquis site. Flow at gauge 05JG004 is also plotted. Both sites are sampled on the same days, although the time between the sampling is not known. The spike in total phosphorus at Marquis in February 1990 reflects an outlier in the phosphate data.

Terry et al. (2018) puts forward a number of suggestions for improving the accuracy of the WQ model for BPL. This sensitivity investigation strengthens the recommendation for the reinstallation of the WSA flow gauge below the lake that was discontinued in 1996 so that both inflows and outflows to BPL are monitored (note the upstream gauge 05JG004 was reinstalled June 2015). The installation of a meteorological station is recommended for the winter months to

supplement the field data collected by the in-situ research buoy deployed in summer. The WSA are already increasing WQ sampling frequency along the Upper Qu'Appelle river channel and in BPL in the open-water season. However, flow has a major role in constituent transport and sampling flow and WQ data at Highway 2, under a range of flow conditions, may yield better estimates of loading than a monitoring program based on fixed time intervals (Johnes, 2007).

What is interesting is that the two most influential outside variables on modelled WQ are both heavily dependent on climate. The results presented here are for a relatively dry simulation period. In the Canadian Prairies, air temperatures are warming rapidly and the Prairies have experienced severe drought and flood periods in the last couple of decades (Wheater and Gober, 2013). In Canada, a country that contains almost 42% of earth's lakes (with area > 0.1 $km^2$) (Minns, 2013), the impacts of climate change have seen a trend in earlier lake ice break-up dates attributed to warming spring air temperatures (Duguay et al., 2006), and changes in snowpack quantity and duration (Wheater and Gober, 2013). Shallow lakes react quickly to changes in meteorological conditions (Taranu et al., 2010), and the catchment to lake ratio is high for BPL. There is a need to understand how WQ is influenced by the timing of spring break-up and snowpack melt, changing air temperatures and precipitation events. This is also applicable to other aquatic systems that have a large catchment to water surface area ratio as these are most likely to be driven by these catchment climatic conditions.

In addition, there is a need to understand the impacts of changes in flow management strategies. The capacity of the Upper Qu'Appelle River channel is insufficient to meet the needs of a growing region. In 2016-17 the WSA spent $900K stabilizing the channel and maintaining channel capacity (Water Security Agency, 2017). The channel had suffered erosion, sedimentation and macrophyte growth and the original design carrying capacity has been more than halved over recent years (Clifton Associates Ltd, 2012). Recently, the WSA investigated augmenting the delivery of water from LDief to BPL in order to meet increasing water demand. Non-anthropogenic water demand is three times that of human demand, with evaporation constituting 98% of the non-anthropogenic requirements and expected to increase in the face of climate change (Clifton Associates Ltd, 2012). From these results it is apparent that the modelled water quality variables are sensitive to just a 10% increase in flows. If managed flows are to be substantially increased then a reliable water balance may be the most important factor in future modelling efforts.

## 4.7 Conclusions

Sensitivity analyses are useful to investigate a model's response to a change in boundary conditions. The importance of good collection of boundary data is clearly demonstrated. Buffalo Pound Lake has a high catchment to lake ratio (Fig. 4.1a), and the scenario results show that catchment processes have substantial influence on modelled WQ. Flows have the greatest impact on model output for the variables considered. These findings are useful as monitoring resources can now be used strategically for the collection of boundary data. These findings will inform the sampling strategy of the agencies managing the lake.

# CHAPTER 5

# CONCLUSIONS - BUFFALO POUND LAKE MANAGEMENT OPTIONS

The previous chapters present three practical applications of the CE-QUAL-W2 (W2) hydrological-ecological model. Work focusses on Buffalo Pound Lake (BPL) a shallow eutrophic impounded lake in Saskatchewan, Canada. All three chapters look towards testing an alternative approach to the standard model framework to allow increased complexity with limited data. Together the chapters explore the capability of a complex water quality (WQ) model to capture under ice and open water eutrophication processes in a continuous multiyear simulation.

Chapter 2 customises the W2 model to read sediment oxygen demand (SOD) as a time-varying variable in the zero-order sediment compartment. This is in place of the existing fixed coefficient value. The variable rate factors for seasonal variation in SOD dynamics during open water and under-ice conditions. A dissolved oxygen/biochemical oxygen demand model is improved using the variable SOD function. In search of a method to parameterise the new SOD rates with only limited data, in-lake chlorophyll-a (Chl-a) concentrations are found to be a good proxy measurement for estimating summer SOD demand and rate of winter decay.

Chapter 3 adapts the ice module of W2 to include a variable albedo rate function. This better simulates natural changes in ice and snow albedo. Simulated ice cover dates are improved using the variable function with predicted ice-off dates shown to be sensitive to end of season albedo values. The timing of algae spring blooms are shifted in the model using the variable rate. Improvements to WQ predictions are limited by the model structure and linkage of the ice and eutrophication modules. Chapter 2, for example, presents a ‘quick fix’ to better simulate ice cover dates by adding two empirical coefficients to the existing W2 ice module algorithm. These coefficients act as snow cover in the model by reducing heat transfers at the ice-air interface during simulated ice formation and melt. The chapter ends by suggesting a better parameterisation would be to substitute a variable albedo function in the ice module code. This will control the amount of

solar radiation penetrating the ice and solve for snow cover. This will also improve WQ calibration as a fixed albedo coefficient cannot capture the under-ice light environment when modelling winter primary productivity. Testing this suggested improvement in Chapter 3 finds the albedo coefficient in the W2 ice model has no connection to the light extinction coefficient - W2 has two additional coefficients to control light absorption at the ice surface (BETAI), and light decay through the ice (GAMMAI). As a result, when the model code is adapted to read a variable albedo rate the timing of the algal blooms are shifting due to albedo's minor influence on the heat budget, but not on the light environment as would occur in real life.

Linking an ice model and eutrophication model is going to be challenging - especially in simulations spanning multiple years. The dynamic nature of ice formation and melt occurrences, and their dependency on both long and short term weather events means ice cover is variable among years. Regardless, Chapters 2 and 3 demonstrate that there is a reason to parameterise the ice cover-eutrophication processes. WQ variables in BPL follow seasonal trends that differ too greatly between open water and under-ice processes to have just one set of WQ model coefficients. The current information gap is huge; substantial amounts of winter ice and snow data are required to properly calibrate WQ models – this data is expensive to collect, and its applicability for modelling ice dynamics in different time periods is highly uncertain. In addition, too few under-ice eutrophication modelling studies have been conducted to assist with calibration assumptions. Chapters 2 and 3 take essential steps in exploring how WQ models may be adapted to better represent under-ice processes - as published manuscripts they are available for the scientific community at large to move forward this research.

Chapter 4 evaluates the most influential boundary conditions affecting select eutrophication variables in the BPL model. Catchment conditions are found to have more influence on the model than in-lake processes with inflow discharge having the greatest sensitivity for all five modelled eutrophication variables considered. The high sensitivity of inflows in BPL is concerning. Uncertainty becomes an issue with highly sensitive parameters. As the relative importance in the model increases for an input variable or fixed parameter, the greater the risk of model error propagating from inaccuracies in input data and calibrated coefficients. Chapter 3 points out potential instability in the calibrated model in both the ice module (Fig. 3.3), and the modelled results for $NH_4^+$-N (Fig. 3.4). Chapter 3 also discusses a number of uncertainties with the available data for the BPL system. Inflows and outflows are particularly problematic with

ungauged tributaries and wetlands, an unknown transition from riverine to lacustrine flow rates, and the confluence of Moose Jaw River all confounding gauging station data. Other boundary data are also inadequate to properly calibrate the water balance and lake hydrodynamics. In example, capturing water movements in the model has been made difficult due to the limited availability of climate stations for BPL. Climatic forcing is a major driver of turbulent motion behind horizontal and vertical mixing. The closest year-round meteorological station to BPL is 30 km south. Estimates for boundary data are based on comparing recent data between this station and the weather station on the in-situ data collecting buoy deployed over summer. Assumptions are that the summer relationships between the two meteorological stations are still valid when estimating winter values. Wind direction was not recorded by the buoy and thus the wind direction used in the WQ model is for the station 30 kms south. BPL's supply reservoir, Lake Diefenbaker (LDief), has similar challenges with meteorological data. The LDief model is highly sensitive to wind (Sadeghian, 2017), and needs onsite measurements for accurate calibration, yet the closest meteorological station is kilometres from the lake. LDief is a large, deep (max depth 60 m), man-made reservoir located 97 kms (channel length) upstream on the Upper Qu'Appelle River. In LDief the stratification is stronger and the main concern for the model is the depth of the thermocline and mixing in the epilimnion. The BPL model is more challenging as uncertainty in wind data is more impactful on a shallow system. In BPL the shallow depth and large fetch facilitates wind induced shear stresses to the lake bed and it is far more difficult to parameterise wind's impact on mixing conditions in the model – particularly with the lack of temperature profile data for BPL.

Chapter 4 concludes, from the results of the model, that flow management strategy may be the most important aspect of WQ management in BPL. The chapter discussion introduces Water Security Agency (WSA) investigations for meeting increasing water demand with the current level of inflows, and their exploration into increasing the volume of water delivered from LDief to BPL. From the results of Chapter 4 it appears that any proposed change in flow regime may have considerable impact on BPL's WQ based on the model's response. The calibrated WQ model of BPL developed in Chapters 2 to 4 can be applied to assist the WSA with their decision making. A scenario-based investigation is presented next:

The main inflows into BPL are through controlled releases from the upstream LDief in the Qu'Appelle River system (Fig. 5.1). The capacity of the Upper Qu'Appelle River channel, a

combination of improved channelized river (35 km) and meandering natural river channel (62km) flowing between the two reservoirs, can transport insufficient volume to meet future water demand.

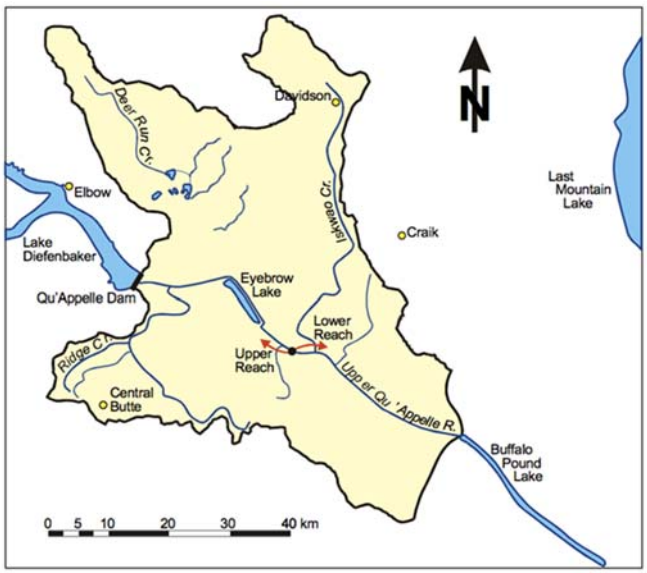


Figure 5.1. The Upper Qu'Appelle River System showing the 97 km stretch between the Qu'Appelle Dam on Lake Diefenbaker and Buffalo Pound Lake (from Acharya and Kells, 2005).

Several studies have been undertaken to evaluate options for augmenting water supply. One project idea put forward by AECOM in 2009 was the construction of an upland conveyance canal (Clifton Associates Ltd, 2012). Alternative options include a gravity pipeline from LDief to BPL, or improving the existing river channel (Stantec, n.d.). According to Clifton Associates Ltd (2012) the AECOM project report stated that the benefits of a new purpose built canal would be an 'incremental' increase of flows from 115,000 $dam^3$ to 326,419 $dam^3$ between the two reservoirs. As a new upland route, a secondary benefit would be the bypassing of agricultural run-off and nutrient loading, and evasion of the algal blooms and sediments found in the current river channel system (Clifton Associates Ltd, 2012).

However, the construction of the conveyance canal would be a major undertaking and may not occur. The existing river channel may need to cope with additional volume of releases from LDief. The WSA are already investigating the benefits of LDief waters, which are cleaner waters than BPL, flowing into BPL. In the summer of 2015 the WSA conducted controlled releases of LDief in an attempt to more rapidly flush BPL WQ at the request of the Buffalo Pound Water

Treatment Plant (WTP). A mild winter with early ice-off saw the appearance of early algal blooms that produced unexpected amounts of oxygen in the lake. This disrupted treatment processes at the WTP as the plant design was not set-up for these conditions. The problems were augmented by a lack of mixing due to unusually calm spring weather, warm temperatures and a summer stratification of 8°C difference (Helen Baulch, personal communication). The Qu'Appelle catchment is flat landscape and the WSA has to carefully manage additional releases so as not to create high water levels downstream. Analysis when scoping the effect from the flushing was that the additional amounts of water entering BPL were too small to impact the WQ status in the short-term, but would form part of a longer term investigation. The spring algae problem improved independently (John-Mark Davies, personal communication).

The WTP administration board considers that WQ in BPL may not improve until such time that the WSA increases LDief contributions more permanently. The WSA, however, cannot simply increase flows due to the catchment's limited capacity to receive additional water, including downstream stakeholder considerations. The management of flows into BPL from LDief is also dependent on the amount of upstream runoff from BPL's local catchment in any given year. This local runoff has elevated concentrations of nutrients, organic carbon, and salts relative to LDief and affects WQ in BPL. In years with high local runoff, including those preceding 2015, the capacity of the system to receive water from LDief is reduced (John-Mark Davies, personal communication). With the WTP having to restrict water supplies to the Cities of Moose Jaw and Regina over the 2015 summer due to substandard WQ and issues with plant design, it is beneficial that the WSA are provided tools and information to help inform their decision on flow management and flushing rates. Notably, an understanding of the constraints of catchment management on improving WQ in BPL need to be defined so residual risks from that approach are accounted for when revising water treatment plant processes. The developed WQ model for BPL is shown to be highly sensitive to the hydrology of the catchment. Lake inflows have the greatest influence on model WQ conditions out of all boundary conditions tested (Terry et al., 2018). The type of modelling approach used in this study can provide an informative tool for investigating this important management question.

At the start of this project there were two options being considered for augmenting the supply of incoming water to BPL: The first was to increase the capacity of the existing Upper Qu'Appelle River channel so that more water can be released from LDief through the existing

system. Over the past number of years, the WSA has worked to improve channel conveyance including erosion control. Apart from expanded irrigation proposals, the current channel capacity is considered sufficient to meet present and future anticipated water demands. The second was the construction of an upland canal conveyance system that would carry water directly from LDief to BPL. As a complex hydrological-ecological model W2 has numerous options for representing the hydrodynamics of natural and man-made waterbodies. This means both management options can be investigated using the same calibrated WQ model of Terry et al. (2018).

Three scenarios are modelled to investigate the effect of augmented water supply on WQ in BPL. The first is to simulate doubling the amount of water being released from LDief through the existing Upper Qu'Appelle River channel and into BPL. For this scenario, the measured boundary daily inflow data are increased by a factor of two. No changes are made to the model hydraulic set-up, and it is assumed all other inflow and outflows, such as ungauged inflows or piped withdrawals for the WTP, remain as per the base model. Inflow temperature and constituent files are as per the base model and described in Terry et al (2018). The base model constituent values are measured data recorded at Highway 2 at the downstream end of the river channel (and forming the upstream boundary of the BPL model). The model assumes that these base model constituent values are not affected by the increased flows.

The second scenario again doubles the amount of water released from LDief into BPL, yet assumes the flows travelling through the Upper Qu'Appelle River channel remain the same as the base model. The additional volume of water is conveyed to BPL along the projected upland canal. The upland canal is added to the model as an inflowing tributary entering the most upstream segment of the lake model grid. It is assumed that flows running through the conveyance canal will remain consistent through the length of the channel. Inflow temperatures are assumed the same as the existing river channel. Inflow constituent concentrations for the upland canal are averages of historical LDief concentrations (so as would be released into the upstream end of the canal) and are a constant value (Table 5.1).

Table 5.1 Lake Diefenbaker constituent concentration values used for upland canal inflow constituent file in W2 model scenario.

| Inflow constituent | Value mg/l (constant) | Data source |
|---|---|---|
| Total dissolved solids | 362 | WSA data: 1986-2006 (107 samples) |
| Inorganic suspended solids | 2 | (Sadeghian et al., 2018) |
| Phosphate | 0.003 | WSA data: 2013-2015 (33 samples) |
| Ammonium | 0.04 | WSA data: 2010-2015 (60 samples) |
| Nitrate | 0.14 | WSA data: 2013-2015 (55 samples) |
| Chlorophyll-a (as algae dry weight organic matter) | 5 | (Sadeghian et al., 2018) |
| Labile dissolved organic matter | 2 | WSA data: 1983-2009 (134 samples – DOC) |
| Refractory dissolved organic matter | 7.8 | WSA data: 1983-2009 (134 samples – DOC) |
| Labile particulate organic matter | 0.1 | WSA data: 1983-2009 (134 samples – DOC) |
| Refractory particulate organic matter | 0.4 | WSA data: 1983-2009 (134 samples – DOC) |
| Biochemical oxygen demand | 2 | WSA data: 2010-2015 (39 samples) |
| Dissolved oxygen | 11.4 | WSA data: 2010-2015 (78 samples) |
| Total inorganic carbon | 39 | WSA data: 1975-1982 (51 samples) |
| Alkalinity | 173 | WSA data: 1974-2009 (203 samples) |

The third scenario assumes that volume releases are made from LDief so as to reach the maximum capacity of the projected upland canal at peak flow rates. The assumed flow rates in the upland canal are based on a hydrograph of historical monthly average flow data (Fig. 5.2) for a Water Survey of Canada gauge below the Qu'Appelle River dam, which releases water from LDief into the Upper Qu'Appelle River channel. Historical monthly averages are multiplied by a factor of 4.5 to produce a maximum flow rate of 65 cms, which is the proposed capacity of the new upland canal (Lindenschmidt and Carstensen, 2015). Proposed winter flows are 6 cms in order to avoid ice damage to the canal as described in Lindenschmidt and Carstensen (2015). Here, ice cover is assumed between October and March. Inflow temperatures are assumed the same as the existing river channel. Inflow constituent concentrations are as scenario two. Flows travelling through the Upper Qu'Appelle River channel are kept the same as per the base model.

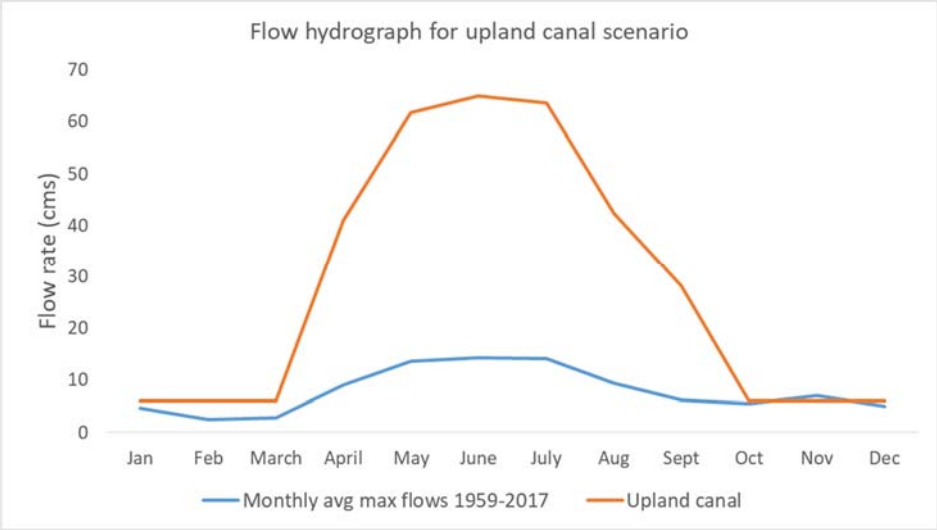


Figure 5.2. Estimated monthly maximum flows for the projected upland canal based on historical monthly average maximum flows recorded for station #05JG006 below Qu'Appelle Dam on the Upper Qu'Appelle River Channel. Maximum capacity of the projected upland canal is 65 cms, with proposed winter flows of 6 cms (Lindenschmidt and Carstensen, 2015)

Results of the first scenario compared against the base model are presented in Figure 5.3. Output is for the downstream segment encompassing the sampling point location of the WTP, as per Terry et al. (2018). Model results indicate that doubling the volume of water released into BPL from LDief does not improve predicted WQ when pushed along the existing Upper Qu'Appelle River channel. Chlorophyll-a (Chl-a) increases from baseline over each winter as well as spring/summer (from here on just summer) periods 1986, 1987 and 1992. Chl-a concentrations are calculated by W2 and represent algae biomass in the BPL model using an algae/Chl-a ratio. Nutrient loading of phosphate ($PO_4$-P), ammonium ($NH_4^+$-N), and nitrate ($NO_3$-N) increase. BPL has a greater amount of total nitrogen (TN) in the scenario run in all but the winter of 1988. Dissolved oxygen (DO), DOC and total dissolved solids (TDS) concentrations show some fluctuation although are not impacted greatly. Algal growth appears to be phosphorus limited in the scenario model. A maximum capacity for nitrogen uptake leads to excess concentrations of $NH_4^+$-N and $NO_3$-N including periods where algae previously suffered nitrogen limited growth (1987, 1988 and 1992).

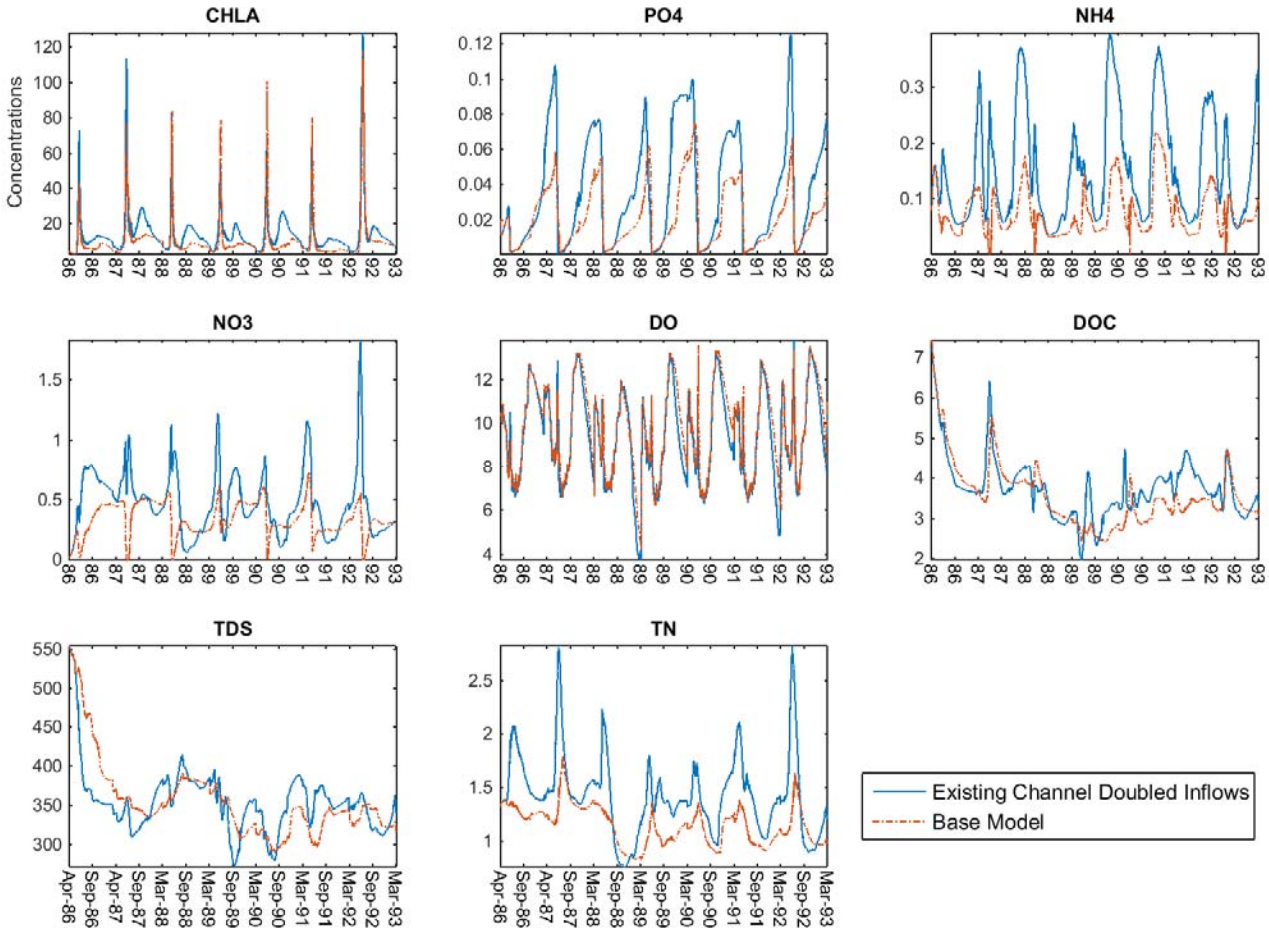


Figure 5.3. Scenario results where flows in the existing Upper Qu'Appelle River channel are doubled. Concentrations are mg/l.

Results of the second scenario show modelled Chl-a summer concentrations are slightly greater than the base model in 1986 and 1987, although the latter five-years demonstrate a significant reduction in peak values in the scenario model (Fig. 5.4). Winter concentrations of Chl-a still reach higher values than concentrations in the base model although show improvement over scenario one results. Chl-a concentrations are depleted lower than the base model by the end of most winters. This may explain why the summer peaks do not reach the same scale as the base model. Nutrient concentrations are clearly reduced from scenario one by the diversion of the additional discharge volume through the projected upper canal. DOC levels, however, increase over the latter half of the simulation period from both the base model and from scenario one. The

diverted inflows through the upper canal use constant nutrient concentration values (Table 5.1) and the calculated DOC loading appears greater in the upper canal than in the original channel in these later years leading to the overall increase in DOC.

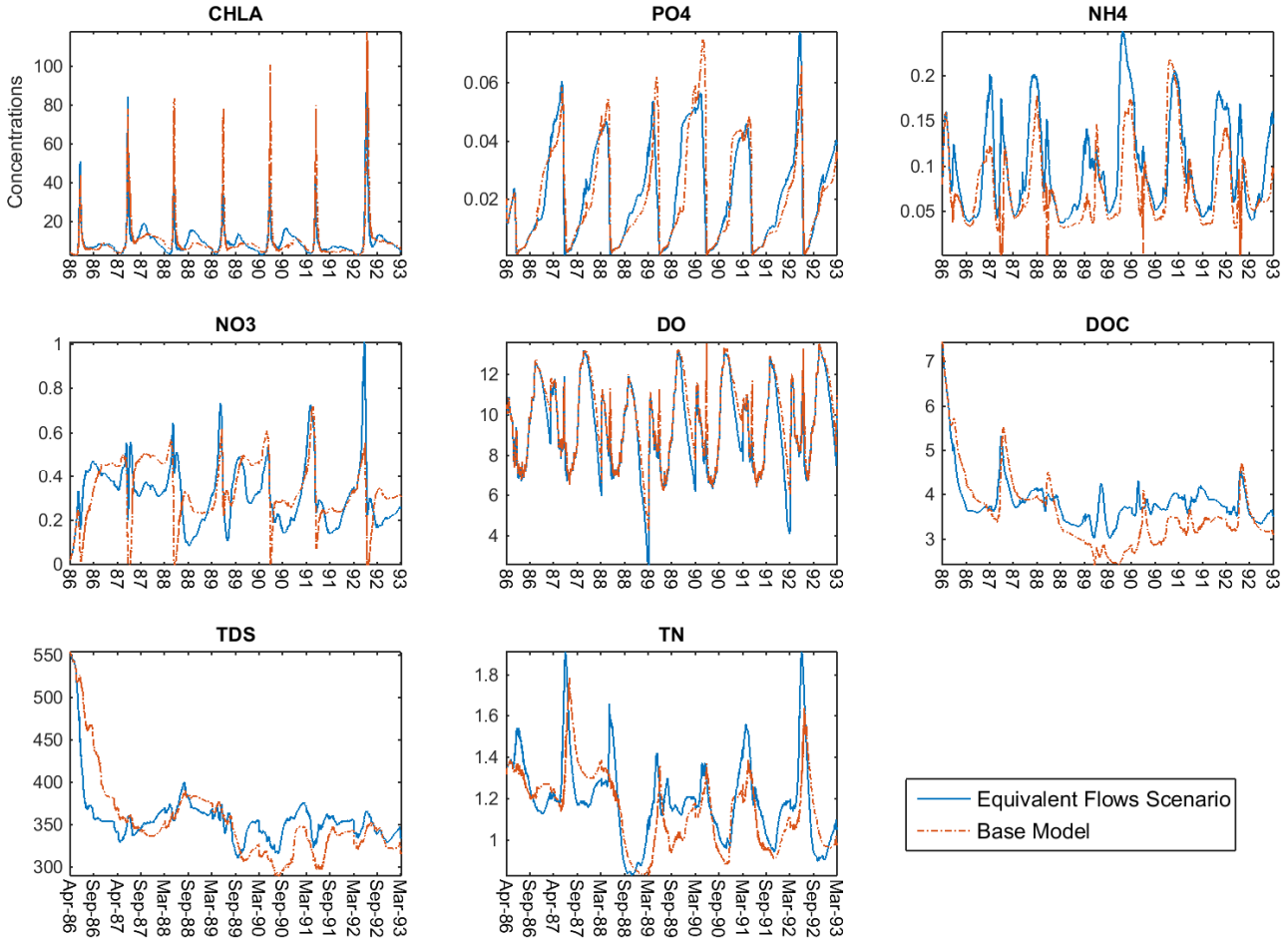


Figure 5.4. Scenario results where flows in the existing Upper Qu'Appelle River channel are doubled with the extra water then transported to BPL through the projected upland canal (flows in the existing river channel remain the same). Concentrations are mg/l.

Most notable from the third scenario results is the predicted reduction in overall Chl-a concentrations as a result of the influx of cleaner water from LDief conveyed along the projected upper canal (Fig. 5.5). Algal growth once again appears to be phosphorus limited in the model. Nutrient concentrations are again substantially reduced from the base model. DOC and TDS

concentrations level out within the first year as a result of the majority of flows now carrying a constant loading concentration.

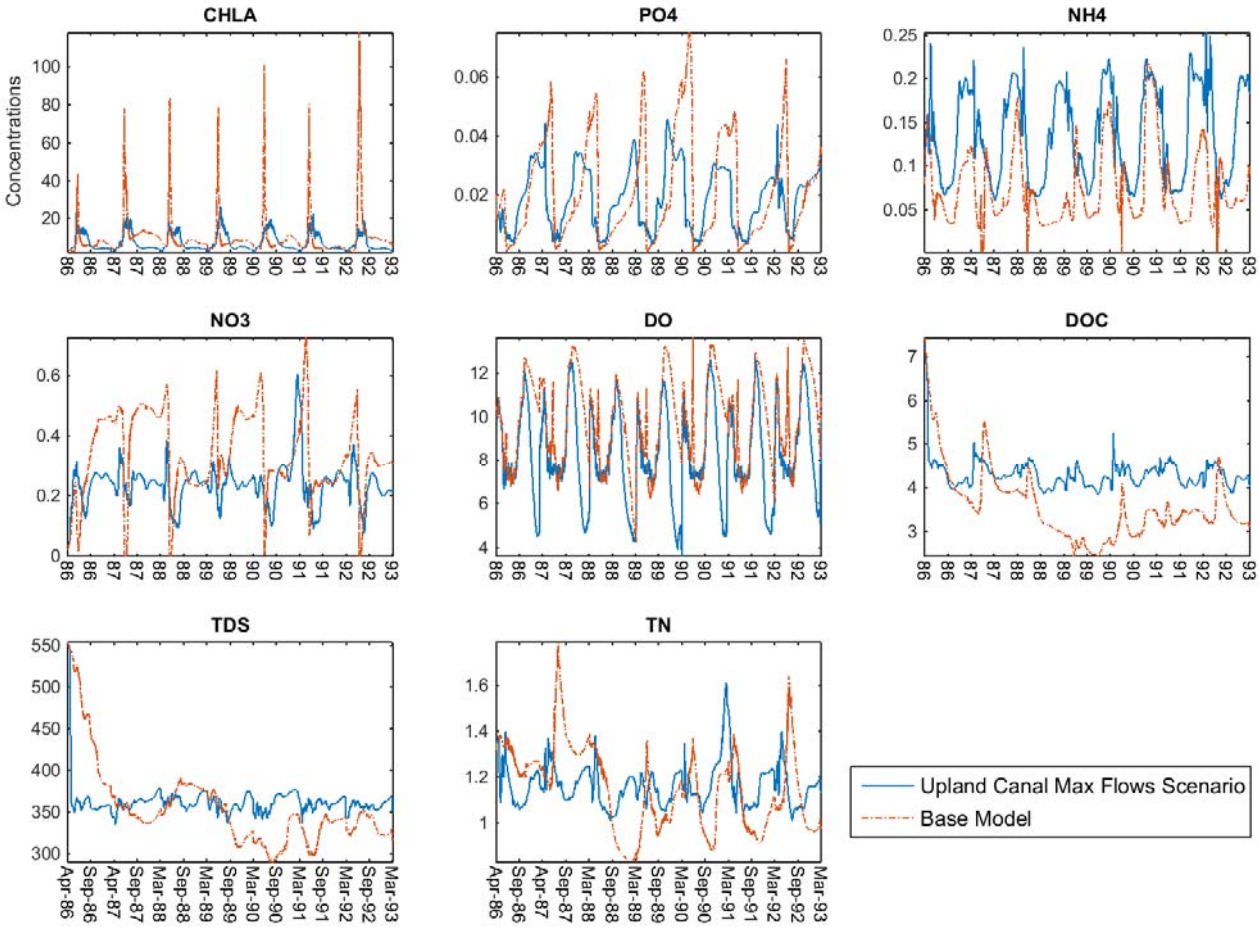


Figure 5.5. Scenario results where maximum flow rates are assumed along the projected upland canal. Flows in existing Upper Qu'Appelle River channel remain the same. Concentrations are mg/l.

These flow scenarios underscore several important factors regarding increasing the volume of water moving from LDief to BPL to meet rising water demands. A core finding of the preceding chapters is that BPL's WQ model is highly influenced by lake inflows as discussed in Chapter 4. The scenarios presented here identify that both the volume of water, and the concentration of WQ constituents entering the lake are contributing factors to the lake's predicted WQ status.

The first scenario predicts that increasing the volume of water released from LDief though the existing river channel does not result in decreased BPL nutrient concentrations. This is not

entirely unexpected because the first scenario model assumptions were that boundary condition WQ concentrations at Highway 2 remained consistent with the base model. In reality these concentrations are anticipated to change with increased flow; however, the scenario is useful for assessing maximum expected differences among different inflow conditions. Almost all variables plotted in Figure 5.3 are increased with the additional discharge volume. The exception to this are DO concentrations that display little change. This DO result agrees with Hosseini et al. (2018) in a similar scenario increasing flow between LDief to BPL using the WASP7 model. It is worth mentioning that while a 10% increase in inflows cause most sensitivity for DO (Chapter 4: Fig. 4.3) the maximum change from baseline is less than 0.8 mg/l. TDS is another exception as concentrations decrease slightly in the initial years of the simulation period. Although not plotted here, further simulations of triple and quadruple flows released from LDief into the existing river channel confirm that as discharge volumes increase so do predicted Chl-a and nutrient concentrations in BPL. WQ challenges appear amplified in line with the additional loading amounts entering the lake through the river channel due to the higher flows. The WASP7 simulations in Hosseini et al. (2018) also find predicted Chl-a and $NO_3$-N concentrations increase in BPL when more water is released from LDief along the original channel. $NH_4^+$-N and $PO_4$-P, however, are shown by WASP7 to decrease with the greater flow volume. The authors state the main source of $NH_4^+$-N and $PO_4$-P in BPL are sediment fluxes, which they specify in the WASP7 model as a fixed daily flux (loading) rate. The authors suggest the increased inflow volume thus dilutes these flux concentrations. In the W2 scenarios presented here the $NH_4^+$-N and $PO_4$-P fluxes are calculated internally by the model as discussed in Chapters 3 and 4, and flux rates differ between both models. The time periods of the two model simulations are almost two decades apart and WQ data are not directly comparable.

Nutrient loading in these W2 scenarios follows basic assumptions. Loading concentrations in the original river channel remain the same in both the base model and in scenario one – the doubling of inflows therefore doubles the inflow constituent loading. In reality, doubling the discharge volume may lead to a dilution of inflow nutrient concentrations as the cleaner LDief waters 'wash out' the channel. Conversely, the additional discharge volume travelling the channel on any given day may lead to additional scour of river banks and movement of the sediment bed as shear stresses increase. In turn this will likely increase inflow nutrient concentrations entering BPL from the original channel. W2 has the ability to link a number of waterbodies together in one

model structure, and the BPL WQ model could be extended to include the Upper Qu'Appelle River channel as a means to investigate this. Both the W2 model and the WASP7 river-lake model predict that BPL remains eutrophic after augmenting inflows from LDief to BPL along the existing channel.

In the second and third scenarios, inflow constituent concentrations for the projected upland canal are constant values throughout the simulation period - being estimated from average LDief concentrations. The concentrations listed in Table 1 are based on long-term historical data, and should be reasonably representative of expected loadings. Interannual and seasonal changes in concentrations will occur in LDief that are not factored into the inflow constituent file - Chl-a in particular will fluctuate seasonally. For these scenarios, potential substances input to the canal through runoff are not considered. It is also assumed that there will be no transformation of LDief constituents being transported through the canal. These assumptions are made as it is not possible to predict how the constituents will transform as they travel through the channel or canal - nor the amount of water and substances abstracted or emitted into the waterbodies from the catchment areas. As with scenario one, these assumptions are useful for establishing contrasting inflow scenarios for comparative purposes. It is assumed in scenarios two and three that flows along the upland canal will remain the same along the whole stretch. In reality, the primary purpose of the upland canal is to provide water for irrigation with water abstracted along the length of the canal.

The inflow temperature file is the same for both the existing river channel and the projected upland canal in all scenarios. In real life inflow temperatures along the existing river channel will be influenced by a number of inflowing tributaries along the river stretch. Inflow temperatures in the upland canal will remain more consistent being a function of flow volume and local climate. Results of a further scenario simulation where inflow temperatures are increased by 2°C indicate inflow temperatures have little impact on the overall outcome of the simulations – the in-lake temperature being more important for WQ processes in this case. Output variables such as Chl-a are therefore not impacted by the inflow temperature assumptions made for this scenario study.

The flow scenarios have no discernible relationship with the simulated dates of ice cover, although scenario two appears to cause both earlier ice formation and melt events. The ice equations in W2 are a function of a number of heat balance equations including ice-to-air surface heat exchange, ice-conduction through the ice, and a function of water conditions below the surface (this includes inflow temperatures as well as water turbulence and movement). Surface heat

exchange computations are the primary terms of the equations. The influence of water movement is set through a coefficient of water-to-ice exchange (*Hwi*) that is set empirically by the user for lakes, and is a function of water velocity for rivers. The WQ model of BPL uses the W2 default value for *Hwi* for both the base model and the scenarios. A test simulation doubling the value of *Hwi* resulted in negligible impact on ice cover dates and ice thickness. The simulation discussed above with increased inflow temperatures of 2°C also has negligible impact on ice cover and minimal impact (*in the range of millimetres on average*) on ice thickness. The potential instability in the ice model has already been discussed.

For the scenarios it is assumed lake water levels will remain close to full supply level of 509.47 masl and the dynamic pump option in the W2 model is used to calculate the appropriate outflow files. The ability of the Buffalo Pound Dam structure to cope with the increased volume of inflows and outflows in BPL is not considered in these analyses. Existing reports establish that the movement of water across the dam structure during flood events is extremely complex with tailwater creating a significant drop in capacity of the spillway to deal with outflows. Several instances of water backflowing into BPL from the downstream Moose Jaw Creek have occurred during high water events after waters overtop the dam (MPE Engineering, 2013). Moose Jaw Creek backflows are discussed in Chapter 3.

Figure 5.6 plots the residence time of the lake water in the model segment selected for the constituent comparisons in Figures 5.3-5.5. The segment is located approximately four kilometres before the downstream model boundary, and the plots show mid-depth values. In the third scenario, where flows are maximised in the projected upland canal, the residence time of BPL decreases substantially. It is likely that modelled algae populations are negatively impacted by the rapid residence time in the new scenario. The base model has one algal group with a growth rate of 1.2 per day that represents an average of the different species and growth rates in BPL. This is a relatively slow growth rate, and with the rapid changeover of lake water and nutrients the group are unable to establish high population growth in the scenario. A plot of limiting factors for algal growth, per W2, indicates algae have sufficient light, nitrogen and phosphorus resources. Water movement will therefore be the detrimental factor with algae populations washed out of BPL before large blooms can establish.

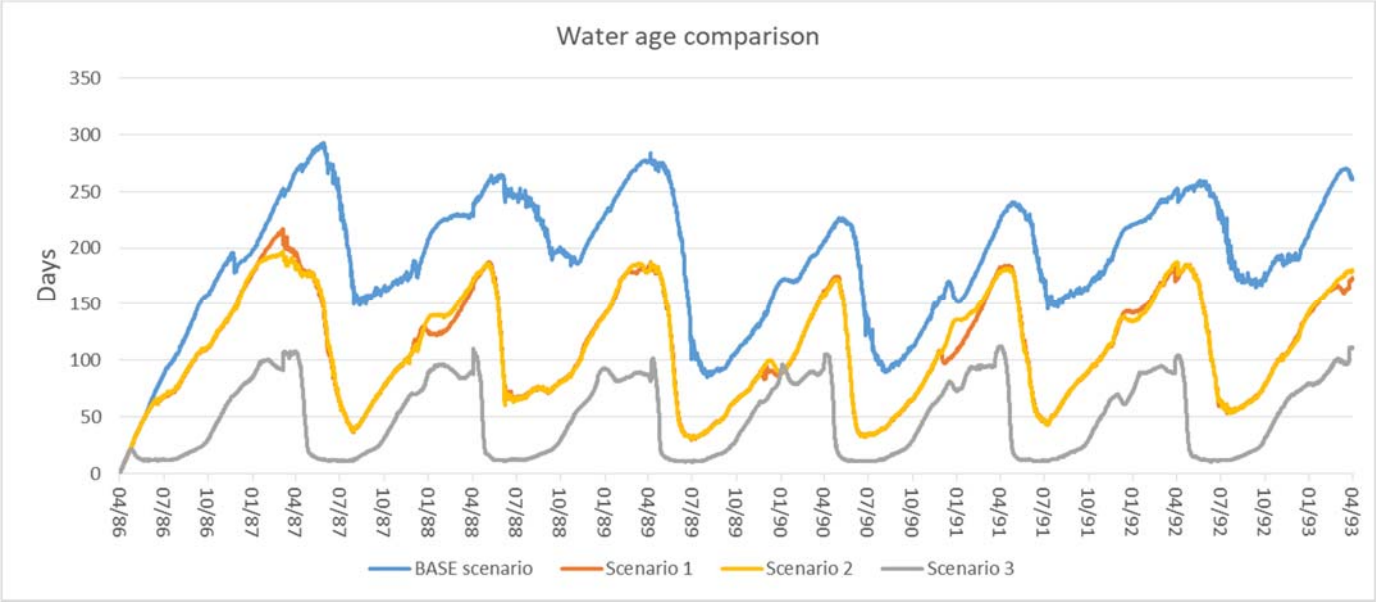


Figure 5.6. Comparison of water residence time between the base model and scenario simulations.

The modelled results show that, dependent on the quantity of water transferred, the increased volume of water may improve WQ in BPL as well as provide additional lake water to meet growing demand. The greater the amount of water that can be transported from LDief along the projected upland canal the greater the improvement in the modelled in-lake Chl-a concentrations. At this point it is worth clarifying that the scenarios were based on three different methods of water transfer used to define the quality of water entering BPL. The basic assumptions made for the treatment of both flows and constituents in both the original channel and the upland canal mean the scenarios do not necessarily hold true in the real world. What the model does support is that increasing the volume of inflows that reflect the WQ of LDief will improve WQ in BPL as the WTP administration board have suggested. If the increase of flows through the original channel results in sufficient dilution of inflow constituents to be closer to the WQ of LDief then the WQ may improve in BPL regardless of whether the upland canal is constructed or not.

There is some uncertainty in the results due to the high sensitivity of the model to small changes in parameter settings, as discussed in Chapter 3. Further investigation would be warranted to ascertain if the findings presented in this study are biased based on model accuracy. Model output can be assessed through uncertainty analysis, which would be an interesting step to take

forward. In addition, recent WQ monitoring in BPL and along the Upper Qu'Appelle River has increased spatially and temporally, and lake profile data are now available. With the reinstallation of the flow gauge 05JG004 above the lake there is the opportunity to validate, and fine tune the BPL model with new simulation periods in future projects.

Chapters 2 through 5 have addressed the three research themes introduced in Chapter 1. For the first research theme, catchment processes, inflows and air temperature in particular, appear to have the most influence on the WQ model of BPL. The hydrology of the Upper Qu'Appelle River basin is indicated as the most sensitive factor behind simulated WQ conditions in the BPL model. An accurate water balance will be essential for successful WQ modelling. Flow is also considered a primary uncertainty in boundary constituent data. This is due to the shallow, macrophyte-bedded section of lake above the Highway 2 divide acting as a flow transition zone. Catchment meteorological conditions also have considerable influence on modelled WQ results with local air temperatures having the second greatest impact to predicted WQ after flows. One caveat is the relatively low flux rates used for $PO_4$-P and $NH_4^+$-N, as discussed in Chapter 4. The model may show more sensitivity to internal flux processes with greater flux rates.

The second research theme is answered in Chapters 4 and 5. For algal bloom development in particular, in Chapter 4 increased air temperatures are shown to increase bloom amplitude, and shift the timing of blooms in the model to earlier in the open water season. Modelled wind speed is also shown to impact Chl-a, although it cannot be said at present how wind speeds across the lake will vary with future climate change. Flow management strategy implications are discussed in detail within the text of Chapter 5. These scenarios are based on a greater volume of controlled flows from LDief. A change in flows due to climate change is more difficult to predict. Climate change impacts may bring increased precipitation and snow melt flows into the lake via ungauged inflows and overland run-off. The Upper Qu'Appelle River channel and BPL will have lower capacity for LDief releases, and WQ will be reduced in these years due to higher inputs of nutrients and organic materials washed in from overland (Hosseini et al., 2018).

For the third research theme, it is evident that the W2 model can be improved/adapted to better represent under-ice conditions during simulations. In example, in Chapters 2 and 3 model results are improved by changing a fixed parameter coefficient to be treated the same as a time-varying boundary variable with time-series data as input. This allowed individual parameterisation

of open water and under-ice processes as would occur in real life. Nonetheless, modelling under-ice processes in BPL has not been altogether successful. The work presented here is unable to influence the under-ice environment to a point where noticeable improvements in the WQ results occur. Linking ice dynamics and eutrophication processes remains the biggest challenge WQ modellers have at the moment with winter modelling. It is clear a number of limitations remain in the W2 ice model compartment, and its connection to the model's WQ compartment, that restrict the ability to use an extended algorithm as intended. Potential improvements would involve major adjustments to the programming code, and in a model as complex as W2 should be performed by the model's own developers. This result is of great significance to those involved with modelling under-ice WQ. There is clearly a missing link in the applicability of current WQ models to high-latitude lakes that needs to be addressed. It is imperative that model developers learn from the challenges that are presenting themselves in real world studies, such as presented in this thesis, so that they can begin to tackle these limitations.

# APPENDIX

## TECHNICAL NOTES MODEL SET-UP

### A.1 Bathymetry

Bathymetry measurements of Buffalo Pound Lake (BPL) were collected by boat (Paul Jones). The provided sonar measurements were converted for Excel using Sonar Log Viewer 2.1.2 (Jay Sagin), and adjusted for the depth of the boat drive. Data collection took place over two field days on 19 June 2014 and 14 August 2014. High-frequency water level data were available at 5-minute intervals from the Water Security Agency (WSA) in-situ gauge at the southern end of the lake. Water level fluctuations during data collection (e.g. due to wind) were not statistically significant (Relative Standard Deviation > 0.000% over each 24-hr period), and the mean water level was taken to be representative for each day (Table A1). The 14 August 2014 was selected as the base data, and 0.136 m (3 d.p.) added to 19 June 2014 values to compensate for water level differences between the bathymetry datasets.

Table A1: Water level statistics for Buffalo Pound Lake for the two data collection field days. Full data record available for each day.

| | **19 Jun 2014** | **14 Aug 2014** |
|---|---|---|
| Mean ($\bar{x}$) (288 measurements) | 509.497 | 509.633 |
| Standard Deviation (s) | 0.0038 | 0.0040 |
| % Relative Standard Deviation (%RSD = (s/x¯)*100) | $7.46 * 10^{-6}$ | $7.85 * 10^{-6}$ |

The sonar dataset was re-projected to WGS84 UTM 13N for ArcGIS processing. To reduce interpolation error due to large areas of lake with no data, additional bathymetry points were included from a digitised version of a 1959 bathymetry map of BPL provided by the WSA. While sedimentation and structure changes on the lake will mean these data are obsolete, for the interpolation it was deemed better than having large gaps with zero information. For the 1959

depth points, the map gave the water level at 1671 ft (509.321 m), and it was assumed that the published data had been corrected for fluctuations in water level during collection. On merging the datasets, 2014 was selected as the base data, and the 1959 values adjusted by 0.3 m (1959 values to 1 d.p.) using the field calculator in ArcMap.

The digital elevation model (DEM) (Figure 2.1) was generated in ArcGIS (Heather Wilson) following the methodology described in Dost and Mannaerts (2008) where the sonar dataset is merged with shoreline level data prior to interpolation of the lake area. The lake extent polygon was provided by the WSA, and digitised from 2006 SPOT 5 2.5 meter imagery when the lake level was 509.58 m. Surface interpolation was performed using a deterministic Spline with Barriers Raster Interpolation at a resolution of 15m.

The lake bathymetry file was created using the Watershed Modeling System (WMS) version 9.1. The ArcGIS DEM was converted into a digitised triangulated irregular network (TIN) file, the format required for generating the CE-QUAL-W2 bathymetry file. WMS supports the CE-QUAL-W2 model and provides GIS tools for creating and editing the bathymetry data before saving in the required *.npt* format of the CE-QUAL-W2 control file. To represent a water body, WMS requires the user to define branches (locations of significant inflow), segments (areas of similar hydrodynamics), and flow direction, and calculates vertical layers and cell-widths based on user preferences. The lake morphology of BPL is such that only one main branch was required to be modelled in WMS.

# REFERENCES


Acharya, M. & Kells, J. A. (2005) Conveyance capacity investigations for the Upper Qu'Appelle River Channel. *17th Canadian Hydrotechnical Conference*. Edmonton, Alberta, Canada.

Adrian, R., Reilly, C., Zagarese, H., Baines, S., Hessen, D., Keller, W., Livingstone, D., Sommaruga, R., Straile, D., Van Donk, E., Weyhenmeyer, G. & Winder, M. (2009) Lakes as sentinels of climate change. *Limnology and Oceanography,* **54,** 2283-2297.

Adrian, R., Walz, N., Hintze, T., Hoeg, S. & Rusche, R. (1999) Effects of ice duration on plankton succession during spring in a shallow polymictic lake. *Freshwater Biology,* **41,** 621-634.

Babin, J. & Prepas, E. E. (1985) Modelling winter oxygen depletion rates in ice-covered temperate zone lakes in Canada. *Canadian Journal of Fisheries and Aquatic Sciences,* **42,** 239-249.

Bertilsson, S., Burgin, A., Carey, C. C., Fey, S. B., Grossart, H. P., Grubisic, L. M., Jones, I. D., Kirillin, G., Lennon, J. T., Shade, A. & Smyth, R. L. (2013) The under-ice microbiome of seasonally frozen lakes. pp. 1998-2012.

Beven, K. (2006) A manifesto for the equifinality thesis. *Journal of Hydrology,* **320,** 18-36.

Blanchfield, P. J., Paterson, M. J., Shearer, J. A. & Schindler, D. W. (2009) Johnson and Vallentynes legacy: 40 years of aquatic research at the Experimental Lakes Area. *Canadian Journal of Fisheries and Aquatic Sciences,* **66,** 1831-1836.

Boegman, L., Loewen, M. R., Hamblin, P. F. & Culver, D. A. (2001) Application of a two-dimensional hydrodynamic reservoir model to Lake Erie. *Canadian Journal of Fisheries and Aquatic Sciences,* **58,** 858-869.

Buffalo Pound Water Administration Board (2015) Annual Report 2015.

Canadian Council of Ministers of the Environment (1999) Canadian water quality guidelines for the protection of aquatic life: Dissolved oxygen (freshwater). In: Canadian environmental quality guidelines. Canadian Council of Ministers of the Environment, Winnipeg.

Cavaliere, E. & Baulch, H. M. (2018) Denitrification under lake ice. *Biogeochemistry***,** 1-11.

Chapra, S. C. (1997) *Surface water-quality modeling.* Boston, Mass. ; New York : McGraw-Hill, Boston, Mass. ; New York.

Clifton Associates Ltd (2012) Upper Qu'Appelle Water Supply Project: Economic Impact & Sensitivity Analysis. pp. 101. Regina, SK.

Cole, T. M. & Wells, S. A. (2015) CE-QUAL-W2: A Two-Dimensional, Laterally Averaged, Hydrodynamic and Water Quality Model, Version 3.72. Department of Civil and Environmental Engineering, Portland State University, Portland.

Cole, T. M. & Wells, S. A. (2016) CE-QUAL-W2: A Two-Dimensional, Laterally Averaged, Hydrodynamic and Water Quality Model, Version 4.0. Department of Civil and Environmental Engineering, Portland State University, Portland, OR.

Cross, T. & Summerfelt, R. (1987) Oxygen demand of lakes: sediment and water column BOD. *Lake and Reservoir Management,* **3,** 109-116.

D'Silva, L. P. (2017) Biological and physicochemical mechanisms affecting phosphorus and arsenic efflux from prairie reservoir sediment, Buffalo Pound Lake, SK, Canada. (ed C. o. G. S. a. R. University of Saskatchewan).

Debele, B., Srinivasan, R. & Parlange, J. Y. (2008) Coupling upland watershed and downstream waterbody hydrodynamic and water quality models (SWAT and CE-QUAL-W2) for better water resources management in complex river basins. *Environ Model Assess,* **13,** 135-153.

Deliman, P. & Gerald, J. (2002) Application of the two- dimensional hydrothermal and water quality model, CE-QUAL-W2, to the Chesapeake Bay - Conowingo Reservoir. *Lake And Reservoir Management,* **18,** 10-19.

Dost, R. J. J. & Mannaerts, C. M. M. (2008) Generation of lake bathymetry using sonar, satellite imagery and GIS. *2008 Esri International User Conference*. ESRI, San Diego, CA.

Duguay, C. R., Prowse, T. D., Bonsal, B. R., Brown, R. D., Lacroix, M. P. & Menard, P. (2006) Recent trends in Canadian lake ice cover. *Hydrological Processes,* **20,** 781-801.

Environment Canada Climate Normals 1981-2010 station data for Moose Jaw A station.

Environment Canada (2015) MANOBS: Manual of Surface Weather Observations. Monitoring and Data Services Directorate, QC, Canada.

Fang, X. & Stefan, H. G. (2000) Projected Climate Change Effects on Winterkill in Shallow Lakes in the Northern United States. *Environmental Management,* **25,** 291-304.

Fang, X. & Stefan, H. G. (2009) Simulations of climate effects on water temperature, dissolved oxygen, and ice and snow covers in lakes of the contiguous U.S. under past and future climate scenarios. *Limnology and Oceanography,* **54,** 2359-2370.

Finlay, K., Leavitt, P. R., Patoine, A. & Wissel, B. (2010) Magnitudes and controls of organic and inorganic carbon flux through a chain of hard-water lakes on the northern Great Plains. *Limnology and Oceanography,* **55,** 1551-1564.

Folkard, A., Sherborne, A. & Coates, M. (2007) Turbulence and stratification in Priest Pot, a productive pond in a sheltered environment. *Limnology,* **8,** 113-120.

Gelda, R. K., Owens, E. M. & Effler, S. W. (1998) Calibration, verification, and an application of a two-dimensional hydrothermal model (CE-QUAL-W2 (t)) for Cannonsville Reservoir. *Lake and Reservoir Management,* **14,** 186-196.

Golosov, S., Maher, O., Schipunova, E., Terzhevik, A., Zdorovennova, G. & Kirillin, G. (2007) Physical background of the development of oxygen depletion in ice- covered lakes. *Oecologia,* **151,** 331-340.

Hall, R. I., Leavitt, P. R., Dixit, A. S., Quinlan, R. & Smol, J. P. (1999) Limnological succession in reservoirs: a paleolimnological comparison of two methods of reservoir formation. *Canadian Journal of Fisheries and Aquatic Sciences,* **56,** 1109-1121.

Hammer, U. (1971) Limnological Studies of the Lakes and Streams of the Upper Qu'Appelle River System, Saskatchewan, Canada. *Hydrobiologia,* **37,** 473-507.

Hampton, S. E., Galloway, A. W. E., Powers, S. M., Ozersky, T., Woo, K. H., Batt, R. D., Labou, S. G., Reilly, C. M., Sharma, S., Lottig, N. R., Stanley, E. H., North, R. L., Stockwell, J. D., Adrian, R., Weyhenmeyer, G. A., Arvola, L., Baulch, H. M., Bertani, I., Bowman, L. L., Carey, C. C., Catalan, J., Colom-Montero, W., Domine, L. M., Felip, M., Granados, I., Gries, C., Grossart, H. P., Haberman, J., Haldna, M., Hayden, B., Higgins, S. N., Jolley, J. C., Kahilainen, K. K., Kaup, E., Kehoe, M. J., Macintyre, S., Mackay, A. W., Mariash, H. L., McKay, R. M., Nixdorf, B., Nõges, P., Nõges, T., Palmer, M., Pierson, D. C., Post, D. M., Pruett, M. J., Rautio, M., Read, J. S., Roberts, S. L., Rücker, J., Sadro, S., Silow, E. A., Smith, D. E., Sterner, R. W., Swann, G. E. A., Timofeyev, M. A., Toro, M., Twiss, M. R., Vogt, R. J., Watson, S. B., Whiteford, E. J. & Xenopoulos, M. A. (2017) Ecology under lake ice. *Ecology Letters,* **20,** 98-111.

Havens, K. (2008) Cyanobacteria blooms: effects on aquatic ecosystems. *Cyanobacterial Harmful Algal Blooms: State Of The Science And Research Need,* **619,** 733-747.

Ho, J. C. & Michalak, A. M. (2015) Challenges in tracking harmful algal blooms: A synthesis of evidence from Lake Erie. *Journal of Great Lakes Research,* **41,** 317-325.

Hondzo, M. & Stefan, H. G. (1993) Regional water temperature characteristics of lakes subjected to climate-change. *Climatic Change,* **24,** 187-211.

Hosseini, N., Akomeah, E., Davies, J-M. & Baulch, H. (2018) Water quality modeling of a prairie river-lake system. *Environmental Science and Pollution Research International,* **25,** 31190-31204.

Hosseini, N., Chun, K. P., Wheater, H. & Lindenschmidt, K.-E. (2017) Parameter Sensitivity of a Surface Water Quality Model of the Lower South Saskatchewan River—Comparison Between Ice-On and Ice-Off Periods. *Environmental Modeling & Assessment,* **22,** 291-307.

Huber, V., Wagner, C., Gerten, D. & Adrian, R. (2012) To bloom or not to bloom: contrasting responses of cyanobacteria to recent heat waves explained by critical thresholds of abiotic drivers. *Oecologia,* **169,** 245-256.

Huisman, J., Sharples, J., Stroom, J. M., Visser, P. M., Kardinaal, W. E. A., Verspagen, J. M. H. & Sommeijer, B. (2004) Changes in turbulent mixing shift competition for light between phytoplankton species. *Ecology,* **85,** 2960-2970.

Jewson, D., Granin, N., Zhdanov, A. & Gnatovsky, R. (2009) Effect of snow depth on under-ice irradiance and growth of Aulacoseira baicalensis in Lake Baikal. *Aquat Ecol,* **43,** 673-679.

Johnes, P. J. (2007) Uncertainties in annual riverine phosphorus load estimation: Impact of load estimation methodology, sampling frequency, baseflow index and catchment population density.(Author abstract). *Journal of Hydrology,* **332,** 241.

Kehoe, M., Chun, K. & Baulch, H. (2015) Who Smells? Forecasting Taste and Odor in a Drinking Water Reservoir. *Environmental Science & Technology,* **49,** 10984-10984.

Kelley, D. E. (1997) Convection in ice- covered lakes: effects on algal suspension. *Journal of Plankton Research,* **19,** 1859-1880.

Kirillin, G., Leppäranta, M., Terzhevik, A., Granin, N., Bernhardt, J., Engelhardt, C., Efremova, T., Golosov, S., Palshin, N., Sherstyankin, P., Zdorovennova, G. & Zdorovennov, R. (2012) Physics of seasonally ice-covered lakes: a review. *Aquat Sci,* **74,** 659-682.

Knightes, C. D., Sunderland, E. M., Barber, M. C., Johnston, J. M. & Ambrose, R. B. (2009) Application of ecosystem- scale fate and bioaccumulation models to predict fish mercury response times to changes in atmospheric deposition. *Environmental Toxicology and Chemistry,* **28,** 881-893.

Leppi, J., Arp, C. & Whitman, M. (2016) Predicting Late Winter Dissolved Oxygen Levels in Arctic Lakes Using Morphology and Landscape Metrics. *Environmental Management,* **57,** 463-473.

Leppäranta, M. (2010) Modelling the Formation and Decay of Lake Ice. *The Impact of Climate Change on European Lakes* (ed D. G. George). Dordrecht : Springer Science+Business Media B.V., Dordrecht.

Leppäranta, M. (2014) Interpretation of statistics of lake ice time series for climate variability. *Hydrology Research,* **45,** 673.

Leppäranta, M. (2015) *Freezing of Lakes and the Evolution of their Ice Cover.* Springer-Verlag, Berlin.

Likens, G. E. (2009) Inland Waters. *Encyclopedia of Inland Waters* (ed G. E. Likens), pp. 1-5. Elsevier, Amsterdam ; Boston.

Lindenschmidt, K.-E. (2006) The effect of complexity on parameter sensitivity and model uncertainty in river water quality modelling. *Ecological Modelling,* **190,** 72-86.

Lindenschmidt, K.-E. & Carstensen, D. (2015) The upper Qu'Appelle water supply project in Saskatchewan, Canada: upland canal ice study. *Österreichische Wasser- und Abfallwirtschaft,* **67,** 230-239.

Lindenschmidt, K.-E. & Chorus, I. (1998) The effect of water column mixing on phytoplankton succession, diversity and similarity. **20,** 1927-1951.

Lindenschmidt, K.-E., Fleischbein, K. & Baborowski, M. (2007) Structural uncertainty in a river water quality modelling system. *Ecological Modelling,* **204,** 289-300.

Lindenschmidt, K.-E., Pech, I. & Baborowski, M. (2009) Environmental risk of dissolved oxygen depletion of diverted flood waters in river polder systems – A quasi-2D flood modelling approach. *Science of The Total Environment,* **407,** 1598-1612.

Martin, J. L. (1988) Application of two-dimensional water-quality model. *Journal of Environmental Engineering-Asce,* **114,** 317-336.

Martin, N., McEachern, P., Yu, T. & Zhu, D. Z. (2013) Model development for prediction and mitigation of dissolved oxygen sags in the Athabasca River, Canada. *Science of the Total Environment,* **443,** 403-412.

Martynov, A., Sushama, L. & Laprise, R. (2010) Simulation of temperate freezing lakes by one-dimensional lake models: Performance assessment for interactive coupling with regional climate models. *Boreal Environment Research,* **15,** 143-164.

McGowan, S., Leavitt, P. & Hall, R. (2005) A Whole- Lake Experiment to Determine the Effects of Winter Droughts on Shallow Lakes. *Ecosystems,* **8,** 694-708.

Meding, M. E. & Jackson, L. J. (2003) Biotic, chemical, and morphometric factors contributing to winter anoxia in prairie lakes. *Limnology and Oceanography,* **48,** 1633-1642.

Michalak, A., Anderson, E., Beletsky, D., Boland, S., Bosch, N., Bridgeman, T., Chaffin, J. D., Cho, K., Confesor, R., Daloglu, I., Depinto, J., Evans, M. A., Fahnenstiel, G., He, L., Ho, J., Jenkins, L., Johengen, T., Kuo, K., Laporte, E., Liu, X., McWilliams, M., Moore, M., Posselt, D., Richards, R., Scavia, D., Steiner, A. L., Verhamme, E., Wright, D. M. & Zagorski, M. A. (2013) Record-setting algal bloom in Lake Erie caused by agricultural and meteorological trends consistent with expected future conditions. *Proceedings Of The National Academy Of Sciences Of The United States Of Ame,* **110,** 6448-6452.

Minns, C. (2013) The science of ecosystem-based management on a global scale: The Laurentian Great Lakes, Lake Ontario, and the Bay of Quinte as a nested case study. *Aquatic Ecosystem Health & Management,* **16,** 229-239.

Mooij, W. M., Trolle, D., Jeppesen, E., Arhonditsis, G., Belolipetsky, P. V., Chitamwebwa, D. B. R., Degermendzhy, A. G., DeAngelis, D. L., Domis, L. N. D. S., Downing, A. S., Elliott, J. A., Fragoso, C. R., Jr., Gaedke, U., Genova, S. N., Gulati, R. D., Hakanson, L., Hamilton, D. P., Hipsey, M. R., t Hoen, J., Huelsmann, S., Los, F. H., Makler-Pick, V., Petzoldt, T., Prokopkin, I. G., Rinke, K., Schep, S. A., Tominaga, K., Van Dam, A. A., Van Nes, E. H., Wells, S. A. & Janse, J. H. (2010) Challenges and opportunities for integrating lake ecosystem modelling approaches. *Aquatic Ecology,* **44,** 633-667.

MPE Engineering (2013) Water Security Agency, Buffalo Pound Dam - Dam Safety, Data Book - Draft.

Oveisy, A., Boegman, L. & Imberger, J. (2012) Three- dimensional simulation of lake and ice dynamics during winter. *Limnology and Oceanography,* **57,** 43-57.

Oveisy, A., Rao, Y. R., Leon, L. F. & Bocaniov, S. A. (2014) Three-dimensional winter modeling and the effects of ice cover on hydrodynamics, thermal structure and water quality in Lake Erie. *Journal of Great Lakes Research,* **40,** 19-28.

Puschner, B., Hoff, B. & Tor, E. R. (2008) Diagnosis of anatoxin-a poisoning in dogs from North America. *Journal of veterinary diagnostic investigation : official publication of the American Association of Veterinary Laboratory Diagnosticians, Inc,* **20,** 89.

Quiblier, C., Wood, S., Echenique-Subiabre, I., Heath, M., Villeneuve, A. & Humbert, J.-F. (2013) A review of current knowledge on toxic benthic freshwater cyanobacteria – Ecology, toxin production and risk management. *Water Research,* **47,** 5464-5479.

Reckhow, K. (1999) Water quality prediction and probability network models. *Canadian Journal of Fisheries and Aquatic Sciences,* **56,** 1150-1158.

Robarts, R. D., Waiser, M. J., Arts, M. T. & Evans, M. S. (2005) Seasonal and diel changes of dissolved oxygen in a hypertrophic prairie lake. *Lakes & Reservoirs: Research & Management,* **10,** 167-177.

Rodell, M., Famiglietti, J. S., Wiese, D. N., Reager, J. T., Beaudoing, H. K., Landerer, F. W. & Lo, M. H. (2018) Emerging trends in global freshwater availability. *Nature,* **557,** 651-659.

Ruuhijärvi, J., Rask, M., Vesala, S., Westermark, A., Olin, M., Keskitalo, J. & Lehtovaara, A. (2010) Recovery of the fish community and changes in the lower trophic levels in a eutrophic lake after a winter kill of fish. *Hydrobiologia,* **646,** 145-158.

Sadeghian, A. (2017) Water quality modeling of Lake Diefenbaker. (ed C. o. G. S. a. R. University of Saskatchewan).

Sadeghian, A., Chapra, S. C., Hudson, J., Wheater, H. & Lindenschmidt, K.-E. (2018) Improving in-lake water quality modeling using variable chlorophyll a/algal biomass ratios. *Environmental Modelling and Software,* **101,** 73-85.

Sadeghian, A., de Boer, D., Hudson, J. J., Wheater, H. & Lindenschmidt, K.-E. (2015) Lake Diefenbaker temperature model. *Journal of Great Lakes Research,* **41,** 8-21.

Salonen, K., Leppäranta, M., Viljanen, M. & Gulati, R. (2009) Perspectives in winter limnology: closing the annual cycle of freezing lakes. *A Multidisciplinary Journal Relating to Processes and Structures at Different Organizational Levels,* **43,** 609-616.

Saltelli, A. & Annoni, P. (2010) How to avoid a perfunctory sensitivity analysis. *Environmental Modelling & Software,* **25,** 1508-1517.

Scardina, P. & Edwards, M. (2001) Prediction and measurement of bubble formation in water treatment. *Journal of Environmental Engineering,* **127,** 968.

Scheffer, M. (2004) *Ecology of shallow lakes.* Dordrecht ; Boston : Kluwer Academic Publishers, Dordrecht ; Boston.

Schindler, D. W. (2009) Lakes as sentinels and integrators for the effects of climate change on watersheds, airsheds, and landscapes. *Limnology and Oceanography,* **54,** 2349-2358.

Semmler, T., Cheng, B., Yang, Y. & Rontu, L. (2012) Snow and ice on Bear Lake (Alaska) – sensitivity experiments with two lake ice models. *Tellus A: Dynamic Meteorology and Oceanography,* **64**.

Shoemaker, L., Dai, T., Koenig, J. & Hantush, M. (2005) TMDL model evaluation and research needs. *EPA/600/R-05/149*. EPA, National Risk Management Laboratory, Cincinnati, Ohio:U.S.

Singleton, V. L., Jacob, B., Feeney, M. T. & Little, J. C. (2013) Modeling a proposed quarry reservoir for raw water storage in Atlanta, Georgia.(Author abstract). *Journal of Environmental Engineering,* **139,** 70.

Slater, G. P. & Blok, V. C. (1983) Isolation and identification of odourous compounds from a lake subject to cyanobacterial blooms. *Water Science and Technology,* **15,** 229-240.

Sommer, U., Adrian, R., De Senerpont Domis, L., Elser, J. J., Gaedke, U., Ibelings, B., Jeppesen, E., Lrling, M., Molinero, J. C., Mooij, W. M., van Donk, E. & Winder, M. (2012) Beyond the Plankton Ecology Group ( PEG) Model: Mechanisms Driving Plankton Succession. *Annu. Rev. Ecol. Evol. Syst.*, pp. 429-448.

Stantec (n.d.) Upper Qu'Appelle Channel Feasibility Study.

Stokstad, E. (2008) Canada's experimental lakes. *Science (New York, N.Y.),* **322,** 1316.

Svacina, N. A., Duguay, C. R. & Brown, L. C. (2014) Modelled and satellite-derived surface albedo of lake ice – Part I: evaluation of the albedo parameterization scheme of the Canadian Lake Ice Model. *Hydrological Processes,* **28,** 4550-4561.

Taranu, Z., Köster, D., Hall, R., Charette, T., Forrest, F., Cwynar, L. & Gregory-Eaves, I. (2010) Contrasting responses of dimictic and polymictic lakes to environmental change: a spatial and temporal study. *Aquat. Sci.,* **72,** 97-115.

Taranu, Z. E., Gregory-Eaves, I., Leavitt, P. R., Bunting, L., Buchaca, T., Catalan, J., Domaizon, I., Guilizzoni, P., Lami, A., McGowan, S., Moorhouse, H., Morabito, G., Pick, F. R., Stevenson, M. A., Thompson, P. L. & Vinebrooke, R. D. (2015) Acceleration of cyanobacterial dominance in north temperate- subarctic lakes during the Anthropocene. *Ecology Letters,* **18,** 375-384.

Taranu, Z. E., Zurawell, R. W., Pick, F. & Gregory-eaves, I. (2012) Predicting cyanobacterial dynamics in the face of global change: the importance of scale and environmental context. *Global Change Biology,* **18,** 3477-3490.

Terry, J. A., Sadeghian, A., Baulch, H. M., Chapra, S. C. & Lindenschmidt, K.-E. (2018) Challenges of modelling water quality in a shallow prairie lake with seasonal ice cover. *Ecological Modelling,* **384,** 43-52.

Terry, J. A., Sadeghian, A. & Lindenschmidt, K.-E. (2017) Modelling Dissolved Oxygen/Sediment Oxygen Demand under Ice in a Shallow Eutrophic Prairie Reservoir. *Water,* **9,** 131.

Thornton, K. W., Kimmel, B. L. & Payne, F. E. (1990) *Reservoir limnology : ecological perspectives.* New York : Wiley, New York.

Vavrus, S. J., Wynne, R. H. & Foley, J. A. (1996) Measuring the sensitivity of southern Wisconsin lake ice to climate variations and lake depth using a numerical model. *Limnology and Oceanography,* **41,** 822-831.

Vehmaa, A. & Salonen, K. (2009) Development of phytoplankton in Lake Pääjärvi (Finland) during under- ice convective mixing period. *Aquat Ecol,* **43,** 693-705.

Venkiteswaran, J. (2012) Up close and personal. *Alternatives Journal,* **38,** 16-19,6.

Vörösmarty, C. J., McIntyre, P. B., Gessner, M. O., Dudgeon, D., Prusevich, A., Green, P., Glidden, S., Bunn, S. E., Sullivan, C. A., Liermann, C. R. & Davies, P. M. (2010) Global threats to human water security and river biodiversity. *Nature,* **467,** 555.

Wang, Q., Li, S., Jia, P., Qi, C. & Ding, F. (2013) A Review of Surface Water Quality Models. *The Scientific World Journal,* **2013**.

Water Security Agency (2017) Annual Report for 2016-17. Government of Saskatchewan.

Watson, S. & Lawrence, J. (2003) Introductory remarks -- Drinking water quality and sustainability. *Water Qual. Res. J. Can,* **38,** 3-13.

Wetzel, R. G. (2001) *Limnology : lake and river ecosystems.* San Diego : Academic Press, San Diego.

Wheater, H. & Gober, P. (2013) Water security in the Canadian Prairies: science and management challenges. *Philosophical transactions. Series A, Mathematical, physical, and engineering sciences,* **371,** 20120409.

Wheater, H. S. & Gober, P. (2015) Water security and the science agenda. *Water Resources Research,* **51,** 5406-5424.

White, J. D., Prochnow, S. J., Filstrup, C. T., Scott, J., Byars, B. & Zygo-Flynn, L. (2010) A combined watershed-water quality modeling analysis of the Lake Waco reservoir: I. Calibration and confirmation of predicted water quality. *Lake And Reservoir Management,* **26,** 147-158.

Williams, R., Keller, V., Vo, A., Barlund, I., Malve, O., Riihimaki, J., Tattari, S. & Alcamo, J. (2012) Assessment of current water pollution loads in Europe: estimation of gridded loads for use in global water quality models.(Report). *Hydrological Processes,* **26**.

Williamson, C. E., Saros, J. E. & Schindler, D. W. (2009) Climate change. Sentinels of change. *Science (New York, N.Y.),* **323,** 887.

Yang, Y., Pettersson, K. & Padisák, J. (2016) Repetitive baselines of phytoplankton succession in an unstably stratified temperate lake (Lake Erken, Sweden): a long-term analysis. *Hydrobiologia,* **764,** 211-227.

Zhang, Z., Sun, B. & Johnson, B. E. (2015) Integration of a benthic sediment diagenesis module into the two dimensional hydrodynamic and water quality model – CE- QUAL- W2. *Ecological Modelling,* **297,** 213-231.